D2-113016-5
April 10, 1967

STUDY OF NAVIGATION AND GUIDANCE OF LAUNCH VEHICLES HAVING CRUISE CAPABILITY FINAL REPORT, VOLUME 2 of 4 TRAJECTORY PARAMETRIC AND OPTIMIZATION STUDIES

by

D. S. Hague and C. R. Glatt

Prepared for

NATIONAL AERONAUTICS AND SPACE ADMINISTRATION

Contract NAS 2-3691

Technical Management
NASA Mission Analysis Division
Moffett Field, California
Mr. Hubert Drake

Aerospace Group
THE BOEING COMPANY
Seattle, Washington

FOREWARD

This document reports on an investigation by The Boeing Company from June 10, 1966 to March 10, 1967 of the navigation and guidance of a two stage launch vehicle (hypersonic Stage 1/rocket Stage 2) under contract NAS 2-3691. The Technical Monitor for the study was Mr. Hubert Drake of the NASA Mission Analysis Division, Moffett Field, California with Co-monitor Mr. Frank Carroll of the NASA Electronics Research Center, Cambridge, Massachusetts.

The Final Report is prepared in four volumes:

Volume 1 - Summary Report, Boeing Document D2-113016-4

Volume 2 - Trajectory Parametric and Optimization Studies, D2-113016-5

Volume 3 - Alternate Navigation-Guidance Concepts (Phase I), D2-113016-6

Volume 4 - Detailed Study of Two Selected Navigation-Guidance Concepts (Phase II), D2-113016-7.

Boeing personnel who participated in the study reported in this volume (Volume 2) are D. S. Hague and C. R. Glatt. J. A. Retka was the program manager.

Acknowledgment is given to Mr. B. R. Bensen of the Air Force Flight Dynamics Laboratory, Wright-Patterson Air Force Base, Ohio for permission to reproduce the optimization theory originally developed under USAF Contract Number AF 33(657)-8829.

CONTENTS

CONTENTS - Cont.

ILLUSTRATIONS

ILLUSTRATIONS - Cont.

ILLUSTRATIONS - CONT.

INTRODUCTION

This study is directed at determining the feasibility, capabilities, and limitations of navigation and guidance systems for a two stage launch vehicle having an aerodynamic, air breathing first stage and a rocket second stage. The basic mission is to fly a 3704 km (2000 nautical mile) offset distance to the orbital plane of a satellite, turn into the plane and separate the second stage which then accomplishes rendezvous of the payload with a target satellite; the first stage then returns to its base. Phase I, the first four months of the nine month study, is a comparative analysis of alternate navigation and guidance concepts. Phase II, the second half of the study is a detailed study of two selected navigation-guidance concepts.

The overall objective of the study is to determine if substantial improvements in navigation and guidance technology are required or if significant losses in mission performance occur in carrying out a rendezvous mission with this launch vehicle. A rescue mission is a typical rendezvous mission that the launch vehicle is required to perform.

The Final Report for the Study of Navigation and Guidance of Launch Vehicles Having Cruise Capability has four volumes.

Volume 1 - Summary Report, Boeing Dcoument D2-113016-4.

Volume 2 - Trajectory Parametric and Optimization Studies, D2-113016-5

Volume 3 - Analyses and Tradeoffs of Alternate Navigation - Guidance Concepts (Phase I) D2-113016-6.

Volume 4 - Detailed Studies of Two Selected Navigation - Guidance Concepts (Phase II), D2-113016-7.

This volume reports the work accomplished on development of the nominal flight profile and is divided into two parts. Part I describes the flight performance work accomplished in Phase I, and Part II gives the trajectory optimization study results obtained in Phase II.

The Phase I study was done by parametrically analyzing the Stage 1 flight profile by breaking the trajectory into distinct subarcs or segments; the Stage 1 pullup and Stage 2 trajectory to the rendezvous point was developed using a steepest-descent optimization computer program. The payload into orbit capability obtained by this approach was 6,230 kg (13,720 lbs).

The trajectory optimization work reported in Part II was done with a variable staging point steepest-descent optimization computer program. The complete Stage 1 and Stage 2 trajectory from takeoff to the rendezvous point was optimized; ignoring the Stage 1 return to base constraint. The resulting staging conditions were then used as the initial conditions for a separate optimization of the Stage 1 return path. The takeoff weight and landing weight of Stage 1 were specified. Stage 1 fuel savings were converted to payload in orbit. The payload in orbit performance capability obtained with this approach was 8,022 kg (17,690 lbs). This is a 29% increase in performance.

PART I. PHASE I TRAJECTORY STUDY RESULTS

1.0 FLIGHT PERFORMANCE

The objective of the Phase I flight performance studies was to define the launch vehicle operational techniques which minimize mission performance losses and/or reduce complexity in the navigation and guidance system for a 3704 km (2000 NM) offset rendezvous mission. The 9,270 km (5000 NM) cruise mission is also investigated. The approach involves the determination of the maximum performance by classical methods with the specified vehicle characteristics and perfect guidance and navigation. The perfect guidance and navigation system as used here is one which duplicates the specified mission profile exactly with no mass penalty. The performance of a real system then is measured in terms of system mass and fuel/propellant penalties, converted to orbital payload penalty. The specified mission profile was determined within the following design constraints.

Stage 1

Maximum Mach Number	7	
Maximum Dynamic Pressure	95,760. N/M^2	(2000 psf)
Maximum Propulsion System Internal Pressure	1,379,000. N/M^2	(200 psi)
Maximum Normal Load Factor	2.5	
Maximum Sonic Boom Overpressure	143.6 N/M^2	(3 psf)

Stage 2

Maximum Dynamic Pressure	9,576 N/M^2	(200 psf)

Figure 1-1 shows the applicable vehicle constraints as a function of Mach number and altitude.

The gross weight and empty weight were specified by the statement of work. Fuel and payload were traded using appropriate exchange ratios for orbital payload as described in Appendix A1 of D2-113016-6 (Volume 3).

2.0 NOMINAL VEHICLE CHARACTERISTICS

The vehicle under consideration is an earth-to-orbit launch system composed of an aerodynamically supported air-breathing first stage and a ballistic rocket second stage represented schematically in Figure 1-2. The first stage structure is made up of nickel alloy heat shields and aerodynamic control surfaces, high temperature insulation and titanium load carrying structure for wing and body. The propulsion system consists of subsonic burning liquid hydrogen turboramjets with sea level static thrust of 1,220,000 newtons (275,000 lbs.) Thrust and specific fuel consumption data are described

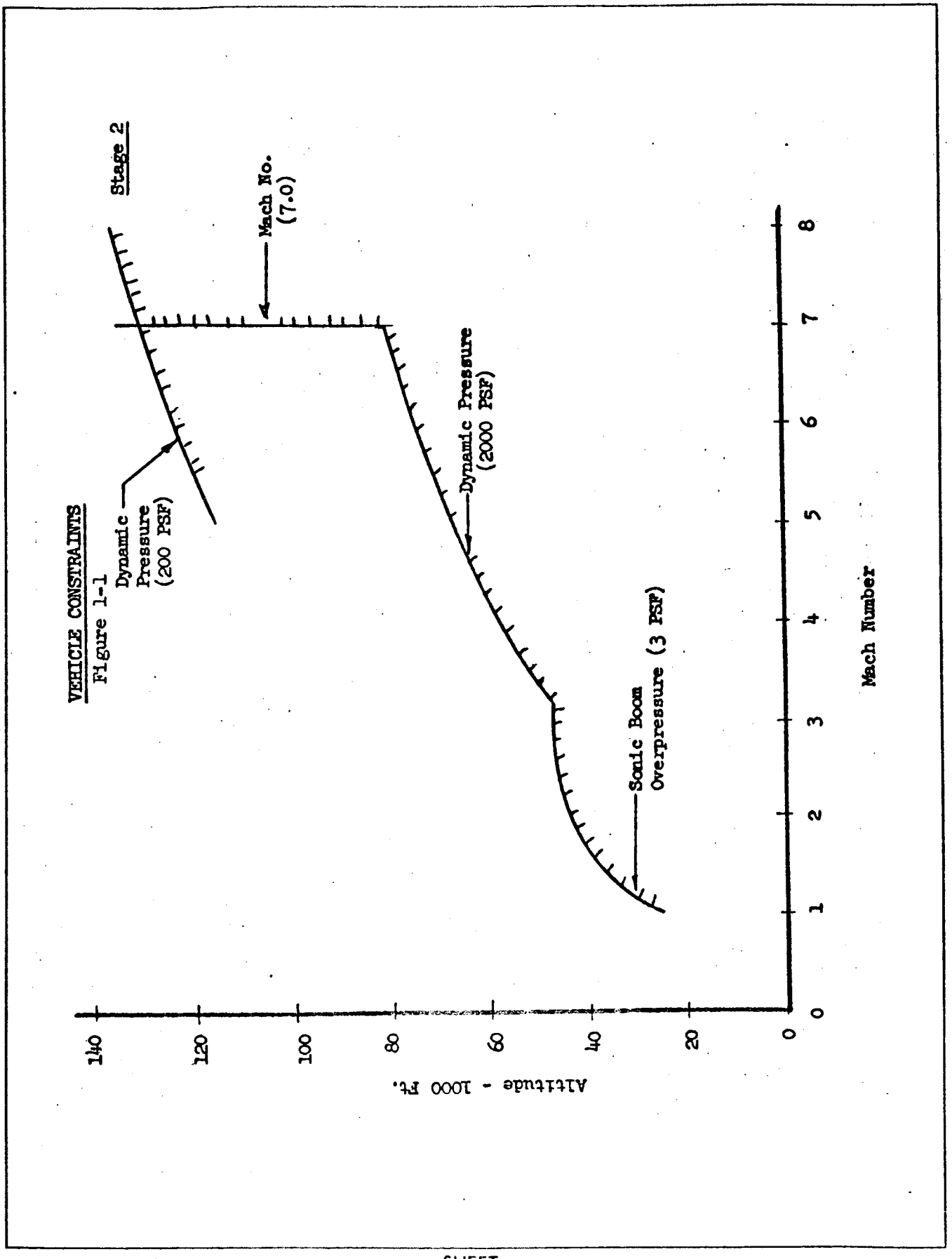

NOMINAL VEHICLE CONFIGURATION

Figure 1-2

- Two Stage Earth-to-Orbit Launch System
- Aerodynamically Supported, Airbreathing First Stage
- Rocket Powered Second Stage
- Manned or Unmanned Payload

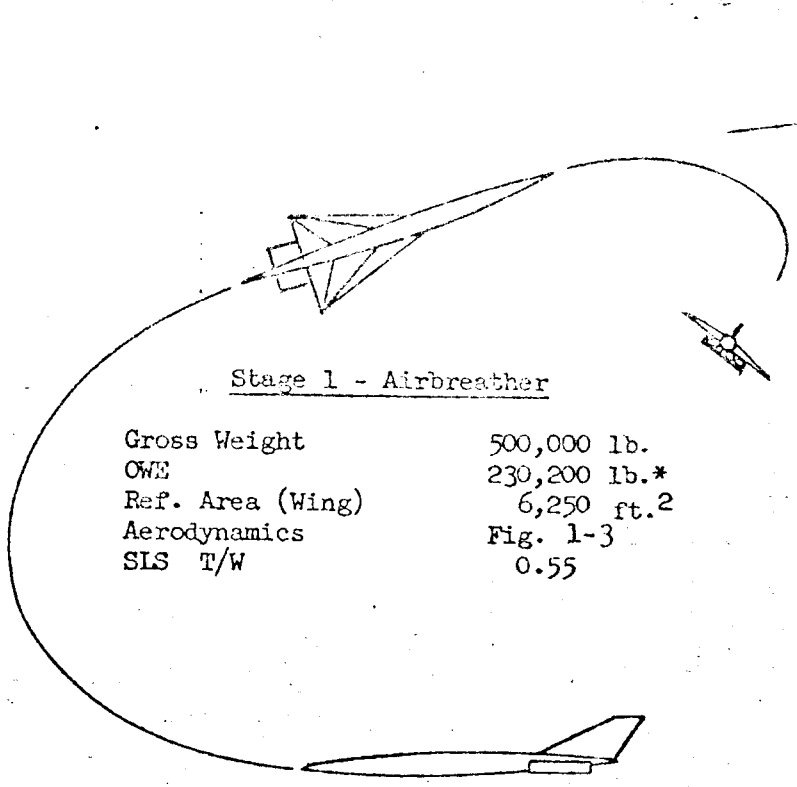

Stage 1 - Airbreather

Gross Weight	500,000 lb.
OWE	230,200 lb.*
Ref. Area (Wing)	6,250 ft.^{2}
Aerodynamics	Fig. 1-3
SLS T/W	0.55

Stage 2 - Rocket

Startburn Wt.	125,500 lb.
Inert Wt.	13,250 lb.
Ref. Area (Base)	62.2 ft^2
Drag Coefficient	0.13
Vac Specific Impulse	420 secs.
Vac T/W	1.5
Payload	13,720 lbs.

* 289,300 for cruise vehicle

in Reference 1. The second stage is an expendable liquid oxygen/liquid hydrogen rocket vehicle with start burn thrust-to-weight ratio of 1.5. The vacuum specific impulse is specified to be 420 sec. The structural weight is considered to be 13.3% of the propellant weight as implied by the work statement. The configuration geometry is as follows:

Stage 1

Length	87.78 M	(288 ft.)*
Body Volume (Sears-Haack Shape)	17251.68 M	(56,600 ft.^{3})*
Wing Planform (edges extended to vehicle center line)	1905. M	(6,250 ft.^{2})
Wing Aspect Ratio (Delta Planform)	1.455	1.455
Wing chord thickness ratio	.04	.04

*312 feet, 71,500 ft^3 for cruise vehicle

Stage II

Length	32.6 M	(107 ft.)
Diameter	2.7 M	(8.9 ft.)
Reference area	19.0 M^2	(62.2 ft.^{2})

The aerodynamic data for the first stage vehicle is shown in Figure 1-3. It is based on the cruise vehicle but is considered satisfactory for the boost vehicle as well. The drag coefficient of the second stage was assumed to be a constant value of 0.13 based on the reference area of 19.0 M^2 (62.2 ft.^{2})

The vehicle characteristics were taken directly from the specifications for the study and supplemented where necessary with reasonable assumptions. No attempt was made to improve or alter the prescribed data. Trade studies considered no feedback on vehicle characteristics. Further vehicle configuration data are given in Reference 2 and 3.

3.0 NOMINAL MISSION

The nominal mission is an offset mission where the hydrogen fueled, turboramjet powered, aerodynamically supported first stage transports an expendable LO/H$_2$ rocket to a launch plane 3,704 km (2000 nautical miles) from the take off base, provides a launch platform for the upper stage, then returns to base. The ground track and velocity-altitude profile are sketched in Figure 1-4. A mission performance summary in terms of weight, range and altitude follows:

AERODYNAMIC CHARACTERISTICS
STAGE 1

FIGURE 1-3

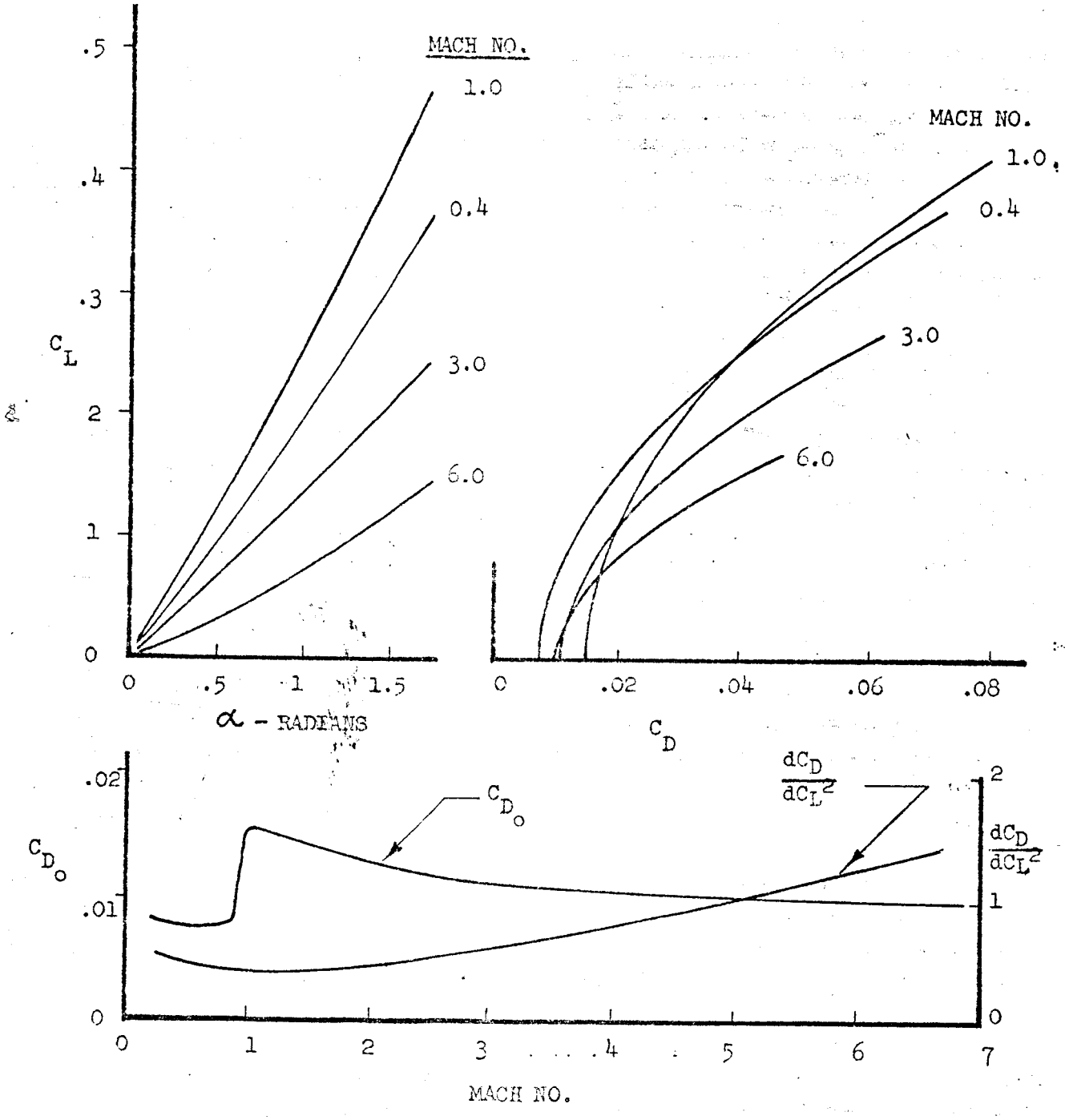

THE NOMINAL MISSION

Figure 1-4

- Take-Off
- Climb and Accelerate to Cruise Conditions
- Cruise and Turn Into Orbit Plane Followed by Pull-Up
- Launch Stage 2
  - Boost to Transfer Orbit
  - Coast to Apogee
  - Insert in 262 NM Circular Orbit
- Cruise Back to Base

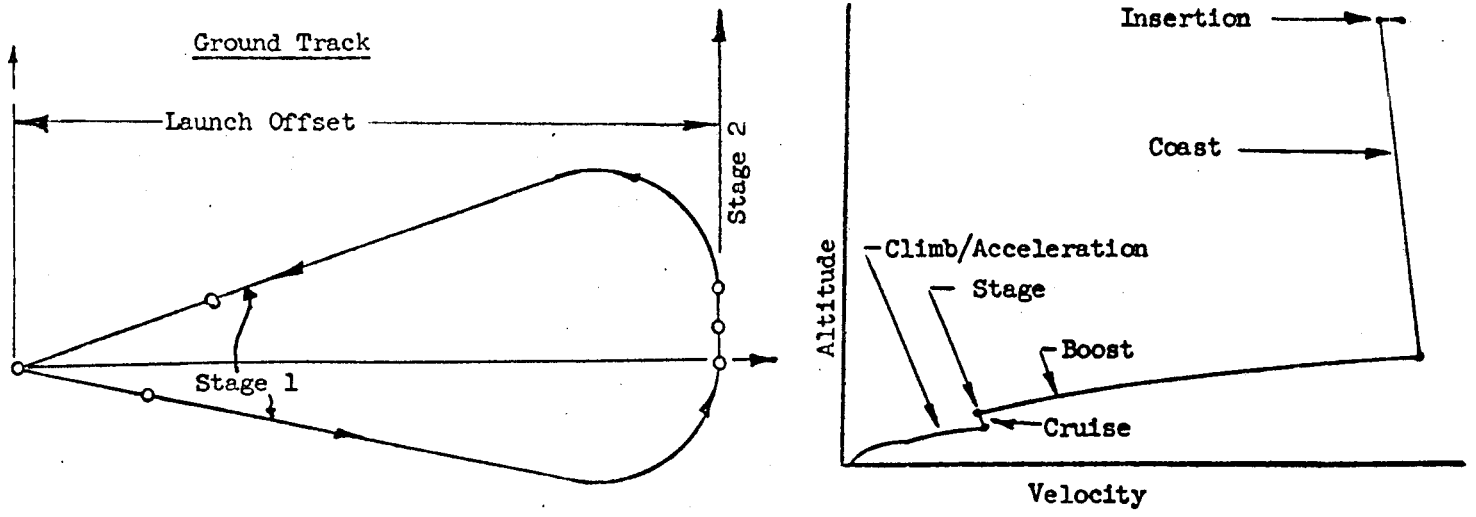

MISSION PERFORMANCE SUMMARY

Initial Condition	Weight kg	Weight Lbs.	Range km	Range N.M.	Altitude km	Altitude Ft.
Take off	227,000	(500,000)	0	0	0	0
Cruise/Turn	203,000	(447,750)	750	(405)	28.3	(92,600)
Pullup	177,000	(391,200)	4,100	(2,216)	29.2	(95,600)
Staging	176,000	(387,800)	4,230	(2,316)	38.9	(127,500)
Turn/Cruise	118,000	(260,200)	4,470	(2,416)	31.9	(104,500)
Descent	105,400	(232,300)	7,280	(3,934)	32.6	(107,100)
Landing	104,500	(230,200)	8,400	(4,534)	0	0
Staging	57,000	(125,600)	--	--	38.9	(127,500)
Insertion	12,200*	(26,890)*	--	--	486.	(1,593,000)

*Payload = 6,230 kg, (13,720 lb.)

Alternate missions include 1852 km (1000 N.M.) and zero offset missions as well as the 9,260 km (5,000 N.M.) cruise missions. These missions are summarized in Figure 1-5. The ground tracks for the several missions are shown approximately to scale for comparison. The weight summary for the Phase I parametric performance study shows a maximum orbital payload of 9,250 kg (20,390 lb.) in a zero offset orbit as compared to 6,220 kg (13,720 lb.) for the nominal mission. The payload for the cruise mission is 18,200 kg (40,200 lb.).

ALTERNATE MISSIONS

Figure 1-5

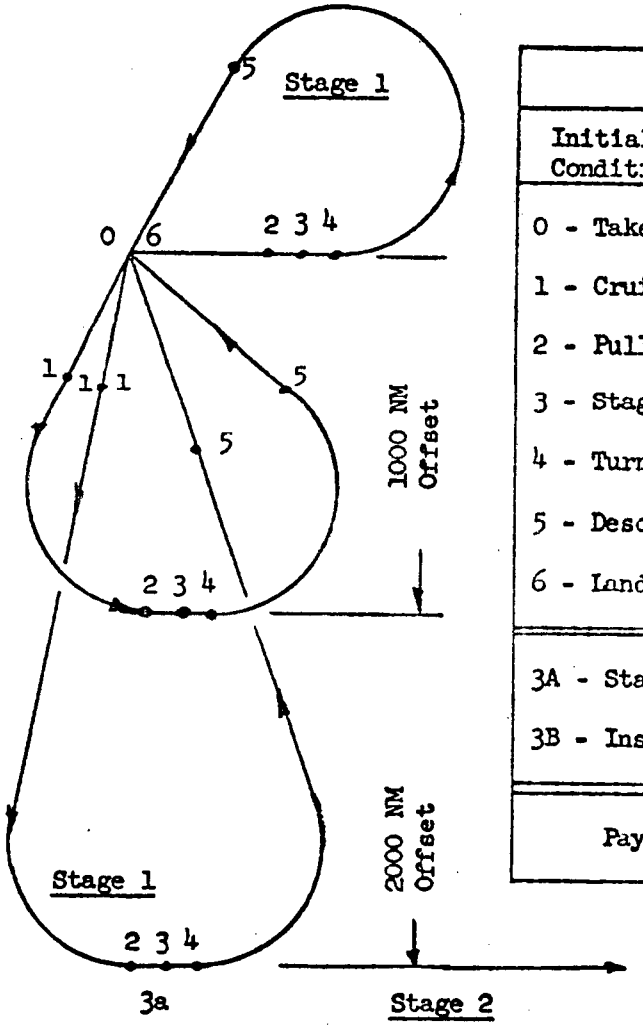

WEIGHT SUMMARY				
Initial Condition	2000 NM Offset	1000 NM Offset	Zero Offset	5000 NM Cruise
0 - Take off	500,000	500,000	500,000	500,000
1 - Cruise/Turn	447,750	447,750	--	447,750
2 - Pull up	391,200	420,500	447,750	--
3 - Stage	387,800	417,000	445,000	--
4 - Turn/Cruise	260,200	245,500	256,300	--
5 - Descent	232,300	232,300	232,300	331,600
6 - Landing	230,200	230,200	230,200	329,500
3A - Stage	125,600	180,640	186,650	--
3B - Insertion	26,890	38,670	39,960	--
Payload	13,720	19,730	20,390	40,200

Baseline Mission

4.0 Stage 1 Parametric Study Results

4.1 Takeoff

The flight profile begins with the start of the ground run attime zero. No fuel allowance is made for warm-up or taxi purposes. Low angle of attack is used for ground roll acceleration. Ground rotation to 15 degrees angle of attack is assumed to occur at 120 percent of the stall speed. Fifteen (15) degrees is considered the maximum angle which allows launch vehicle tail clearance. No high lift devices were considered. The take-off angle of attack is held until 16 degrees flight path angle is reached. This flight path angle is maintained until the vehicle reaches 305 meters (1000 feet) of altitude where level flight is established and a 180 degree turn is initiated.

4.2 Climb/Acceleration

The assumed minimum fuel climb/acceleration profile is defined by the sonic boom overpressure, the dynamic pressure limit and the design Mach number. The fuel requirements and trajectory characteristics for this flight phase were determined by a 20 point mass trajectory program utilizing a velocity-altitude flight plan programmer. Other velocity-altitude profiles in the region of the boundary were investigated but no more economical path was found which satisfied the inequality constraints.

4.3 Cruise/Turn

The cruise/turn path segment starts after climb-acceleration and continues through the turn into the target orbital plane. The cruise phase was studied for two ramjet sizes. First, the ramjet was sized for acceleration under the criterion of minimum excess thrust at the end of the climb/acceleration phase.

$$\frac{T-D}{W} = 0.15$$

at 24.7 km (81,000 feet)

where:
- T = thrust
- D = drag
- W = weight

This is the criterion normally used for airbreathing launch vehicles when hypersonic cruise (i.e. launch offset) is not required. In this case the cruise and turn were performed at constant altitude corresponding to the altitude at the end of the climb.

In the second case the ramjet was sized for cruise at optimum altitude with no excess thrust.

$$\frac{T-D}{W} = 0$$

at Cruise Altitude

Since flight at Mach 7 requires a fuel equivalence ratio of at least unity for inlet cooling, no performance advantage is expected for throttling. Therefore, the above criterion is expected to yield the minimum fuel usage for cruise. The larger ramjet also has significant performance advantage in the acceleration phase.

Several alternatives to the cruise/turn ground rules were considered including (1) cruise at optimum altitude and sacrifice of speed in the turn, (2) cruise at optimum altitude and sacrifice of altitude during the turn or (3) cruise at the lower altitude necessary to obtain minimum fuel for cruise plus steady state turn. For the first alternative, it was assumed that the vehicle would be reaccelerated after the turn. It is shown in Appendix A2 of Volume 3 that loitering time delay in the target plane is very expensive in terms of payload penalty so any turn technique involving loss of speed has been ruled out. For the second alternative, the altitude is reduced during the turn. It was shown in Phase 2 studies that this may be the way to perform the turn because of the improvement in Stage 2 performance resulting from the Stage 1 energy gain at staging by this method. The third method holds some promise because the cruise efficiency has a low sensitivity to change in altitude at the optimum cruise altitude while the load factor capability is quite sensitive under the same conditions. To demonstrate this trade, the minimum fuel cruise/turn was determined by performing the cruise and turn at various increments below cruise altitude. The results are shown in Figure 1-6 for 1852 and 3704 km (1000 and 2000 N.M.) offset missions. These results did not take into account the climb to cruise altitude following acceleration.

Sensitivity studies of the effects of heading change on mission performance indicated possible gains by altering the ground track. The results of an investigation of cruise heading angle for minimum total Stage 1 mission fuel usage is shown in Figure 1-7. This figure shows changes in fuel requirements for changes in outbound cruise heading from the zero heading path. It can be seen that as relative heading angle is increased the extra fuel used for the outbound cruise is more than compensated by the fuel saved on the inbound cruise. This results in a desired relative heading angle of 12° for the 3704 km (2000 N.M.) offset mission. Under the same conditions with 1852 km (1000 N.M.) offset the best outbound relative heading angle is 26° West.

FUEL FOR CRUISE PLUS TURN
CRUISE ALTITUDE REDUCTION

FIGURE 1-6

NOTES:

1. Engine sized for cruise
2. Equivalence ratio at 7000 FPS - 1.0
3. Data does not include fuel for climb/acceleration

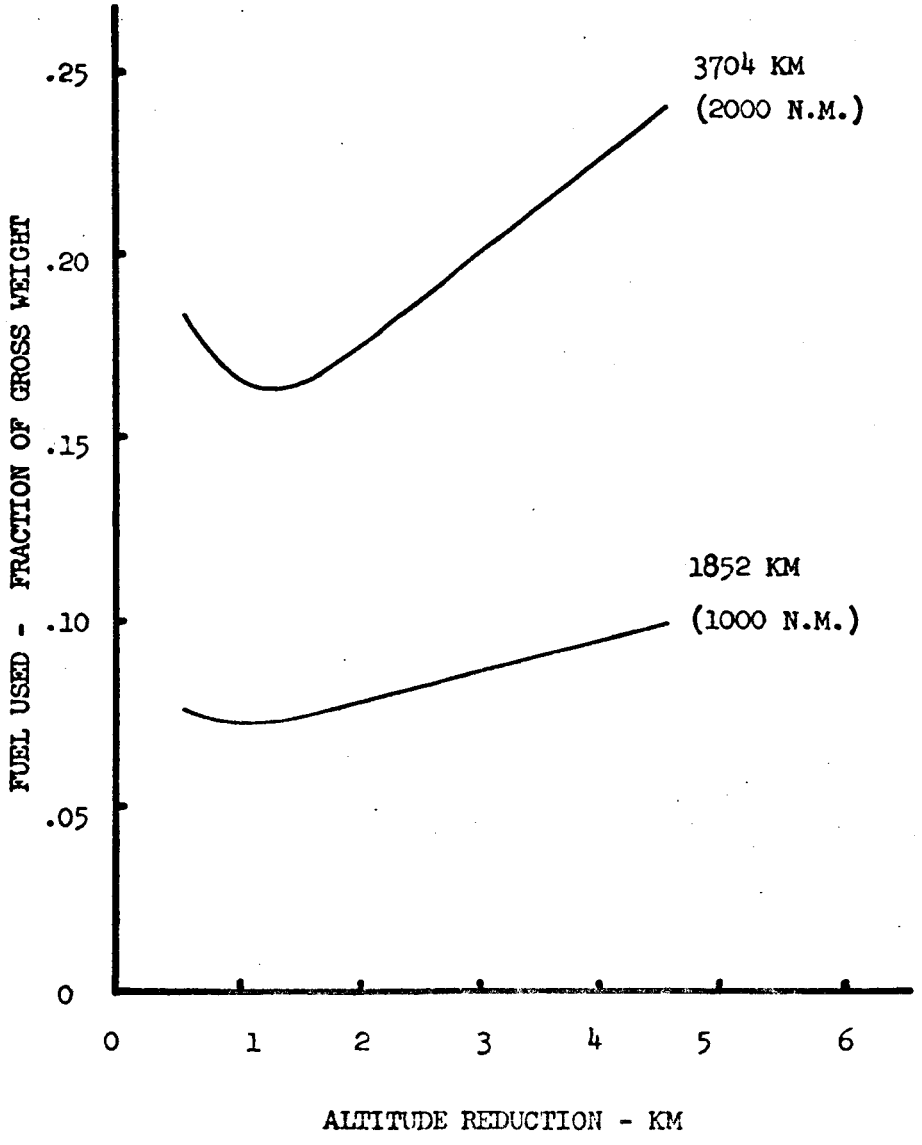

MINIMUM FUEL OUTBOUND HEADING ANGLE

FIGURE 1-7

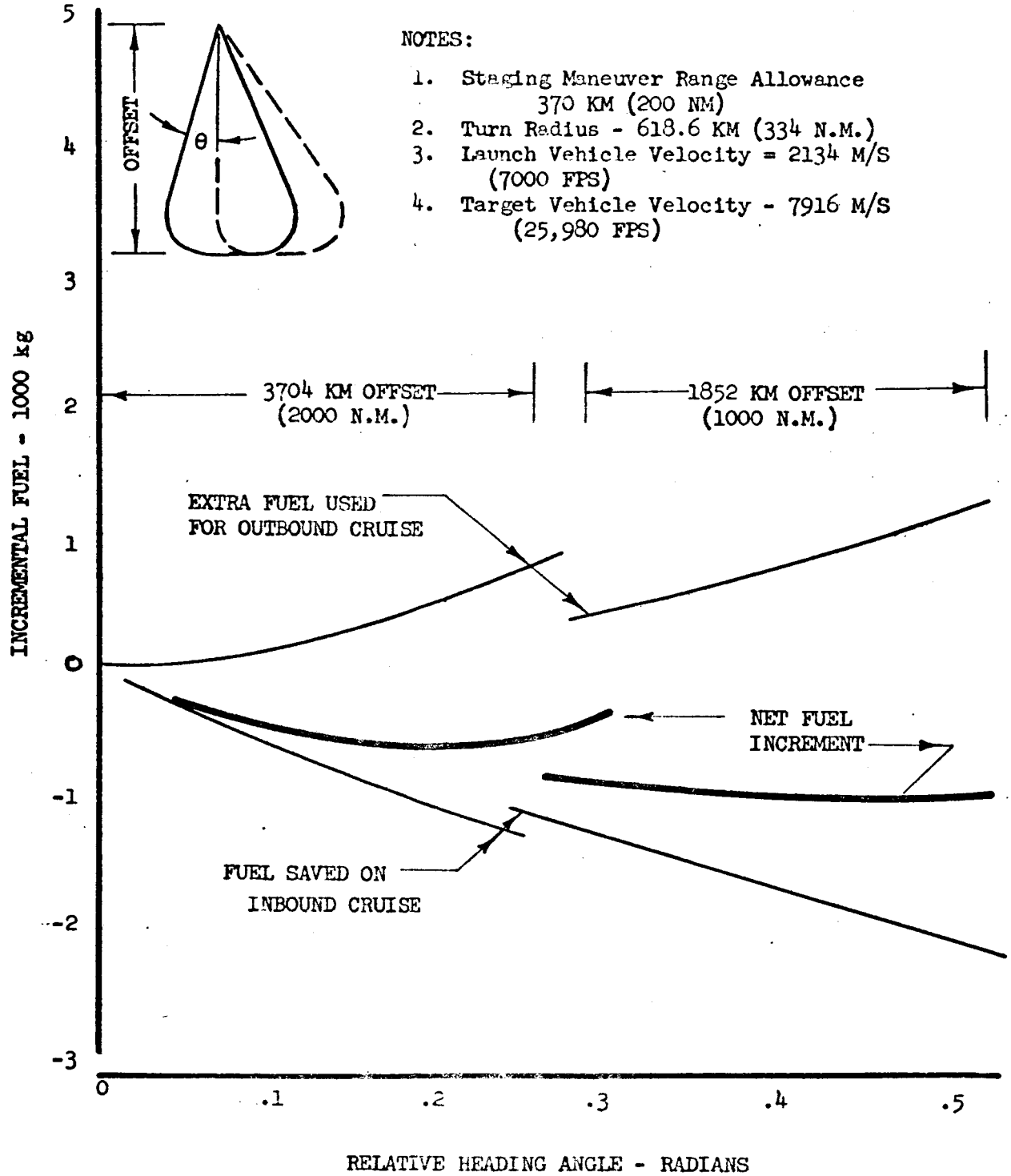

4.4 Post Staging Maneuver

The recovery of the stage 1 vehicle following staging is a difficult problem. In its simplest definition, the trajectory follows a decelerating coast to apogee, then an accelerating descent back to cruise altitude and velocity, where the turn to the return-to-base heading is initiated. This method has been used for the nominal profile. 185 km (100 NM) of ground track range was covered during the recovery. A more efficient means of performing a combination of recovery and turn-to-base is developed in the Phase II trajectory study results.

4.5 Descent and Deceleration

The turn to base and cruise back were performed in a manner similar to the cruise out and turn into the target plane. The descent was flown at maximum lift-to-drag ratio and idle thrust after an initial deceleration to this velocity-altitude profile.

5.0 Stage 2 Ascent to Orbit

Second stage boost commences with separation from the launch vehicle. The velocity, altitude and flight path angle at which staging should occur and the ensuing Stage 2 trajectory have been studied with a fixed stage time steepest-descent computer program.

In the absence of atmospheric effects an efficient means of achieving circular orbit is with a Hohmann transfer orbit; a low perigee altitude for the transfer orbit gives the most efficient operation of the booster. At some altitude, the decrease in velocity losses due to gravity are offset by the increase in velocity losses due to aerodynamic drag. Drag losses can be reduced by inserting in the transfer orbit at a positive flight path angle. In this case the transfer trajectory has a central angle change of less than 180°.

The Stage 1 pullup and Stage 2 ascent to rendezvous were optimized as a unit. The end constraints were defined by a 485 km (262 nautical mile) circular orbit. The initial conditions were Stage 1 level flight conditions at Mach 7 and 24.7 km (81,000 ft). Initially, no inflight constraints were used because it was uncertain which constraints, if any, would apply. The velocity-altitude profile is shown in Figure 1-8.

The unconstrained solution shown in Figure 1-9 indicates the desired transfer orbit insertion conditions are

Velocity = 8,000 M/Sec. (26,190 fps)

Flight Path Angle = 0.64 deg.

Altitude = 74,200 M (243,200 ft.)

These data confirm that the optimum transfer orbit is not exactly a Hohmann transfer.

The unconstrained optimum trajectory showed dynamic pressure at staging to be a problem. Constraint of the dynamic pressure to 9,576 newtons per meter^2 (200 psf) at staging resulted in a payload penalty of 159 kg (350 pounds). This trajectory is shown in Figure 1-10. Rapid changes at the beginning of this trajectory indicate a more efficient maneuver may have resulted if the first stage effects are investigated further. This has been done in the Phase II studies.

Phase I analysis of the effect of increasing the altitude for initiating the first stage pullup indicated a payload penalty would result. Distinct payload advantage has been shown to result from both cruising at high altitude and initiating pullup from lower altitude. Therefore a decreasing altitude turn which would take advantage of the higher cruise altitude and lower staging initiation altitude while shortening the effective cruise range seems to suggest a more efficient operating mode. Further investigation of this interaction was accomplished during Phase II studies.

STAGE 2 FLIGHT PROFILE

Figure 1-8

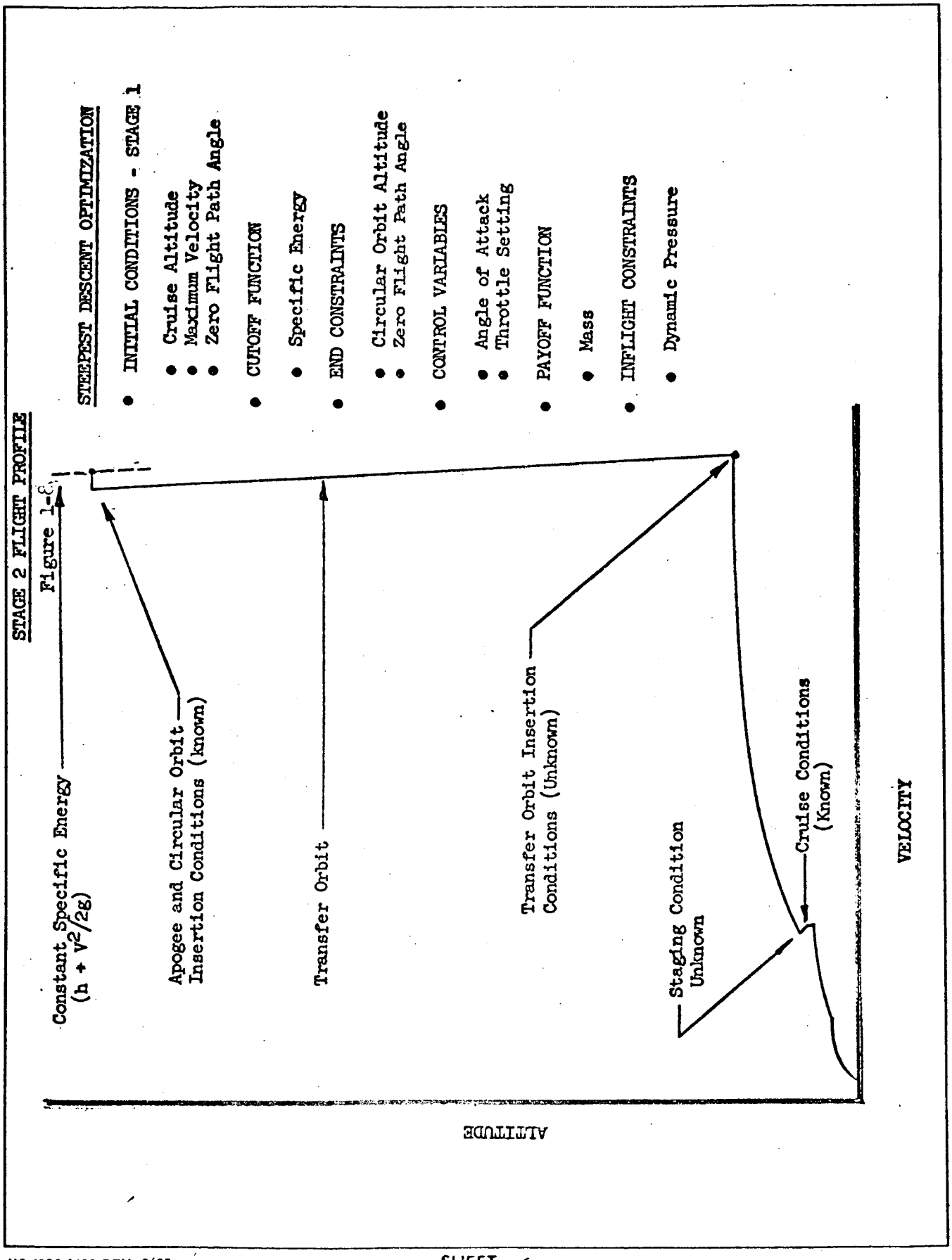

STAGE 2

UNCONSTRAINED OPTIMUM BOOST TRAJECTORY

485 KM (262 N.M.) Circular Orbit

Figure 1-9

No Inflight

Inequality Constraints

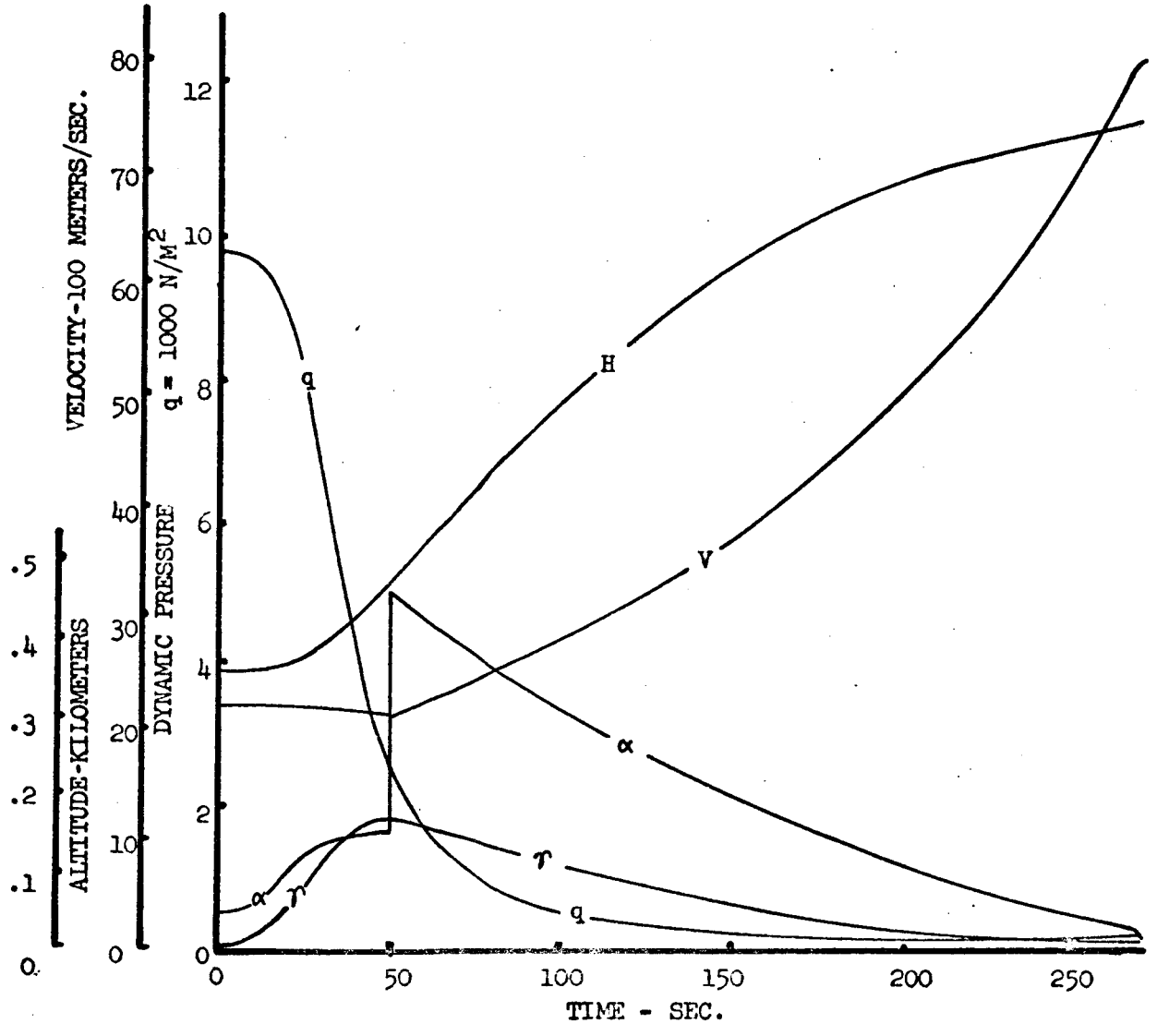

STAGE 2
CONSTRAINED OPTIMUM TRAJECTORY
Dynamic Pressure - 9576 N/M^2 (200 PSF) @ Staging
Figure 1-10
485 KM (262 N.M.) Circular Orbit

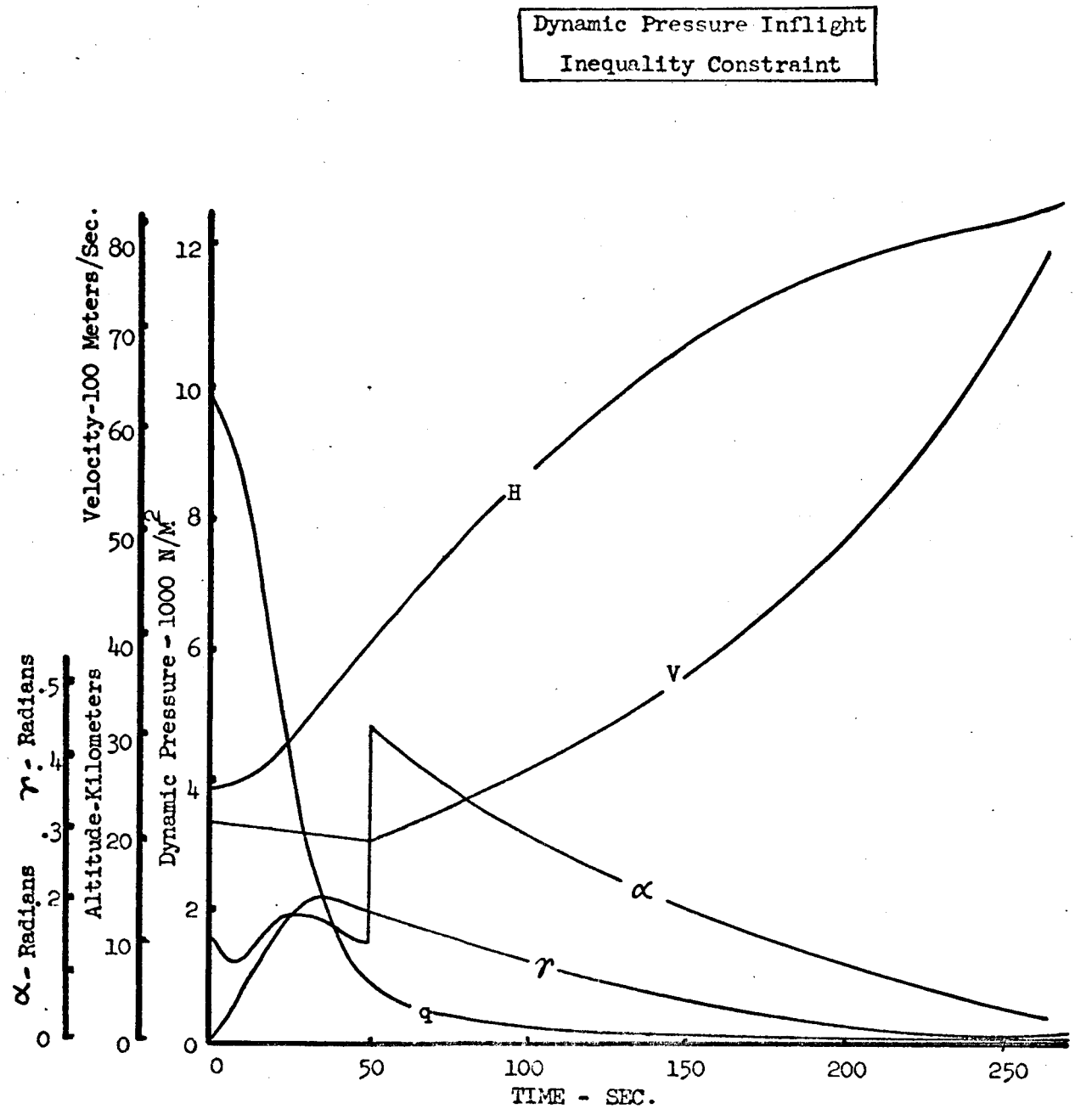

6.0 CONCLUSIONS:

The methods employed in the Phase I trajectory study represent the classical approach to mission analysis. That is, the mission is segmented into subarcs and these subarcs are analyzed in isolation. The analyst then considers trades which hold the most promise for performance gain and selects the most efficient result. The nominal trajectory established by the Stage 1 parametric studies and the Stage 2 partial optimization results were used as the reference for the Phase I navigation-guidance trades reported in Volume 3, D2-113016-6. These results were the starting point for the more complete optimization studies performed in Phase II and reported in the following part of the report.

PART I REFERENCES

1. "Estimated Performance of a Mach 8.0 Hydrogen Fueled Wrap-Around Turboramjet", Pratt & Whitney Aircraft Report TDM-1805, June 3, 1963. (Confidential)

2. Richard H. Peterson, Thomas J. Gregory, and Cynthia L. Smith, "Some Comparisons of Turbojet-Powered Hypersonic Aircraft for Cruise and Boost Missions, "AIAA Paper No. 65-759, Nov. 15-18, 1965, Los Angeles, California, National Aeronautics and Space Administration, Moffett Field, California.

3. Thomas J. Gregory, Richard H. Peterson, and John A. Wyss, "Performance Tradeoffs and Research Problems for Hypersonic Transports, "Journal of Aircraft Vol. 2, No. 4, July-August, 1965.

PART II. TRAJECTORY OPTIMIZATION STUDY RESULTS

1.0 INTRODUCTION

The past decade has seen the accumulation of a wealth of information on the operational and performance characteristics of vertical ascent launch vehicles. A similar background for recoverable launch vehicles having cruise capability has yet to be developed. Recent developments in the field of flight path performance analysis utilizing numerical optimization techniques offer means for rapidly acquiring a similar store of information for these vehicles. This section is devoted to the study of one cruise launch vehicle mission, a 3704 km (2000 NM) offset launch to orbital conditions. The vehicle consists of two stages. The first stage of the hybrid launch system is a lifting turboramjet vehicle capable of horizontal takeoff and hypersonic cruise. The second stage is an expendable rocket.

Flight path analysis of this vehicle presents several unusual problems. The mission involves two distinct sets of terminal constraints. The first stage cruises out to some as yet unspecified point, releases the second stage, and returns to base. Following release the second stage ascends to orbital rendezvous conditions at a prespecified point. The optimization problem is to maximize the orbital payload, while satisfying the above double set of constraints. Atmospheric flight problems of this complexity can be solved only by numerical techniques. The present approach is based upon the steepest descent method, References 1 and 2.

Some insight into the staging problem can be gained by a breakdown of the trajectory into distinct subarcs or segments. For example, one might define an initial acceleration and ascent to cruise conditions, followed by a cruise segment, a turn into the desired orbital plane, and a final pullup maneuver to the staging point. The second stage flight profile can then be determined by the iterative guidance technique, Reference 3, or other appropriate techniques. The Stage I return can be handled by conventional methods. Using such a model, the staging point can be obtained by parametric analysis. An approach of this nature was followed in Phase I of the present study, but does not provide optimum performance.

In Phase II a steepest descent algorithm utilizing simultaneous perturbation of the control histories and the staging point was used to obtain the optimal trajectory. A generalized algorithm of this type is presented in Reference 2. Solutions utilizing this algorithm have previously been reported in Reference 4 for less complicated missions. A computer program embodying this approach was constructed within the framework of the program of Reference 5, and applied to the present mission. The optimal Stage I/Stage II ascent to orbit was determined as a single optimal staging problem, ignoring the Stage I return constraint. The resulting staging conditions were then used for the

Stage I return. This segment was optimized as a single stage problem in isolation from the remainder of the mission. Useful follow-on research would be the development of an optimization program, specifically tailored to the requirements of a multi-vehicle launch system.

The next three sections of this report presents the theory of the steepest-descent methods. Section 2.0 covers optimization of a single stage trajectory. Then, Section 3.0 extends the results to the optimization of a multi-stage trajectory where the location of the staging points is included in the characteristics being optimized. Section 4.0 discusses convergence of the steepest descent method. This theory was originally presented in Reference 2. It has been reproduced here since it is the basis for the trajectory optimization work done in the current study. The reader who does not have the time to review the theory should turn to Section 5.0 on page 52 where the presentation of the trajectory optimization results is started.

2.0 THE STEEPEST DESCENT METHOD FOR A SINGLE STAGE TRAJECTORY

2.1 Problem Statement

The analysis of single stage trajectories by the steepest-descent method has been thoroughly treated in the literature. One of the clearest treatments available is that of Bryson and Denham in Ref. 1. For convenience and as an aid in the understanding of the optimal staging method of the following section, the analysis will be repeated here.

Point mass motion is governed by three second order differential equations of position together with a first order differential equation governing the mass. By suitably defining additional state variables, it is possible to reduce these equations to a set of first order differential equations. We can therefore consider point mass motion to be governed by a set of first order differential equations. The form of these equations is

$$\left\{\dot{x}_n(t)\right\} = \left\{f\left(x_n(t),\ \alpha_m(t),\ t\right)\right\} \qquad 2.1.1$$

$$n = 1,2 \ldots\ldots\ldots N$$
$$m = 1,2 \ldots\ldots\ldots M$$

That is, we have N state variables whose derivatives $\dot{x}_n(t)$, are defined by N first order differential equations involving the state variables, together with M control variables, $\alpha_m(t)$, and t, the independent variable itself.

We may wish to constrain a set of functions of the state variables and time to particular values at the end of the trajectory. In this case a set of constraint functions of the form

$$\left\{\psi_p\right\} = \left\{\psi_p\left(x_n(T),\ T\right)\right\} = 0 \qquad 2.1.2$$

$$p = 1,2 \ldots\ldots\ldots P$$

can be constructed, which our final trajectory must satisfy. Any one of the constraints may be used as a cut-off function which, when satisfied, will terminate a particular trajectory. The cut-off function can therefore be written in the form

$$\Omega = \Omega\left(x_n(T),\ T\right) = 0 \qquad 2.1.3$$

and determines the trajectory termination time T. In all then, when the cut-off function is included, we have P + 1 end constraints.

Finally we may wish to optimize some other function of the state variables and time at the end of the trajectory; hence a pay-off function

$$\phi = \phi\left(x_n(T),\ T\right) \qquad 2.1.4$$

can be constructed, which is to be maximized or minimized.

Now suppose that we have a nominal trajectory available. The requirements of this trajectory are modest; it must of course, satisfy the cut-off condition, Eqn. (2.1.3), but it need not optimize the pay-off function or satisfy the constraint equations. To generate this nominal trajectory by integrating Eqns. (2.1.1) we will need to know the vehicle characteristics, the initial state variable values, and a nominal control variable history. Having obtained a nominal trajectory we are now in a position to apply the steepest descent process. To do this we seek the trajectory showing the greatest improvement in the pay-off function, while at the same time eliminating a given amount of the end point errors as measured by Eqns. (2.1.2), for a given size of control variable perturbation.

Eqns. (2.1.2) provide an end point error measure for they will only be satisfied if the end points have been achieved. Therefore any non-zero ψ_p represents an end point error which must be corrected. As a convenient measure of the control variable perturbation we can define the scalar quantity

$$DP^2 = \int_{t_o}^{T} \left[\delta\alpha(t)\right]\left[W(t)\right]\left\{\delta\alpha(t)\right\} dt \qquad 2.1.5$$

where W is any arbitrary symmetric matrix. In the usual case W is taken equal to the unit matrix and DP^2 then becomes the integrated square of the control variable perturbations, $\delta\alpha(t)$. It might be noted that it is essential, for Eqn. (2.1.5) to have any meaning, that all control variables have the same dimensions. To meet this requirement we will henceforth require the control variables to be non-dimensional.

The constraint on control variable perturbation size represented by Eqn. (2.1.5) is an essential element of the steepest descent process. For we will be seeking the optimum perturbation by a local linearization of the non-linear trajectory equations about the nominal trajectory. To ensure the validity of the linearized approximation, we must limit ourselves to small control variable perturbations by using Eqn. (2.1.5) which provides an integral measure of the local perturbation magnitudes.

2.2 Single Stage Analysis

An outline of the steepest descent process has been given in Section (2.1). To implement this method we must carry out an analysis of all perturbations about the nominal trajectory. In the present report all perturbations will be linearized; that is, we will assume that only first order perturbations in the control and state variables need to be considered. Our task will be completed when the optimum control variable perturbation, in the sense discussed in Section (2.1), has been found.

Let us denote variables on the nominal trajectory by a bar, thusly:

$$\left\{\alpha_m(t)\right\}_{\text{nominal}} = \left\{\bar{\alpha}_m(t)\right\} \qquad 2.2.1$$

and

$$\left\{x_n(t)\right\}_{\text{nominal}} = \left\{\bar{x}_n(t)\right\} \qquad 2.2.2$$

where we have M control variables and N state variables.

Now consider a small perturbation to the control variable history, $\delta\alpha(t)$; this in turn will cause a small perturbation in the state variable history, $\delta x(t)$. The new values of the variables will become

$$\left\{\alpha(t)\right\} = \left\{\bar{\alpha}(t)\right\} + \left\{\delta\alpha(t)\right\} \qquad 2.2.3$$

and

$$\left\{x(t)\right\} = \left\{\bar{x}(t)\right\} + \left\{\delta x(t)\right\} \qquad 2.2.4$$

We can also write the nominal state variable and perturbed state variable histories as

$$\left\{\bar{x}(t)\right\} = \left\{x(t_o)\right\} + \int_{t_o}^{t} \left\{f\left(\bar{x}\,(t),\ \bar{\alpha}\,(t),\ t\right)\right\} dt \qquad 2.2.5$$

$$\left\{x(t)\right\} = \left\{x(t_o)\right\} + \int_{t_o}^{t} \left\{f\left(\bar{x} + \delta x,\ \bar{\alpha} + \delta\alpha,\ t\right)\right\} dt \qquad 2.2.6$$

Subtracting Eqn. (2.2.5) from Eqn. (2.2.6) and using Taylor's expansion to first order,

$$\left\{x(t)\right\} - \left\{\bar{x}(t)\right\} = \int_{t_o}^{t} \left\{\frac{\partial \bar{f}}{\partial x_n} \cdot \delta x^n + \frac{\partial \bar{f}}{\partial \alpha_m} \cdot \delta\alpha^m\right\} dt = \left\{\delta x(t)\right\} \qquad 2.2.7$$

where:

$$\bar{f} = f\left(\bar{x}(t),\ \bar{\alpha}\,(t),\ t\right) \qquad 2.2.8$$

and where the repeated index indicates a summation over all possible values. Differentiation leads to

$$\frac{d}{dt}\left\{\delta x(t)\right\} = \left\{\frac{\partial \bar{f}}{\partial x_n}\ \delta x^n + \frac{\partial \bar{f}}{\partial \alpha_m}\ \delta\alpha^m\right\} \qquad 2.2.9a$$

or in matrix form

$$\frac{d}{dt}\left\{\delta x(t)\right\} = \left[F\right]\left\{\delta x\right\} + \left[G\right]\left\{\delta\alpha\right\} \qquad 2.2.9b$$

where:

$$F_{ij} = \frac{\partial \bar{f}_i}{\partial x_j} \text{ and } G_{ij} = \frac{\partial \bar{f}_i}{\partial \alpha_j} \qquad 2.2.10$$

Here the $(i,j)^{th}$ element lies in the i^{th} row and j^{th} column of the matrices; F is an N x N matrix and G is an N x P matrix.

We must now find the effect of these perturbations on the pay-off, cut-off and constraint functions. A general way of obtaining these effects, known as the 'adjoint method', Ref. 2, is to define a new set of variables by the equations

$$\left[\dot{\lambda}(t)\right] = -\left[F(t)\right]'\left[\lambda(t)\right] \qquad 2.2.11$$

By specifying various boundary conditions on the λ, the changes in all functions of interest can be found in turn. To show this we commence by pre-multiplying Eqn. (2.2.9b) by λ' and Eqn. (2.2.11) by $\delta x'$, transpose the second of these equations and sum with the first, giving

$$\left[\lambda\right]'\cdot\left\{\frac{d}{dt}(\delta x)\right\} + \left[\dot{\lambda}\right]'\left\{\delta x\right\} = \left[\lambda\right]'\left[F\right]\left\{\delta x\right\} + \left[\lambda\right]'\left[G\right]\left\{\delta\alpha\right\} - \left[\lambda\right]'\left[F\right]\left\{\delta x\right\} \qquad 2.2.12$$

which may be written as

$$\left\{\frac{d}{dt}\left(\lambda'\delta x\right)\right\} = \left[\lambda\right]'\left[G\right]\left\{\delta\alpha\right\} \qquad 2.2.13$$

Integrating Eqn. (2.2.13) over the trajectory we obtain

$$\left\{\lambda'\delta x\right\}_T - \left\{\lambda'\delta x\right\}_{t_o} = \int_{t_o}^{T}\left[\lambda\right]'\left[G\right]\left\{\delta\alpha\right\}dt \qquad 2.2.14$$

We will now define three distinct sets of λ functions by applying the following boundary conditions at t = T:

$$\left\{\lambda(T)\right\} = \left\{\frac{\partial\phi}{\partial x_i}\right\}_T = \left\{\lambda_\phi(T)\right\} \qquad 2.2.15a$$

$$\left\{\lambda(T)\right\} = \left\{\frac{\partial\Omega}{\partial x_i}\right\}_T = \left\{\lambda_\Omega(T)\right\} \qquad 2.2.15b$$

$$\left[\lambda(T)\right] = \left[\frac{\partial\psi_j}{\partial x_i}\right]_T = \left[\lambda_\psi(T)\right] \qquad 2.2.15c$$

We may directly integrate Eqn. (2.2.11) in a reverse direction (i.e., from T to t_o) to obtain the functions, $\{\lambda_\phi(t)\}$, $\{\lambda_\Omega(t)\}$ and $[\lambda_\psi(t)]$.

Substituting each of these functions into Eqn. (2.2.14) in turn and noting that

$$\left[\lambda_\phi(T)\right]\left\{\delta x\right\} = \left[\frac{\partial \phi}{\partial x}\right]\left\{\delta x\right\} = \delta\phi_{t=T} \qquad 2.2.16a$$

$$\left[\lambda_\Omega(T)\right]\left\{\delta x\right\} = \left[\frac{\partial \Omega}{\partial x}\right]\left\{\delta x\right\} = \delta\Omega_{t=T} \qquad 2.2.16b$$

$$\left[\lambda_\psi(T)\right]'\left\{\delta x\right\} = \left[\frac{\partial \psi_i}{\partial x_j}\right]\left\{\delta x\right\} = \left\{\delta\psi_{t=T}\right\} \qquad 2.2.16c$$

we obtain

$$\delta\phi_{t=T} = \int_{t_o}^{T}\left[\lambda_\phi\right]\left[G\right]\left\{\delta\alpha\right\}dt + \left[\lambda_\phi(t_o)\right]\left\{\delta x(t_o)\right\} \qquad 2.2.17a$$

$$\delta\Omega_{t=T} = \int_{t_o}^{T}\left[\lambda_\Omega\right]\left[G\right]\left\{\delta\alpha\right\}dt + \left[\lambda_\Omega(t_o)\right]\left\{\delta x(t_o)\right\} \qquad 2.2.17b$$

$$\left\{\delta\psi\right\}_{t=T} = \int_{t_o}^{T}\left[\lambda_\psi\right]'\left[G\right]\left\{\delta\alpha\right\}dt + \left[\lambda_\psi(t_o)\right]'\left\{\delta x(t_o)\right\} \qquad 2.2.17c$$

Now, Eqns. (2.2.17) would give us the changes in the pay-off function, cut-off function and constraint functions, if they were measured at the terminal time of the nominal trajectory; however, on the perturbed trajectory the cut-off will usually occur at some perturbed time, T + ΔT. In this case the total change in the above quantities will become

$$d\phi = \int_{t_o}^{T}\left[\lambda_\phi\right]\left[G\right]\left\{\delta\alpha\right\}dt + \left[\lambda_\phi(t_o)\right]\left\{\delta x(t_o)\right\} + \dot\phi(T)\,\Delta T \qquad 2.2.18a$$

$$d\Omega = \int_{t_o}^{T}\left[\lambda_\Omega\right]\left[G\right]\left\{\delta\alpha\right\}dt + \left[\lambda_\Omega(t_o)\right]\left\{\delta x(t_o)\right\} + \dot\Omega(T)\,\Delta T \qquad 2.2.18b$$

$$\left\{d\psi\right\} = \int_{t_o}^{T}\left[\lambda_\psi\right]'\left[G\right]\left\{\delta\alpha\right\}dt + \left[\lambda_\psi(t_o)\right]'\left\{\delta x(t_o)\right\} + \left\{\dot\psi(T)\right\}\Delta T \qquad 2.2.18c$$

Eqns. (2.2.18) give us the changes in pay-off, cut-off and constraint functions on the perturbed trajectory.

We can eliminate the time perturbation in Eqns. (2.2.18a) and (2.2.18c) by noting that, by definition of the cut-off function, Eqn. (2.2.18b) must be zero.

$$\therefore \Delta T = -\frac{1}{\dot\Omega(T)}\left(\int_{t_o}^{T}\left[\lambda_\Omega\right]\left[G\right]\left\{\delta\alpha\right\}dt + \left[\lambda_\Omega(t_o)\right]\left\{\delta x(t_o)\right\}\right) \qquad 2.2.19$$

Substituting Eqn. (2.2.19) into Eqns. (2.2.18a) and (2.2.18c) results in

$$d\phi = \int_{t_o}^{T} \left[\lambda_{\phi\Omega}\right]\left[G\right]\left\{\delta\alpha\right\}dt + \left[\lambda_{\phi\Omega}(t_o)\right]\left\{\delta x(t_o)\right\} \qquad 2.2.20a$$

$$\left\{d\psi\right\} = \int_{t_o}^{T} \left[\lambda_{\psi\Omega}\right]' \left[G\right]\left\{\delta\alpha\right\} dt + \left[\lambda_{\psi\Omega}(t_o)\right]' \left\{\delta x(t_o)\right\} \qquad 2.2.20b$$

where:

$$\left\{\lambda_{\phi\Omega}\right\} = \left\{\lambda_{\phi}\right\} - \frac{\dot{\phi}(T)}{\dot{\Omega}(T)}\left\{\lambda_{\Omega}\right\} \qquad 2.2.21a$$

$$\left[\lambda_{\psi\Omega}\right]' = \left[\lambda_{\psi}\right]' - \frac{\left\{\dot{\psi}(T)\right\}\left|\lambda_{\Omega}\right|}{\dot{\Omega}(T)} \qquad 2.2.21b$$

Eqns. (2.2.20) reveal the significance of the λ functions, originally defined by Eqns. (2.2.11) and (2.2.15). At time t_o, $\lambda_{\phi\Omega}$ gives the sensitivity of $\phi(T)$ to small perturbations in the state variables at t_o. Similarly, $\lambda_{\phi\Omega}(t)$ measures the sensitivity of $\phi(T)$ to small perturbations in the state variables at any time t. The sensitivity of the constraints $d\psi$ to small state variable perturbations at any time is likewise defined by each row of the function $\lambda_{\psi\Omega}(t)$.

A measure of the sensitivity of a trajectory to α perturbations can be obtained from the quantities $\lambda_{\phi\Omega}'G$ and $\lambda_{\psi\Omega}'G$. Suppose we have a pulse type of α perturbation at time t', that is $\delta(t-t')$, where δ is the Dirac delta function. With this type of control variable perturbation, it can be seen from Eqns. (2.2.20) that the changes on the pay-off and constraint functions will be $\lambda_{\phi\Omega}(t')' \cdot G(t')$ and $\lambda_{\psi\Omega}(t')' \cdot G(t')$, respectively, for fixed initial conditions.

In order to apply the steepest-descent process to our problem, we must maximize the ϕ change, Eqn. (2.2.20a); subject to a specified change in the constraints, Eqn. (2.2.20b); and a given size of perturbation to the control variables, Eqn. (2.1.5). This can be achieved by constructing an augmented function in the manner of Lagrange and maximizing this instead of $d\phi$. For our problem the augmented function is

$$U = \int_{t_o}^{T} \left[\lambda_{\phi\Omega}\right]\left[G\right]\left\{\delta\alpha\right\} dt + \left[\lambda_{\phi\Omega}(t_o)\right]\left\{\delta x(t_o)\right\}$$

$$+\left[\upsilon\right]\left\{\int_{t_o}^{T} \left[\lambda_{\psi\Omega}\right]'\left[G\right]\left\{\delta\alpha\right\} dt + \left[\lambda_{\psi\Omega}(t_o)\right]' \left\{\delta x(t_o)\right\}\right\}$$

$$+\mu \int_{t_o}^{T} \left[\delta\alpha\right]\left[W\right]\left\{\delta\alpha\right\} dt \qquad 2.2.22$$

where the ν are P undetermined Lagrangian multipliers and μ is a single undetermined Lagrangian multiplier. We wish to find that variation of the control variable history which will maximize U.

Suppose we take a variation of $\delta\alpha$, that is a $\delta(\delta\alpha)$. Then we can always write any $\delta\alpha$ distribution in the form

$$\left\{\delta\alpha\right\} = \left\{A(t)\right\} k, \text{ or } \left\lfloor\delta\alpha\right\rfloor = \left\lfloor A(t)\right\rfloor k \qquad 2.2.23$$

where A(t) prescribes the perturbation shape and k its magnitude. We can write that part of Eqn. (2.2.22) which depends on $\delta\alpha$, the perturbation in the control variable, in the form.

$$\bar{U} = k\int_{t_o}^{T}\left\lfloor\lambda_{\phi\Omega}\right\rfloor\left[G\right]\left\{A(t)\right\}dt + k\left\lfloor\nu\right\rfloor\int_{t_o}^{T}\left[\lambda_{\psi\Omega}\right]'\left[G\right]\left\{A(t)\right\}dt$$

$$+ k^2\mu\int_{t_o}^{T}\left\lfloor A(t)\right\rfloor\left[W\right]\left\{A(t)\right\}dt \qquad 2.2.24$$

Now

$$\frac{\partial\bar{U}}{\partial k} = \int_{t_o}^{T}\left\lfloor\lambda_{\phi\Omega}\right\rfloor\left[G\right]\left\{A(t)\right\}dt + \left\lfloor\nu\right\rfloor\int_{t_o}^{T}\left[\lambda_{\psi\Omega}\right]'\left[G\right]\left\{A(t)\right\}dt$$

$$+ 2k\mu\int_{t_o}^{T}\left\lfloor A(t)\right\rfloor\left[W\right]\left\{A(t)\right\}dt \qquad 2.2.25$$

or

$$\delta\bar{U} = \int_{t_o}^{T}\Big(\left\lfloor\lambda_{\phi\Omega}\right\rfloor\left[G\right]\left\{\delta k\cdot A(t)\right\} + \left\lfloor\nu\right\rfloor\left[\lambda_{\psi\Omega}\right]'\left[G\right]\left\{\delta k\cdot A(t)\right\}$$

$$+ 2\mu\left\lfloor k\cdot A(t)\right\rfloor\left[W\right]\left\{\delta k\cdot A(t)\right\}\Big)dt$$

$$= \int_{t_o}^{T}\left(\left\lfloor\lambda_{\phi\Omega}\right\rfloor\left[G\right] + \left\lfloor\nu\right\rfloor\left[\lambda_{\psi\Omega}\right]'\left[G\right] + 2\mu\left\lfloor\delta\alpha\right\rfloor\left[W\right]\right)\left\{\delta(\delta\alpha)\right\}dt \qquad 2.2.26$$

where we have noted from Eqn. (2.2.23) that

$$\delta(\delta\alpha) = A(t)\,\delta k \qquad 2.2.27$$

Now as Eqn. (2.2.26) holds for any A(t), it follows that it is a general relationship. Further for $\bar{U}$ to be an extremal, $\delta\bar{U}$ must be zero.

If we have maximized $\bar{U}$ by means of a control variable perturbation $\delta\alpha$, $\delta\bar{U}$ must be stationary for all small perturbations to the $\delta\alpha$, that is for all $\delta(\delta\alpha)$. The only way in which Eqn. (2.2.26) can be zero for all $\delta(\delta\alpha)$ is for the coefficient of $\delta(\delta\alpha)$ to be identically zero. That this last statement is true follows from considering the case where, over some finite time interval between t_o and T, the coefficient of $\delta(\delta\alpha)$ is, say, positive. If this were the case we could choose a $\delta(\delta\alpha)$ distribution that was also positive in this same interval and zero elsewhere between t_o and T. It would follow that $\delta\bar{U}$ was also positive and hence $\bar{U}$ could not be maximum. A similar argument holds when $\delta(\delta\alpha)$ is negative over any interval in t_o to T. Hence the coefficient of $\delta(\delta\alpha)$ must be identically zero in the whole interval $t_o \leq t \leq T$. Thus, we can write

$$\left[\left[\lambda_{\phi\Omega}\right] + \left[\nu\right]\left[\lambda_{\psi\Omega}\right]'\right]\left[G\right] = -2\mu\left[\delta\alpha\right]\left[W\right] \qquad 2.2.28$$

Transposing, noting that W is symmetric, and solving for $\delta\alpha$, we obtain

$$\left\{\delta\alpha\right\} = -\frac{1}{2\mu}\left[W\right]^{-1}\left[G\right]'\left\{\left\{\lambda_{\phi\Omega}\right\} + \left[\lambda_{\psi\Omega}\right]\left\{\nu\right\}\right\} \qquad 2.2.29$$

Substituting Eqn. (2.2.29) into Eqn. (2.2.20b) gives

$$\left\{d\beta\right\} = -\frac{1}{2\mu}\left\{\left\{I_{\psi\phi}\right\} + \left[I_{\psi\psi}\right]\left\{\nu\right\}\right\} \qquad 2.2.30a$$

where

$$\left\{d\beta\right\} = \left\{d\psi\right\} - \left[\lambda_{\psi\Omega}(t_o)\right]'\left\{\delta x(t_o)\right\} \qquad 2.2.30b$$

and

$$\left[I_{\psi\psi}\right] = \int_{t_o}^{T}\left[\lambda_{\psi\Omega}\right]'\left[G\right]\left[W\right]^{-1}\left[G\right]'\left[\lambda_{\psi\Omega}\right]dt \qquad 2.2.31a$$

$$\left\{I_{\psi\phi}\right\} = \int_{t_o}^{T}\left[\lambda_{\psi\Omega}\right]'\left[G\right]\left[W\right]^{-1}\left[G\right]'\left\{\lambda_{\phi\Omega}\right\}dt \qquad 2.2.31b$$

For subsequent use we will also define

$$I_{\phi\phi} = \int_{t_o}^{T}\left[\lambda_{\phi\Omega}\right]\left[G\right]\left[W\right]^{-1}\left[G\right]'\left\{\lambda_{\phi\Omega}\right\}dt \qquad 2.2.31c$$

We can express ν in terms of μ from Eqn. (2.2.30a):

$$\left\{\nu\right\} = -\left[I_{\psi\psi}\right]^{-1}\left\{2\mu\left\{d\beta\right\} + \left\{I_{\psi\phi}\right\}\right\} \qquad 2.2.32$$

Substituting Eqn. (2.2.29) into Eqn. (2.1.5) we obtain

$$DP^2 = \frac{1}{4\mu^2}\left(I_{\phi\phi} + \left[I_{\psi\phi}\right]\left\{\nu\right\} + \left[\nu\right]\left\{I_{\psi\phi}\right\} + \left[\nu\right]\left[I_{\psi\psi}\right]\left\{\nu\right\}\right) \qquad 2.2.33$$

Transposing the second term in the right hand side bracket, we obtain

$$DP^2 = \frac{1}{4\mu^2}\left(I_{\phi\phi} + 2\left[\nu\right]\left\{I_{\psi\phi}\right\} + \left[\nu\right]\left[I_{\psi\psi}\right]\left\{\nu\right\}\right) \qquad 2.2.34$$

Substituting Eqn. (2.2.32) in Eqn. (2.2.34), and noting that $\left[I_{\psi\psi}\right]^{-1}$ is symmetrical, gives

$$4\mu^2\, DP^2 = I_{\phi\phi} - \left[I_{\psi\phi}\right]\left[I_{\psi\psi}\right]^{-1}\left\{I_{\psi\phi}\right\} + 4\mu^2\left[d\beta\right]\left[I_{\psi\psi}\right]^{-1}\left\{d\beta\right\} \qquad 2.2.35$$

So that

$$2\mu = \pm\sqrt{\frac{I_{\phi\phi} - \left[I_{\psi\phi}\right]\left[I_{\psi\psi}\right]^{-1}\left\{I_{\psi\phi}\right\}}{DP^2 - \left[d\beta\right]\left[I_{\psi\psi}\right]^{-1}\left\{d\beta\right\}}} \qquad 2.2.36$$

Substituting Eqn. (2.2.36) into Eqn. (2.2.32) we obtain the remaining Lagrangian multipliers in the form

$$\left\{\nu\right\} = -\left[I_{\psi\psi}\right]^{-1}\left\{\left\{I_{\psi\phi}\right\} \pm \sqrt{\frac{I_{\phi\phi} - \left[I_{\psi\phi}\right]\left[I_{\psi\psi}\right]^{-1}\left\{I_{\psi\phi}\right\}}{DP^2 - \left[d\beta\right]\left[I_{\psi\psi}\right]^{-1}\left\{d\beta\right\}}}\left\{d\beta\right\}\right\} \qquad 2.2.37$$

The optimum control perturbation is found by substituting Eqns. (2.2.36) and (2.2.37) back into Eqn. (2.2.29) and is

$$\left\{\delta\alpha\right\} = \mp\left[W\right]^{-1}\left[G\right]'\left\{\left\{\lambda_{\phi\Omega}\right\} - \left[\lambda_{\psi\Omega}\right]\left[I_{\psi\psi}\right]^{-1}\left\{I_{\psi\phi}\right\}\right\} \times \sqrt{\frac{DP^2 - \left[d\beta\right]\left[I_{\psi\psi}\right]^{-1}\left\{d\beta\right\}}{I_{\phi\phi} - \left[I_{\psi\phi}\right]\left[I_{\psi\psi}\right]^{-1}\left\{I_{\psi\phi}\right\}}} + \left[W\right]^{-1}\left[G\right]'\left[\lambda_{\psi\Omega}\right]\left[I_{\psi\psi}\right]^{-1}\left\{d\beta\right\} \qquad 2.2.38$$

With this equation we have achieved our object. Perturbing the control variables according to Eqn. (2.2.38) will give us the optimum change in the trajectory as discussed in Section (2.1), with the added effect of changes in the initial value of the state variables included through the term in $d\beta$. We can determine the appropriate sign to use on the first term of Eqn. (2.2.38) by evaluating $d\phi$. Substituting the optimum α perturbation into Eqn. (2.2.20a) results in

$$d\phi = \pm\sqrt{\left(I_{\phi\phi} - \left[I_{\psi\phi}\right]\left[I_{\psi\psi}\right]^{-1}\left\{I_{\psi\phi}\right\}\right)\left(DP^2 - \left[d\beta\right]\left[I_{\psi\psi}\right]^{-1}\left\{d\beta\right\}\right)}$$
$$+ \left[I_{\psi\phi}\right]\left[I_{\psi\psi}\right]^{-1}\left\{d\beta\right\} + \left[\lambda_{\phi\Omega}(t_o)\right]\left\{\delta x(t_o)\right\} \qquad 2.2.39$$

As the quantity in the radical must be positive to assure that the change in ϕ is real, we see that the negative sign must be taken when minimizing the payoff function and the positive sign when maximizing the payoff function.

3.0 OPTIMIZATION OF A MULTI-STAGE TRAJECTORY

3.1 Introduction

It is not unusual to encounter trajectories in which some of the state variables, or state variable derivatives, have a discontinuity for some value, t', of the independent variable, t. Such a point will be called a stage point, and we shall say that the portion of a trajectory preceding a stage point is in a different "stage" to that following the stage point. The first stage will be that portion of a trajectory lying between t_0 and the first stage point; the s^{th} stage will be that portion of the trajectory lying between the $(s-1)^{th}$ and s^{th} stage points. The final stage will be that portion of the trajectory lying between the last stage point and the final cut-off time.

It will be convenient in the analysis of this section to define a new independent variable to replace t. This new independent variable, the stage time τ, will be defined separately for each stage in the following manner. Let the s^{th} stage commence at time t'_{s-1} and terminate at time t'_s. Then,

$$\tau_s = t - t'_{s-1} \qquad 3.1.1$$

so that when

$$t = t'_{s-1}, \quad \tau_s = 0 \qquad 3.1.2$$

The termination of the s^{th} stage will be determined by some cut-off function Ω_s, assumed to be of the form

$$\Omega_s = \Omega_s\Big(x(T_s),\, T_s \Big) = 0 \qquad 3.1.3$$

where T_s is the stage time at cut-off.

The analysis of Section (2) no longer holds for a staged trajectory, unless the stage points are determined by cut-off functions of the form

$$\Omega_s(T_s) = 0 \qquad 3.1.4$$

That is, the stages are of fixed length in the independent variable.

For suppose the nominal trajectory has an s^{th} stage lying in the region

$$t'_{s-1} \leq t \leq t'_s \qquad 3.1.5$$

Then on the perturbed trajectory, unless the s^{th} stage and the $(s-1)^{th}$ stage are terminated in the manner of Eqn. (3.1.4), the s^{th} stage will occupy the region

$$t'_{s-1} + \Delta t'_{s-1} \leq t \leq t'_s + \Delta t'_s \qquad 3.1.6$$

by virtue of the perturbations in the state variables. This, in turn, will mean that our estimates of the optimum α-perturbation together with the corresponding payoff and constraint function changes, will be in error due to the fact that the F and G matrices are incorrect in the regions between

$$(t'_{s-1},\ t'_{s-1} + \Delta t'_{s-1})$$

and

$$(\tau'_s,\ t'_s + \Delta t'_s)$$

In such a situation, a new factor enters the optimization problem, for it may be that we can exert some control over the position of all or some of the stage points. In this case, we seek to find, not just the optimum control variable perturbation, but rather the optimum combination of control variable and stage point perturbations, when considered simultaneously. Our objective in the following section will be to obtain this optimum combined perturbation.

3.2 Changes in Payoff and Constraint Functions in Combined Perturbation

Given a nominal multi-stage trajectory, suppose we simultaneously perturb the control variable histories and the stage point positions, throughout the whole trajectory. Considering the first stage, the effect of this combined perturbation, when the stage terminates, will appear as some modification in the state variables values. This perturbation in the first stage final state variable values may be looked upon as a perturbation in the initial state variable values to the second stage. The combined effect of stage point, control variables, and initial state variable perturbations in the second stage, will be to produce a perturbation in the state variable values at the second stage termination, and we may proceed in like manner until the last stage is reached.

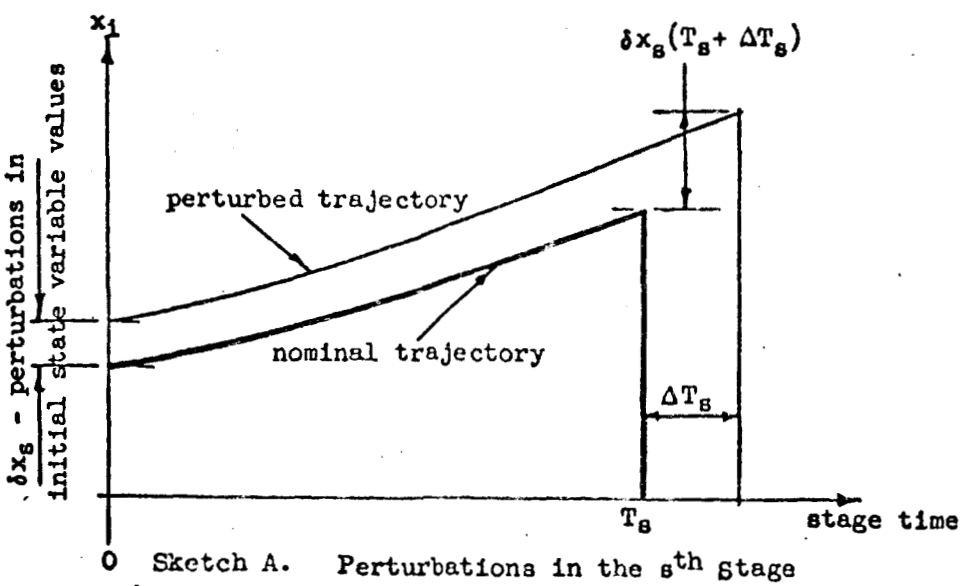

Sketch A. Perturbations in the s^{th} Stage

Consider now, the last stage. The result of the trajectory perturbations ahead of it will appear solely as an initial state variable perturbation. We can therefore find the optimum combined perturbation along the whole trajectory by optimizing the last stage with initial state variable perturbations which are a function of the previous stage perturbations.

We commence this task by considering the s^{th} stage on the perturbed trajectory. As noted above, the effect of perturbations in all the stages preceding the s^{th} will appear as some perturbation in the initial state variable values to the s^{th} stage, say δx_s. Suppose the s^{th} stage is terminated on the nominal trajectory by some function of the form

$$\Omega_s = \Omega_s\Big(x(T_s),\ T_s\Big) = 0 \qquad 3.2.1$$

Then, provided we use the stage time τ_s as the independent variable instead of t, we can find the change in any function of the state variables and τ_s when cut-off is terminated by Eqn. 3.1.3, using the analysis of Section 2. For, analogously to Eqn. 2.2.18c, we can write

$$\Big\{\delta\Psi(T_s)\Big\} = \int_0^{T_s} \Big[\lambda_{\Psi\Omega_s}\Big]' \Big[G\Big] \Big\{\delta\alpha\Big\} d\tau_s + \Big[\lambda_{\Psi\Omega_s}(0)\Big]' \Big\{\delta x_s(0)\Big\} \qquad 3.2.2$$

where Ψ_s is any function of the form

$$\Big\{\dot{\Psi}_s\Big\} = \Big\{\dot{\Psi}_s\Big(x(T_s),\ T_s\Big)\Big\} \qquad 3.2.3$$

and

$$\Big[\lambda_{\Psi\Omega_s}\Big] = \Big[\lambda_{\Psi_s}\Big] - \Big\{\lambda_{\Omega_s}\Big\} \frac{\Big[\dot{\Psi}_s(T_s)\Big]}{\dot{\Omega}_s(T_s)} \qquad 3.2.4$$

Here λ_{Ψ_s} and λ_{Ω_s} are obtained by integrating the adjoint equations in stage time, through the s^{th} stage, subject to the boundary conditions

$$\Big[\lambda_{\Psi_s}(T_s)\Big] = \left[\frac{\partial \Psi_s}{\partial x_j}\right]' \qquad 3.2.5$$

$$\Big\{\lambda_{\Omega_s}(T_s)\Big\} = \left\{\frac{\partial \Omega_s}{\partial x_j}\right\} \qquad 3.2.6$$

So far, the cut-off function has not been perturbed; this can be achieved by terminating the trajectory when

$$\Omega_s + \Delta\Omega_s = 0$$

instead of by Eqn. (3.1.3). Perturbing the cut-off function will cause a change in the trajectory stage time at cut-off which will be given by,

$$\Delta T_s = \frac{\Delta \Omega_s}{\dot{\Omega}_s(T_s)} \qquad 3.2.7$$

The total change in Ψ_s at the termination of the s^{th} stage will then be given by

$$\left\{\delta\Psi_s(T_s + \Delta T_s)\right\} = \int_0^{T_s} \left[\lambda\Psi\Omega_s\right]' \left[G\right]\left\{\delta\alpha\right\} d\tau_s + \left[\lambda\Psi\Omega_s(0)\right]' \left\{\delta x_s(0)\right\} + \left\{\dot{\Psi}_s(T_s)\right\} \Delta T_s \qquad 3.2.8$$

Suppose we choose the state variables as Ψ_s, so that

$$\left\{\Psi_s\right\} = \left\{x(T_s)\right\} \qquad 3.2.9$$

With this choice of Ψ_s, Eqn. (3.2.4) becomes

$$\left[\lambda\Psi_s(T_s)\right] = \left[\frac{\partial x_i}{\partial x_j}\right]' = \left[I\right] \qquad 3.2.10$$

where I is the unit matrix. Denoting the $\lambda\Psi_s$ resulting from this particular choice of boundary conditions by λ_{x_s}, we obtain from Eqn. (3.2.8), the relationship for the change in the state variables at the termination of the s^{th} stage as:

$$\left\{\delta x_s(T_s + \Delta T_s)\right\} = \int_0^{T_s} \left[\lambda_{x\Omega_s}\right]' \left[G\right]\left\{\delta\alpha\right\} d\tau_s + \left[\lambda_{x\Omega_s}(0)\right]' \left\{\delta x_s(0)\right\} + \left\{\dot{x}(T_s)\right\}\Delta T_s \qquad 3.2.11$$

These perturbations are the state variable changes to the left of the s+1 stage point.

The δx to the right of a stage point, $\delta x^{(+)}$, are not necessarily equal to those on the left, $\delta x^{(-)}$, but we can usually define a matrix P_s which will transform the left-hand perturbation into the right hand ones.

$$\left\{\delta x_{s+1}^{(+)}\right\} = \left[P_s\right]\left\{\delta x_{s+1}^{(-)}\right\} = \left[P_s\right]\left\{\delta x_s(T_s + \Delta T_s)\right\} \qquad 3.2.12$$

Typically, for example, consider the case of a multi-stage boost vehicle with a fixed amount of fuel in each stage. The mass of the remaining portions of the vehicle at the commencement of the s^{th} stage

is the sum of the empty weights of the remaining stages, together with the sum of the fuel contained in those stages. Perturbations in mass at the termination of the $(s-1)^{th}$ stage reflect changes in the burning time of that stage. It will usually be physically impossible to transfer any fuel remaining in the $(s-1)^{th}$ stage across the interface with the s^{th} stage and hence changes in the state variable of mass to the left of the stage point may fail to cause a corresponding change to the right of the stage point. In such a case, the P matrix will have a null row for that particular state variable. On the other hand, changes in the state variables of position to the left of a stage point will always appear directly as changes to the right of a stage point. The corresponding row in the P matrix will have unity on the diagonal element and zero elsewhere. This is also true of the state variables of velocity, provided impulsive forces are absent at the stage point.

Substituting Eqn. (3.2.11) into Eqn. (3.2.12), we obtain

$$\left\{\delta x_{s+1}\right\} = \left[P_s\right]\left\{\int_0^{T_s}\left[\lambda_{x\Omega_s}\right]'\left[G\right]\left\{\delta\alpha\right\}d\tau_s + \left[\lambda_{x\Omega_s}(0)\right]'\left\{\delta x_s(0)\right\} + \left\{\dot{x}(T_s)\right\}\Delta T_s\right\}$$

$$= \left[P_s\right]\left\{\left\{K_s\right\} + \left[\bar{\lambda}_{x\Omega_s}\right]'\left\{\delta x_s(0)\right\} + \left\{\bar{\dot{x}}_s\right\}\Delta T_s\right\} \qquad 3.2.13$$

where

$$\left\{K_s\right\} = \int_0^{T_s}\left[\lambda_{x\Omega_s}\right]'\left[G\right]\left\{\delta\alpha\right\}d\tau_s \qquad 3.2.14$$

$$\left[\bar{\lambda}_{x\Omega_s}\right] = \left[\lambda_{x\Omega_s}(0)\right] \qquad 3.2.15$$

and

$$\left\{\bar{\dot{x}}_s\right\} = \left\{\dot{x}_s(T_s)\right\} \qquad 3.2.16$$

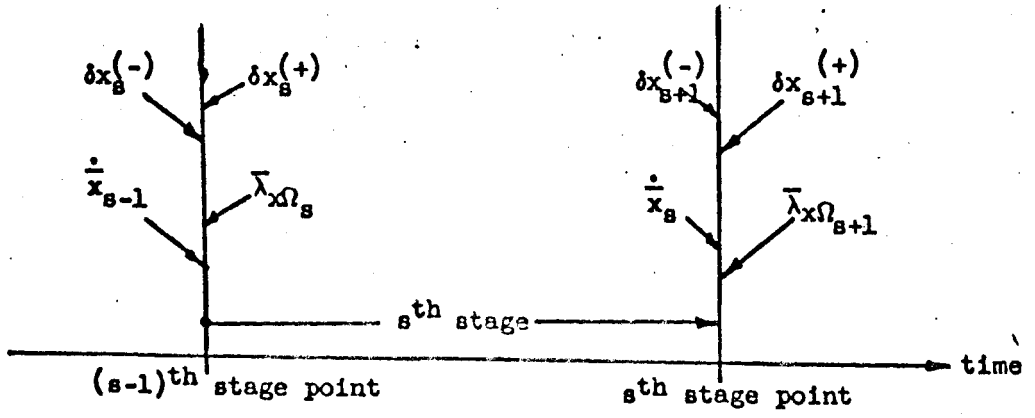

Sketch B - Position of Functions Defined in the s^{th} Stage

Similarly, the components for longitude changes are

$$\left\{\Delta x_1^{\theta}\right\} = \begin{Bmatrix} \frac{\partial \theta}{\partial X_e} \\ \frac{\partial \theta}{\partial Y_e} \\ \frac{\partial \theta}{\partial Z_e} \\ --- \\ 0 \end{Bmatrix} \qquad 3.2.18b$$

In addition to this type of initial point perturbation, we may have some changes resulting from the previous iterations, Δx_1^P . Combining both types of perturbation, the total change in the first stage state variables is

$$\left\{\delta x_1\right\} = \left\{\Delta x_1\right\} = \sum_i \left\{\Delta x_1^i\right\} + \left\{\Delta x_1^P\right\} \qquad 3.2.19$$

Knowing the δx_1 we can compute the total initial value perturbations in the second stage by using Eqn. (3.2.17)

$$\left\{\delta x_2\right\} = \left[P_1\right]\left(\left\{K_1\right\} + \left[\bar{\lambda}_{x\Omega_1}\right]' \left\{\delta x_1\right\} + \left\{\dot{\bar{x}}_1\right\} \Delta T_1\right) + \left\{\Delta x_2\right\} \qquad 3.2.20$$

Proceeding to the next stage,

$$\begin{aligned} \left\{\delta x_3\right\} &= \left[P_2\right]\left(\left\{K_2\right\} + \left[\bar{\lambda}_{x\Omega_2}\right]' \left\{\delta x_2\right\} + \left\{\dot{\bar{x}}_2\right\} \Delta T_2\right) + \left\{\Delta x_3\right\} \\ &= \left[P_2\right]\left\{K_2\right\} + \left[P_2\right]\left[\bar{\lambda}_{x\Omega_2}\right]'\left[P_1\right]\left\{K_1\right\} \\ &+ \left[P_2\right]\left\{\dot{\bar{x}}_2\right\}\Delta T_2 + \left[P_2\right]\left[\bar{\lambda}_{x\Omega_2}\right]'\left[P_1\right]\left\{\dot{\bar{x}}_1\right\} \Delta T_1 \\ &+ \left[P_2\right]\left[\bar{\lambda}_{x\Omega_2}\right]'\left[P_1\right]\left[\bar{\lambda}_{x\Omega_1}\right]'\left\{\Delta x_1\right\} + \left[P_2\right]\left[\bar{\lambda}_{x\Omega_2}\right]'\left\{\Delta x_2\right\} + \left\{\Delta x_3\right\} \end{aligned} \qquad 3.2.21$$

In some cases, we may wish to specify additional perturbations in the state variables to the right of a stage point. For example, returning to the case of a multi-stage booster; in a more sophisticated analysis of booster capability, one may wish to consider variations in the initial mass of fuel contained within each stage. Typically, in a given iteration, the amount of fuel consumed in the $s+1^{th}$ stage may be either less than, or greater than, the total amount of fuel available in that stage. If this, or a similar situation arises, the initial amount of fuel contained in the stage must be adjusted in the next iteration. It is essential to have a mechanism within the optimization analysis, which will permit these required changes to be specified. The P matrix, as described above, is unable to provide this mechanism, for the additional changes may clearly be functions of the state variable perturbations at the termination of the $(s+1)^{th}$ stage, rather than at the termination of the s^{th} stage. The P matrix is primarily introduced to convert changes in the state variables at the termination of the s^{th} stage into state variable changes at the beginning of the $(s+1)^{th}$ stage. Accordingly, a set of additional state variable perturbations $\{\Delta x_{s+1}\}$ which we specify directly will be introduced. The complete expression for the state variable perturbations therefore becomes

$$\left\{\delta x_{s+1}\right\} = \left[P_s\right]\left\{\left\{K_s\right\} + \left[\bar{\lambda}_{x\Omega_s}\right]'\left\{\delta x_s(0)\right\} + \left\{\dot{\bar{x}}_s\right\}\Delta T_s\right\} + \left\{\Delta x_{s+1}\right\} \qquad 3.2.17$$

With Eqn. (3.2.17), we have achieved our first objective: a recursion formula which enables us to predict the initial state variable perturbations in the $(s+1)^{th}$ stage when the perturbations in the s^{th} stage are known and additional changes are directly specified in the initial values of the $(s+1)^{th}$ stage state variables.

The recursion formula Eqn. (3.2.17) can be applied to each stage in turn, commencing with the first. In the case of the first stage, there will be no perturbations of the initial state variable due to prior stages, but there will be perturbations to the state variables if a search for the optimum trajectory initial conditions is being made.

These initial value perturbations will be some combination of state variable vectors dictated by the particular problem under consideration. For example, suppose we seek the optimal launch point for a mobile missile. We may express our nominal launch point in terms of latitude and longitude, and then on successive iterations, perturb the launch point towards the optimal position. The perturbation in latitude is a state variable vector having components corresponding to the position state variables and zeros elsewhere,

$$\left\{\Delta x_1^{\phi}\right\} = \begin{Bmatrix} \frac{\partial \phi}{\partial X_e} \\ \frac{\partial \phi}{\partial Y_e} \\ \frac{\partial \phi}{\partial Z_e} \\ \hline 0 \end{Bmatrix} \qquad 3.2.18a$$

and the next

$$\{\delta x_4\} = [P_3]\left(\{K_3\} + [\bar{\lambda}_x\Omega_3]' \{\delta x_3\} + \{\dot{\bar{x}}_3\}\Delta T_3\right) + \{\Delta x_4\}$$

$$= Q_3Q_2P_1K_1 + Q_3P_2K_2 + P_3K_3$$

$$+ Q_3Q_2P_1 \dot{\bar{x}}_1\Delta T_1 + Q_3P_2 \dot{\bar{x}}_2\Delta T_2 + P_3 \dot{\bar{x}}_3\Delta T_3$$

$$+ Q_3Q_2Q_1 \Delta x_1 + Q_3Q_2 \Delta x_2 + Q_3 \Delta x_3 + \Delta x_4 \qquad 3.2.22$$

where

$$[Q_s] = [P_s][\bar{\lambda}_x\Omega_s]' \qquad 3.2.23$$

In general, the total state variable perturbation at the commencement of the $(s+1)^{th}$ stage is

$$\{\delta x_{s+1}\} = \left(Q_sQ_{s-1}\cdots\cdots Q_2P_1K_1 + Q_sQ_{s-1}\cdots\cdots Q_3P_2K_2 + \cdots\right.$$
$$\left.\cdots + Q_sP_{s-1}K_{s-1} + P_sK_s\right)$$
$$+\left(Q_sQ_{s-1}\cdots\cdots Q_2P_1\dot{\bar{x}}_1\Delta T_1 + Q_sQ_{s-1}\cdots\cdots Q_3P_2\dot{\bar{x}}_2\Delta T_2 + \cdots\right.$$
$$\left.\cdots + Q_sP_{s-1}\dot{\bar{x}}_{s-1}\Delta T_{s-1} + P_s\dot{\bar{x}}_s\Delta T_s\right)$$
$$+\left(Q_sQ_{s-1}\cdots Q_1 \Delta x_1 + Q_sQ_{s-1}\cdots\cdots Q_2 \Delta x_2 + \cdots\right.$$
$$\left.\cdots + Q_sQ_{s-1} \Delta x_{s-1} + Q_s \Delta x_s + \Delta x_{s+1}\right) \qquad 3.2.24$$

At the commencement of the last (N^{th}) stage, we can write

$$\{\delta x_N\} = \sum_{s=1}^{N-1} [A_s^N]\{K_s\} + \sum_{s=1}^{N-1} \{B_s^N\}\Delta T_s + \sum_{s=1}^{N} [C_s^N]\{\Delta x_s\} \qquad 3.2.25$$

where

$$[A_s^N] = Q_{N-1}Q_{N-2} \cdots\cdots Q_{s+1}P_s, \quad s < N-1$$
$$= P_s, \quad s = N-1 \qquad 3.2.26$$

$$\{B_s^N\} = Q_{N-1}Q_{N-2} \cdots\cdots Q_{s+1}P_s \dot{\bar{x}}_s, \quad s < N-1$$
$$= P_s\dot{\bar{x}}_s, \quad s = N-1 \qquad 3.2.27$$

$$[C_s^N] = Q_{N-1}Q_{N-2} \cdots\cdots Q_s, \quad s < N$$
$$= I, \quad s = N \qquad 3.2.28$$

Knowing the initial perturbations to the last stage, we can apply Eqns.(2.2.20) in stage time to find the changes in the payoff function Φ, and the constraints.

$$\delta\phi = \int_0^{T_N} \left[\lambda_{\phi\Omega_N}\right]\left[G\right]\left\{\delta\alpha\right\} d\tau_N + \left[\lambda_{\phi\Omega_N}(0)\right]\left\{\delta x_N\right\} \qquad 3.2.29$$

$$\left\{\delta\psi\right\} = \int_0^{T_N} \left[\lambda_{\psi\Omega_N}\right]'\left[G\right]\left\{\delta\alpha\right\} d\tau_N + \left[\lambda_{\psi\Omega_N}(0)\right]'\left\{\delta x_N\right\} \qquad 3.2.30$$

and on substituting for δx_N

$$\delta\phi = K_{N_\phi} + \left[\bar{\lambda}_{\phi\Omega_N}\right]\left\{\sum_{s=1}^{N-1}\left[A_s^N\right]\left\{K_s\right\} + \sum_{s=1}^{N-1}\left\{B_s^N\right\}\Delta T_s + \sum_{s=1}^{N}\left[C_s^N\right]\left\{\Delta x_s\right\}\right\} \qquad 3.2.31$$

$$\left\{\delta\psi\right\} = \left\{K_{N_\psi}\right\} + \left[\bar{\lambda}_{\psi\Omega_N}\right]'\left\{\sum_{s=1}^{N-1}\left[A_s^N\right]\left\{K_s\right\} + \sum_{s=1}^{N-1}\left\{B_s^N\right\}\Delta T_s + \sum_{s=1}^{N}\left[C_s^N\right]\left\{\Delta x_s\right\}\right\} \qquad 3.2.32$$

where

$$K_{N_\phi} = \int_0^{T_N} \left[\lambda_{\phi\Omega_N}\right]\left[G\right]\left\{\delta\alpha\right\} d\tau_N \qquad 3.2.33$$

$$\left\{K_{N_\psi}\right\} = \int_0^{T_N} \left[\lambda_{\psi\Omega_N}\right]'\left[G\right]\left\{\delta\alpha\right\} d\tau_N \qquad 3.2.34$$

It is convenient to combine the integrals, K_s, through each stage into a single set of integrals throughout the complete trajectory. To accomplish this, we define

$$\left[\Lambda_{\phi\Omega}\right] = \left[\bar{\lambda}_{\phi\Omega_N}\right]\left[A_s^N\right]\left[\lambda_{x\Omega_s}\right]'; \quad s < N \qquad 3.2.35$$

$$= \left[\lambda_{\phi\Omega_N}\right]; \quad s = N$$

$$\left[\Lambda_{\psi\Omega}\right]' = \left[\bar{\lambda}_{\psi\Omega_N}\right]'\left[A_s^N\right]\left[\lambda_{x\Omega_s}\right]'; \quad s < N \qquad 3.2.36$$

$$= \left[\lambda_{\psi\Omega_N}\right]' \quad s = N$$

Expanding Eqn. (3.2.31), we obtain

$$\delta\phi = K_{N_\phi} + \left(\left[\bar{\lambda}_{\phi\Omega_N}\right]\sum_{s=1}^{N-1}\left[A_s^N\right]\left\{K_s\right\}\right) + \left(\left[\bar{\lambda}_{\phi\Omega_N}\right]\left\{\sum_{s=1}^{N-1}\left\{B_s^N\right\}\Delta T_s + \sum_{s=1}^{N}\left[C_s^N\right]\left\{\Delta x_s\right\}\right\}\right)$$

$$= \int_o^{T_N}\left[\lambda_{\phi\Omega_N}\right]\left[G\right]\left\{\delta\alpha\right\}d\tau_N + \sum_{s=1}^{N-1}\left[\bar{\lambda}_{\phi\Omega_N}\right]\left[A_s^N\right]\left\{\int_o^{T_s}\left[\lambda_{x\Omega_s}\right]'\left[G\right]\left\{\delta\alpha\right\}d\tau_s\right\}$$

$$+ \left[\bar{\lambda}_{\phi\Omega_N}\right]\left\{\sum_{s=1}^{N-1}\left\{B_s^N\right\}\Delta T_s + \sum_{s=1}^{N}\left[C_s^N\right]\left\{\Delta x_s\right\}\right\} \qquad 3.2.37$$

$$\therefore \delta\phi = \sum_{s=1}^{N}\int_o^{T_s}\left[\lambda_{\phi\Omega}\right]\left[G\right]\left\{\delta\alpha\right\}d\tau_s + \left[\bar{\lambda}_{\phi\Omega_N}\right]\left\{\sum_{s=1}^{N-1}\left\{B_s^N\right\}\Delta T_s + \sum_{s=1}^{N}\left[C_s^N\right]\left\{\Delta x_s\right\}\right\} \qquad 3.2.38$$

The first term, which is the summation of a set of integrals throughout each stage on the unperturbed trajectory, can be combined into one integral by reverting to the original independent variable t. That is

$$\delta\phi = \int_{t_o}^{T}\left[\lambda_{\phi\Omega}\right]\left[G\right]\left\{\delta\alpha\right\}dt + \left[\bar{\lambda}_{\phi\Omega_N}\right]\left\{\sum_{s=1}^{N-1}\left\{B_s^N\right\}\Delta T_s + \sum_{s=1}^{N}\left[C_s^N\right]\left\{\Delta x_s\right\}\right\} \qquad 3.2.39$$

Similarly

$$\left\{\delta\psi\right\} = \int_{t_o}^{T}\left[\lambda_{\psi\Omega}\right]'\left[G\right]\left\{\delta\alpha\right\}dt + \left[\bar{\lambda}_{\psi\Omega_N}\right]'\left\{\sum_{s=1}^{N-1}\left\{B_s^N\right\}\Delta T_s + \sum_{s=1}^{N}\left[C_s^N\right]\left\{\Delta x_s\right\}\right\} \qquad 3.2.40$$

Eqns. (3.2.39) and (3.2.40) give the total change in payoff and constraint functions when the trajectory simultaneously undergoes perturbations in the control variable histories, stage point positions and initial state variable values in each stage. The sensitivity of payoff and constraint functions to these variations is immediately apparent. For pulse variations in the control variables at time t=t', the individual sensitivities of the payoff function are the elements of the row matrix,

$$\left[\phi_\alpha(t')\right] = \left[\lambda_{\phi\Omega}(t')\right]\left[G(t')\right] \qquad 3.2.41$$

The individual sensitivities of the constraint functions to control variable pulse perturbations are similarly the elements of the rectangular matrix

$$\left[\psi_\alpha(t')\right] = \left[\Lambda_{\psi\Omega}\right]' \left[G\right] \qquad 3.2.42$$

The sensitivity of the payoff function with respect to stage point variations follows directly from the second term of Eqn. (3.2.39). If the s^{th} stage alone is perturbed by ΔT_s, we see that

$$\phi_{\Delta T_s} = \left[\lambda_{\phi\Omega_N}\right] \left\{B_s^N\right\} \qquad 3.2.43$$

Similarly, the constraint sensitivities with respect to stage point perturbations are obtained from Eqn. (3.2.40) as

$$\left\{\psi_{\Delta T_s}\right\} = \left[\lambda_{\psi\Omega_N}\right]' \left\{B_s^N\right\} \qquad 3.2.44$$

Finally, the sensitivities to initial state variable value perturbations in each stage can be obtained from the last terms in Eqns. (3.2.39) and (3.2.40). The payoff function sensitivities for the s^{th} stage are the elements of

$$\left[\phi_{\Delta x_s}\right] = \left[\lambda_{\phi\Omega_N}\right] \left[C_s^N\right] \qquad 3.2.45$$

and the constraint function sensitivities for the s^{th} stage are the elements of the rectangular matrix

$$\left[\psi_{\Delta x_s}\right] = \left[\lambda_{\psi\Omega_N}\right]' \left[C_s^N\right] \qquad 3.2.46$$

In general, we must consider two types of stage points: those whose perturbation is prescribed and those which we are free to optimize. Hence, we can write

$$\sum_{s=1}^{N-1} \left\{B_s^N\right\} \Delta T_s = \sum_{s'=1}^{S'} \left\{B_{s'}^N\right\} \Delta T_{s'} + \sum_{\bar{s}=1}^{\bar{S}} \left\{B_{\bar{s}}^N\right\} \Delta T_{\bar{s}} \qquad 3.2.47$$

where the $\Delta T_{s'}$ are prescribed and the $\Delta T_{\bar{s}}$ are to be optimized. Substituting Eqn. (3.2.47) into Eqn. (3.2.39), we obtain

$$\delta\phi = \int_{t_o}^{T} \left[\Lambda_{\phi\Omega}\right]\left[G\right]\left\{\delta\alpha\right\}dt + \left[\lambda_{\phi\Omega_N}\right]\left\{\sum_{\bar{s}=1}^{\bar{S}} \left\{B_{\bar{s}}^N\right\} \Delta T_{\bar{s}}\right\}$$

$$+ \left[\lambda_{\phi\Omega_N}\right]\left\{\sum_{s'=1}^{S'} \left\{B_{s'}^N\right\} \Delta T_{s'} + \sum_{s=1}^{N} \left[C_s^N\right]\left\{\Delta x_s\right\}\right\} \qquad 3.2.48$$

Substituting Eqn. (3.2.47) into Eqn. (3.2.40), we obtain

$$\{\delta\Gamma\} = \int_{t_o}^{T} [\lambda_{\psi\Omega}]' [G]\{\delta\alpha\}\, dt + [\bar{\lambda}_{\psi\Omega_N}]' \left\{ \sum_{\bar{s}=1}^{\bar{S}} \{B^N_{\bar{s}}\} \Delta T_{\bar{s}} \right\} \qquad 3.2.49$$

where all the quantities which we wish to specify directly are grouped together in the term,

$$\{\delta\Gamma\} = \{\delta\psi\} - [\bar{\lambda}_{\psi\Omega_N}]' \left\{ \sum_{s'=1}^{S'} \{B^N_{s'}\} \Delta T_{s'} + \sum_{s=1}^{N} [C^N_s]\{\Delta x_s\} \right\} \qquad 3.2.50$$

With Eqns. (3.2.48) and (3.2.49), we have attained our first objective: expressions for the change in the payoff and constraint functions resulting from a general perturbation of control variable histories and stage point perturbations. The optimal perturbation has yet to be found. This task will be attempted in the next section.

3.3 Derivation of Variational Equations

The analysis of the preceding section resulted in expressions for the payoff and constraint function changes when a combined perturbation is introduced in the control variable histories, stage point positions and initial state variable values in each stage. We will now attempt to optimize the payoff function change while at the same time directly specifying changes in the constraints, $\{\delta\psi\}$, and the initial state variable values in each stage $\{\Delta x_s\}$. In order to obtain a meaningful solution, we must place limits on the perturbation magnitudes. We limit control variable perturbations in the manner of Section 2 by introducing a constraint

$$DP^2 \doteq \int_{t_o}^{T} \left(\lfloor \delta\alpha \rfloor [W]\{\delta\alpha\} \right) dt \qquad 3.3.5$$

A similar constraint (DT^2) must be introduced to limit the total stage point perturbation.

$$DT^2 = \left(\sum_{\bar{s}=1}^{\bar{S}} V_{\bar{s}}\, \Delta T_{\bar{s}}^2 \right) \qquad 3.3.1$$

where the $V_{\bar{s}}$ are a set of weighting functions which may be used to modulate the optimal stage point perturbations.

Proceeding as in Section (2.2), we may construct an augmented function in the manner of Lagrange and minimize (maximize) this. In the present case, the augmented function is

$$U = \int_{t_o}^{T} \left[\Lambda_{\phi\Omega}\right]\left[G\right]\left\{\delta\alpha\right\}' dt + \left[\bar{\lambda}_{\phi\Omega_N}\right]\left\{\sum_{\bar{s}=1}^{\bar{S}}\left\{B_{\bar{s}}^{N}\right\}\ \Delta T_{\bar{s}}\right\}$$

$$+ \left[\bar{\lambda}_{\phi\Omega_N}\right]\left\{\sum_{s'=1}^{S'}\left\{B_{s'}^{N}\right\}\Delta T_{s'} + \sum_{s=1}^{N}\left[C_{s}^{N}\right]\left\{\Delta x_s\right\}\right\}$$

$$+\left[\vartheta\right]\left\{\int_{t_o}^{T}\left[\Lambda_{\psi\Omega}\right]'\left[G\right]\left\{\delta\alpha\right\}dt + \left[\bar{\lambda}_{\psi\Omega_N}\right]'\left\{\sum_{\bar{s}=1}^{\bar{S}}\left\{B_{\bar{s}}^{N}\right\}\Delta T_{\bar{s}}\right\}\right.$$

$$\left. + \left[\bar{\lambda}_{\psi\Omega_N}\right]'\left\{\sum_{s'=1}^{S'}\left\{B_{s'}^{N}\right\}\Delta T_{s'} + \sum_{s=1}^{N}\left[C_{s}^{N}\right]\left\{\Delta x_s\right\}\right\}\right\}$$

$$+ \mu\int_{t_o}^{T}\left[\delta\alpha\right]\left[W\right]\left\{\delta\alpha\right\}dt + \omega\left(\sum_{\bar{s}=1}^{\bar{S}} V_{\bar{s}}\ \Delta T_{\bar{s}}^{2}\right) \qquad 3.3.2$$

where ω is a Lagrangean Multiplier introduced for the stage point perturbation constraint.

First, we differentiate with respect to each stage point perturbation which we seek to optimize. This results in $\bar{S}$ equations,

$$\frac{\partial U}{\partial(\Delta T_{\bar{s}})} = \left[\bar{\lambda}_{\phi\Omega_N}\right]\left\{B_{\bar{s}}^{N}\right\} + 2\omega V_{\bar{s}}\Delta T_{\bar{s}} + \left[\vartheta\right]\left[\bar{\lambda}_{\psi\Omega_N}\right]'\left\{B_{\bar{s}}^{N}\right\} \qquad 3.3.3$$

These expressions must disappear for U to be extremalized. Solving for the $\Delta T_{\bar{s}}$, we obtain the equations:

$$\Delta T_{\bar{s}} = -\frac{1}{2\omega V_{\bar{s}}}\left[\left[\bar{\lambda}_{\phi\Omega_N}\right] + \left[\vartheta\right]\left[\bar{\lambda}_{\psi\Omega_N}\right]'\right]\left\{B_{\bar{s}}^{N}\right\} \qquad 3.3.4$$

Squaring both sides of Eqn. (3.3.4), multiplying throughout by $V_{\bar{s}}$, summing the $\bar{S}$ equations and using Eqn. (3.3.1)

$$\sum_{s=1}^{\bar{S}} V_{\bar{s}}\,\Delta T_{\bar{s}}^{2} = DT^{2} = \frac{1}{4\omega^{2}} \sum_{s=1}^{\bar{S}} V_{\bar{s}}^{-1}\left(\left[\left[\bar{\lambda}_{\phi\Omega_N}\right] + \left[\vartheta\right]\left[\bar{\lambda}_{\psi\Omega_N}\right]'\right]\left\{B_{\bar{s}}^{N}\right\}\right)^{2}$$

$$= \frac{1}{4\omega^{2}} \sum_{s=1}^{\bar{S}}\left[\left[\bar{\lambda}_{\phi\Omega_N}\right] + \left[\vartheta\right]\left[\bar{\lambda}_{\psi\Omega_N}\right]'\right]\frac{\left\{B_{\bar{s}}^{N}\right\}\left[B_{\bar{s}}^{N}\right]}{V_{\bar{s}}}\left\{\left\{\bar{\lambda}_{\phi\Omega_N}\right\} + \left[\bar{\lambda}_{\psi\Omega_N}\right]\left\{\vartheta\right\}\right\} \qquad 3.3.5$$

Rearranging Eqn. (3.3.5) and taking the summation into the matrix product

$$\omega^{2} = \frac{1}{4\,DT^{2}}\left(L_{\phi\phi} + 2\left[L_{\psi\phi}\right]\left\{\vartheta\right\} + \left[\vartheta\right]\left[L_{\psi\psi}\right]\left\{\vartheta\right\}\right)$$

or

$$4\omega^{2}DT^{2} - L_{\phi\phi} - 2\left[L_{\psi\phi}\right]\left\{\vartheta\right\} - \left[\vartheta\right]\left[L_{\psi\psi}\right]\left\{\vartheta\right\} = 0 \qquad 3.3.6$$

where

$$L_{\phi\phi} = \left[\bar{\lambda}_{\phi\Omega_N}\right]\left[D\right]\left\{\bar{\lambda}_{\phi\Omega_N}\right\} \qquad 3.3.7$$

$$\left[L_{\psi\phi}\right] = \left[\bar{\lambda}_{\phi\Omega_N}\right]\left[D\right]\left[\bar{\lambda}_{\psi\Omega_N}\right] \qquad 3.3.8$$

$$\left[L_{\psi\psi}\right] = \left[\bar{\lambda}_{\psi\Omega_N}\right]'\left[D\right]\left[\bar{\lambda}_{\psi\Omega_N}\right] \qquad 3.3.9$$

and

$$\left[D\right] = \sum_{s=1}^{\bar{S}} V_{\bar{s}}^{-1}\left\{B_{\bar{s}}\right\}\left[B_{\bar{s}}\right] \qquad 3.3.10$$

Second, we take a variation of $\delta\alpha$ to Eqn. (3.3.2) in a similar manner to Section (2.2)

$$\delta U_{(\alpha)} = \int_{t_o}^{T}\left[\Lambda_{\phi\Omega}\right]\left[G\right]\left\{\delta^{2}\alpha\right\}dt + \left[\vartheta\right]\int_{t_o}^{T}\left[\Lambda_{\psi\Omega}\right]'\left[G\right]\left\{\delta^{2}\alpha\right\}dt + 2\mu\int_{t_o}^{T}\left[\delta\alpha\right]\left[W\right]\left\{\delta^{2}\alpha\right\}dt = 0$$

$$3.3.11$$

$$\therefore \left[\Lambda_{\phi\Omega}\right]\left[G\right] + \left[\vartheta\right]\left[\Lambda_{\psi\Omega}\right]'\left[G\right] + 2\mu\left[\delta\alpha\right]\left[W\right] = 0 \qquad 3.3.12$$

$$\therefore \left\{\delta\alpha\right\} = -\frac{1}{2\mu}\left[W\right]^{-1}\left[G\right]'\left\{\left\{\Lambda_{\phi\Omega}\right\} + \left[\Lambda_{\psi\Omega}\right]\left\{\vartheta\right\}\right\} \qquad 3.3.13$$

Substituting into Eqn. (3.2.49)

$$\left\{\delta\Gamma\right\} = -\frac{1}{2\mu}\left\{\left\{J_{\psi\phi}\right\} + \left[J_{\psi\psi}\right]\left\{\vartheta\right\}\right\} + \left[\bar{\lambda}_{\psi\Omega_N}\right]' \left\{\sum_{E=1}^{\bar{S}}\left\{B_E^N\right\}\Delta T_E\right\} \qquad 3.3.14$$

where we define

$$J_{\phi\phi} = \int_{t_o}^{T}\left[\Lambda_{\phi\Omega}\right]\left[G\right]\left[W\right]^{-1}\left[G\right]'\left\{\Lambda_{\phi\Omega}\right\}dt \qquad 3.3.15$$

$$\left\{J_{\psi\phi}\right\} = \int_{t_o}^{T}\left[\Lambda_{\psi\Omega}\right]'\left[G\right]\left[W\right]^{-1}\left[G\right]'\left[\Lambda_{\phi\Omega}\right]dt \qquad 3.3.16$$

$$\left[J_{\psi\psi}\right] = \int_{t_o}^{T}\left[\Lambda_{\psi\Omega}\right]\left[G\right]\left[W\right]^{-1}\left[G\right]'\left[\Lambda_{\psi\Omega}\right]dt \qquad 3.3.17$$

Transposing Eqn. (3.3.4), substituting into Eqn. (3.3.14), and using Eqn. (3.3.10)

$$\left\{\delta\Gamma\right\} = -\frac{1}{2\mu}\left\{\left\{J_{\psi\phi}\right\} + \left[J_{\psi\psi}\right]\left\{\vartheta\right\}\right\} - \frac{1}{2\omega}\left[\bar{\lambda}_{\psi\Omega_N}\right]'\left[D\right]\left\{\left[\bar{\lambda}_{\psi\Omega_N}\right]\left\{\vartheta\right\} + \left\{\bar{\lambda}_{\phi\Omega_N}\right\}\right\} \qquad 3.3.19$$

Substituting Eqns. (3.3.8) and (3.3.9) into Eqn. (3.3.19), multiplying throughout by $2\omega\mu$ and collecting terms on the left

$$2\mu\omega\left\{\delta\Gamma\right\} + \omega\left\{\left\{J_{\psi\phi}\right\} + \left[J_{\psi\psi}\right]\left\{\vartheta\right\}\right\} + \mu\left\{\left[L_{\psi\psi}\right]\left\{\vartheta\right\} + \left\{L_{\psi\phi}\right\}\right\} = 0 \qquad 3.3.20$$

Third, we substitute Eqn. (3.3.13) into Eqn. (2.1.5)

$$DP^2 = \frac{1}{4\mu^2}\int_{t_o}^{T}\left[\left[\Lambda_{\phi\Omega}\right] + \left[\vartheta\right]\left[\Lambda_{\psi\Omega}\right]\right]'\left[G\right]\left[W\right]^{-1}\left[G\right]'\left\{\left\{\Lambda_{\phi\Omega}\right\} + \left[\Lambda_{\psi\Omega}\right]\left\{\vartheta\right\}\right\}dt \qquad 3.3.21$$

Using Eqns. (3.3.15), (3.3.16), and (3.3.17), multiplying by $4\mu^2$ and collecting on the left

$$4DP^2\mu^2 - J_{\phi\phi} - 2\left[J_{\psi\phi}\right]\left\{\vartheta\right\} - \left[\vartheta\right]\left[J_{\psi\psi}\right]\left\{\vartheta\right\} = 0 \qquad 3.3.22$$

Eqns. (3.3.6), (3.3.20) and (3.3.22) are the variational equations which must be solved to obtain the Lagrangean multiplier introduced for the constraints of Eqns. (2.1.5) and (3.3.1)

3.4 Solution Using Combined Step-Size Parameter

A closed form solution to the optimal staging equations can be obtained if separate Lagrangean Multipliers for the control variable, and stage point perturbations are abandoned. Combining these perturbations* and defining a single step-size parameter by the expression

$$DC^2 = \int_{t_o}^{T} \left[\delta\alpha(t)\right] \left[W(t)\right] \left\{\delta\alpha(t)\right\} dt + \sum_{\bar{s}=1}^{\bar{S}} \bar{V}_{\bar{s}} \Delta T_{\bar{s}}^2$$

results in the creation of a single perturbation measure. It should be noted that the weighting function, $\bar{V}_{\bar{s}}$, must now be a dimensional quantity to ensure compatibility between both portions of Eqn. (3.4.1).

*This approach was suggested by Mr. R. L. Mobley now of the Rand Corporation.

Returning to the augmented function of Eqn. (3.3.2), we see that in the last line we must now replace ω by μ. This substitution can also be made in Eqns. (3.3.3) to (3.3.6). Eqns. (3.3.6) and (3.3.22) can then be combined to obtain

$$4\mu^2 .DC^2 - (J_{\phi\phi} + I_{\phi\phi}) - 2\left[\left[J_{\psi\phi}\right] + \left[L_{\psi\phi}\right]\right]\left\{\vartheta\right\}$$

$$-\left[\vartheta\right]\left[\left[J_{\psi\psi}\right] + \left[L_{\psi\psi}\right]\right]\left\{\vartheta\right\} \qquad 3.4.2$$

Substituting μ for ω into the equations leading to Eqn. (3.3.20) results in the expression

$$2\mu\left\{\delta\Gamma\right\} + \left\{\left\{J_{\psi\phi}\right\} + \left\{L_{\psi\phi}\right\}\right\} + \left[\left[J_{\psi\psi}\right] + \left[L_{\psi\psi}\right]\right]\left\{\vartheta\right\} = 0 \qquad 3.4.3$$

It follows, by comparison with Eqns. (2.2.34) and (2.2.30a), that μ and $\{\vartheta\}$ are given by Eqns. (2.2.36) and (2.2.37) provided we replace the $\{d\beta\}$ by $\{\delta\Gamma\}$ and the I by the appropriate (J + L). For example,

$$I_{\phi\phi} \longrightarrow J_{\phi\phi} + L_{\phi\phi} \qquad 3.4.4$$

The optimal control variable perturbation is then given by Eqn. (2.2.38) with the I replaced by the (J+L) and the λ by the appropriate Λ. For example

$$\left\{\lambda_{\phi\Omega}\right\} \longrightarrow \left\{\Lambda_{\phi\Omega}\right\} \qquad 3.4.5$$

Substituting μ and $\{\vartheta\}$ into Eqn. (3.5.1), the optimal stage point perturbations are obtained in the form

$$\left\{\Delta T_{\bar{s}}\right\} = \mp\left[V_s\right]^{-1}\left[B_s^N\right]'\left\{\left\{\bar{\lambda}_{\phi\Omega N}\right\} - \left[\bar{\lambda}_{\psi\Omega N}\right]\left[J_{\psi\psi} + L_{\psi\psi}\right]^{-1}\left\{J_{\psi\phi} + L_{\psi\phi}\right\}\right\} \qquad 3.4.6$$

$$\times\sqrt{\frac{DC^2 - \left[\delta\Gamma\right]\left[J_{\psi\psi} + L_{\psi\psi}\right]^{-1}\left\{\delta\Gamma\right\}}{(J_{\phi\phi} + L_{\phi\phi}) - \left[J_{\psi\phi} + L_{\psi\phi}\right]\left[J_{\psi\psi} + L_{\psi\psi}\right]^{-1}\left\{J_{\psi\phi} + L_{\psi\phi}\right\}}}$$

$$+\left[V_s\right]^{-1}\left[B_s^N\right]'\left[\bar{\lambda}_{\psi\Omega N}\right]\left[J_{\psi\psi} + L_{\psi\psi}\right]^{-1}\left\{\delta\Gamma\right\}$$

With these equations, we have obtained the general solution to the optimal staging problem. The main difficulty in applying the results lies in determining suitable weighting matrices. In this respect, the concepts in Reference 2 serve as a guide.

4.0 CONVERGENCE OF THE STEEPEST-DESCENT METHOD

It should be noted that the optimal control perturbation is directly proportional to the inverse of the weighting matrix W and the optimal stage point perturbations are directly proportional to the inverse of the diagonal matrix formed from weighting parameters V_S. These equations indicate that any descending direction is a possible steepest-descent direction when minimizing and conversely any ascending direction is a possible steepest-ascent direction. By choosing the weighting matrices and weighting parameters appropriately the steepest-descent/ascent direction can be made equal to that of any favorable perturbation which provides the specified end point changes.

From a nominal control history and set of stage times the steepest descent process can be applied iteratively by means of equations 2.2.38 and 3.4.6 until the terminal points are satisfied and the performance ceases to improve. The main difficulty in applying the method lies in the determination of suitable weighting matrices and weighting parameters. To use the method efficiently reasonable values of the perturbation magnitude DC^2 and the constraint change vector $d\bar{\psi}$ must be determined.

A highly successful approach to the determination of these quantities is the convergence scheme of Reference 2. There these quantities are determined by means of a second order approximation to the actual non-linear behavior of the trajectory perturbations introduced by the optimal first order control and stage perturbations of Eqns. (2.2.38) and 3.4.6 and a series of logical decisions. A Taylor expansion in terms of a single scalar perturbation parameter, K, is used for this purpose. The first-order changes in the trajectory functions of interest and the combined perturbation parameter are determined according to the equations

$$DC^2 = K_1^2 \cdot DC_o^2 \qquad 4.1$$

$$d\bar{\psi} = K_1 \cdot d\bar{\psi}_o$$

The nominal control perturbations, DC_o^2, and constraint changes, $d\bar{\psi}_o$, are determined by the convergence logic. It can be seen from the equations of the preceding section that in addition to the linear relationships of Eqn. (4.1) a further linear relationship between the performance function change, $d\phi$, and the scalar perturbation parameter, K, exists for

$$d\phi = K_1 \, d\phi_o \qquad 4.2$$

where $d\phi_o$ is the performance change associated with $d\bar{\psi}_o$ and dC_o^2. It follows from a Taylors expansion for the actual non-linear change in the performance and constraint functions, $\Delta\phi$ and $\Delta\bar{\psi}$ that

$$\Delta\phi = (\Delta\phi_o - d\phi_o) \cdot K^2 + d\phi_o \cdot K$$

$$\Delta\psi = (\Delta\psi_o - d\psi_o) \cdot K^2 + d\psi_o \cdot K \qquad 4.3$$

where $\Delta\phi_o$ and $\Delta\psi_o$ are the actual non-linear payoff and constraint function changes obtained by an exploratory perturbation of the trajectory with K = 1. Further details of this method are contained in Reference 2.

5.0 APPLICATION OF THE STEEPEST-DESCENT METHOD

The purpose of the trajectory optimization application was threefold. First, it was desired to discover and analyze any unique characteristics of this hybrid launch system and to identify any unexpected behavior. Second, it was anticipated that the resultant trajectory could be used to evaluate a lambda guidance simulator which was developed for the study of an advanced guidance technique. Third, it was desired to use optimum baseline performance in an effort to obtain more meaningful payload penalty data.

Phase I studies basically involved classical parametric techniques for determination of performance. The missions were segmented and analyzed as subarcs of the whole trajectory. This technique necessarily neglects the interaction of adjacent flight phases and completely ignores the possibility of unexpected trajectory behavior. Therefore, Phase II studies were directed toward learning as much as possible about the optimal performance and flight path of the hybrid launch system. Detailed consideration of the trajectory optimization problem established that a single trajectory with any of the available optimization computer programs would not produce the desired result. None of the optimization programs presently available has the multiple vehicle capability required by the boundary criteria established by orbital rendezvous and stage one return to base. The computer tool required to obtain the desired trajectory would contain all the features of presently operational steepest descent optimization programs plus the added capability of multiple sets of end constraints or boundary conditions. For the present study, this simply means the end constraints of both the first and second stages must be simultaneously met in such a way as to pass all unused stage one mass into stage two for the purpose of improving payload. Inasmuch as a multiple vehicle program is not presently available an alternate two-step approach was devised which would satisfy the aforementioned objectives.

A. Optimize the Stage 1/Stage 2 trajectory from takeoff to orbital rendezvous using the optimal staging technique.

B. Optimize the Stage 1 return trajectory from the staging conditions established in A. Any excess fuel can then be translated into payload using the mass exchange ratio for Stage 2 established by A.

These studies should produce near maximum payload in orbit and give some insight into optimal launch vehicle operation from a performance aspect.

The Stage 1/Stage 2 optimization problem was first tried with a fixed stage optimization program. The intent was to determine the staging time by parametric variation. This study is described in Section 5.1. The fixed stage program was abandoned in favor of an experimental optimal staging program after the fixed stage program failed to

converge. The Stage 1/Stage 2 optimal staging solution is discussed in Section 5.2. Finally the optimal Stage 1 return trajectory utilizing the stage 1 state at staging as initial conditions is discussed in Section 5.3.

5.1 Fixed Stage Optimization

The Stage I/Stage II trajectory commences immediately after take off with the following vehicle state:

Weight,	W	= (498,000 lbs.)	226,000 kg
Altitude,		= (1,000 ft.)	305 m
Flight path angle,		= 0°	
Velocity,	V	= (400 ft/sec.)	122 m/sec.
Latitude,		= 33.330° N	
Longitude,		= 0°	
Heading Angle		= 180°, (due South)	

A non-rotating earth, and a 1959 ARDC atmospheric model were employed for the calculation. The vehicle physical characteristics employed are contained in Part I of this report.

The terminal conditions imposed on this mission were:

Altitude,		= (262 N.M.) 485 km	
Flight path angle,		= 0°	
Velocity,	V	= (24980 ft/sec)	7,620 m/sec.
Latitude,		= 0°	
Heading angle,		= 90°, (Due East)	

These end constraints impose a 485 km (262 N.M.) circular orbit condition with longitude free, in the equatorial plane. Final orbital mass was maximized. Three continuously varying controls were employed in the calculation, pitch angle, θ, bank angle, B_A, and throttle, N. The actual pitch angle employed in these calculations was the scalar sum of the flight path angle, γ and the total angle of attack, α ; these two angles are not in a plane when the vehicle is banked. Bank angle consists of a rotation about the velocity vector at constant pitch.

In-flight inequality constraints were placed on (1) sonic boom, which was limited to 143.6 N/M^2 (3 psf) differential over-pressure, (2) dynamic pressure, 95,760 N/M^2 (2000 psf) in the first stage and 9576 N/M^2 (200 psf) in the second stage, and (3) throttle. The first stage throttle was limited to 1.0 which corresponds to full throttle, and the second stage throttle was left free. A maximum Mach number constraint of 7.0 was also imposed throughout the first stage flight.

A slowly turning initial nominal trajectory was employed using constant bank angle, full throttle, and constant pitch. This trajectory was deliberately chosen in a non-optimal fashion in order to avoid any pre-supposition with regard to the characteristics of the optimal flight path. It also provides a smoothly varying control history. Past

experience has indicated this to be a desirable feature of an initial control profile to facilitate rapid convergence.

Initially a solution was sought with the program of Reference 7 using a fixed stage time. At this point in the study, the intention was to parametrically vary the stage time, reoptimizing the path each time. By this means the optimal stage point could be located. The optimization program of Reference 7 was chosen to provide compatibility with the lambda guidance simulator of the present report.

The trajectory developed after 32 iterations through this computer program is shown in Figures 5-1 to 5-7 together with the initial nominal profile. During Stage I, the flight path remains close to the inflight inequality constraint boundaries in a Mach-altitude sense. Severe violations of the throttle inequality constraint occur at the beginning and end of Stage I, Figure 5-7. The throttle history for Stage II reveals that a coast had developed, punctuated by short bursts of power. The turn into the equatorial plane is marked by a pronounced dog-leg during the staging maneuver as shown by the ground track of Figure 5-1. The portion of the flight path preceding this motion was practically normal to the equatorial plane. A slight Westerly deviation had occurred with a resulting bowing out of the flight path shown in Figure 5-1. The terminal conditions had significantly improved over the nominal values. The start mass for Stage 1 at this point was about 64,800 kg (143,000 lbs.) The terminal mass in orbit was approximately 12,200 kg (28,000 lbs.) giving a mass ratio of 5.1. Since Phase I studies of Stage 2 performance indicated a weight ratio of 4.65 was attainable, it was concluded that further improvements in the trajectory were possible from a performance standpoint. Accordingly, the calculations were continued until iteration 40 with the results given in Figure 5-8 which show that the calculations were diverging from the desired end point. At this point these calculations were abandoned since this divergence was traced to the presence of spurious perturbations in the control variable history. These spurious perturbations were capable of introducing end point changes of the magnitude of 120 km (400,000 ft.) in the terminal conditions.

5.2 Optimal Staging Solution

At this point in the study the calculations were continued using an experimental optimal staging program developed from the computer program of Reference 5. The parametric study of staging point position is avoided by the use of this program. Further, since it was apparent from the previous calculation that a coast period had developed, the second stage trajectory was divided into a boost-coast-boost mission. Each of these stages retained continuous control of pitch, bank and throttle in the powered stages together with the control of the duration of each stage. Since the duration of the last stage is automatically perturbed by the steepest-descent method, this approach introduced three additional control parameters: one for the end of Stage I, a second for the termination of the first burn of Stage II,

USE FOR DRAWING AND HANDPRINTING — NO TYPEWRITTEN MATERIAL

FINAL GROUND TRACK FIXED STAGE PROGRAM

FIGURE 5-1

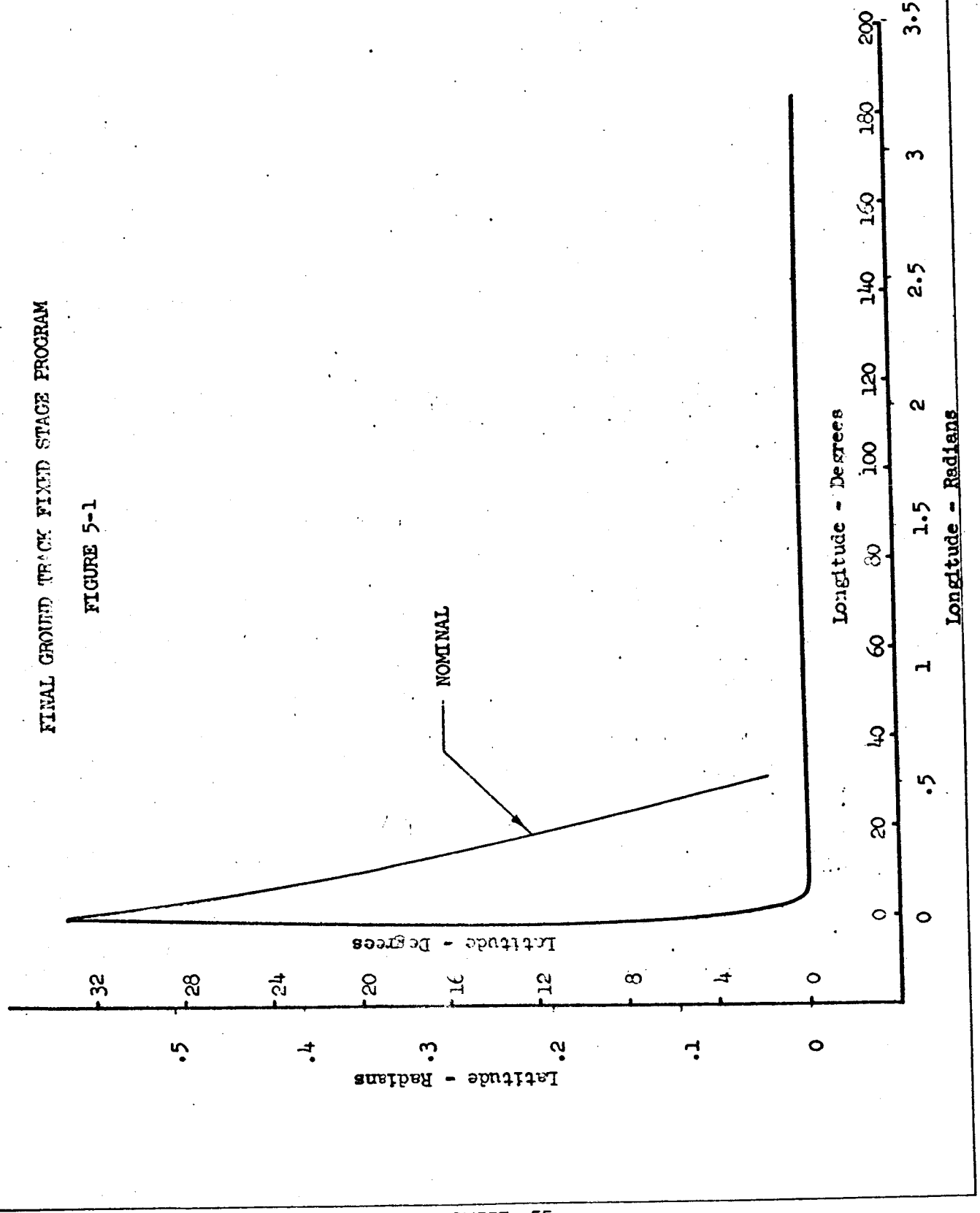

FINAL VELOCITY - ALTITUDE PROFILE
FIXED STAGE PROGRAM

FIGURE 5-2

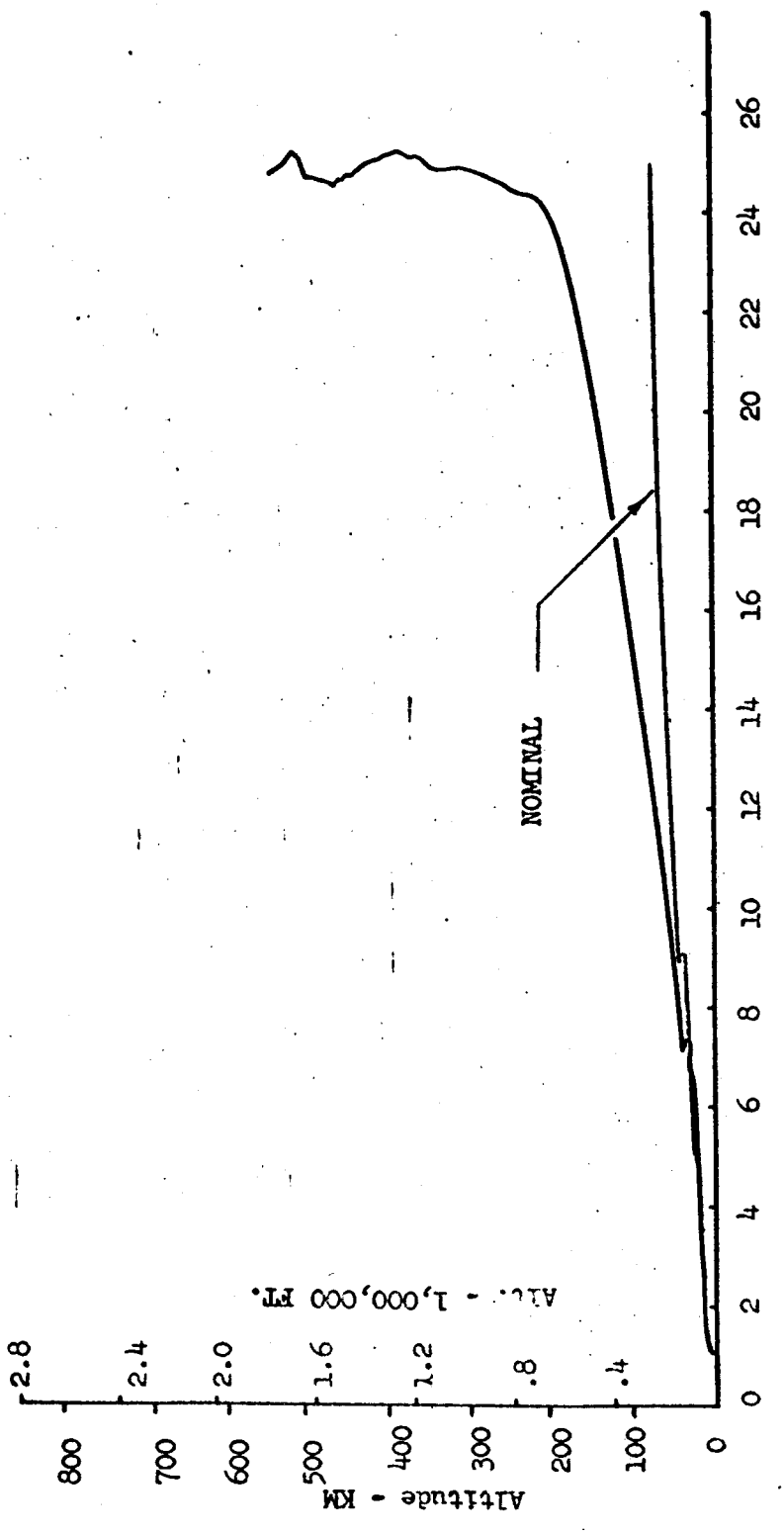

FINAL ALTITUDE HISTORY-FIXED STAGE PROGRAM

FIGURE 5-3

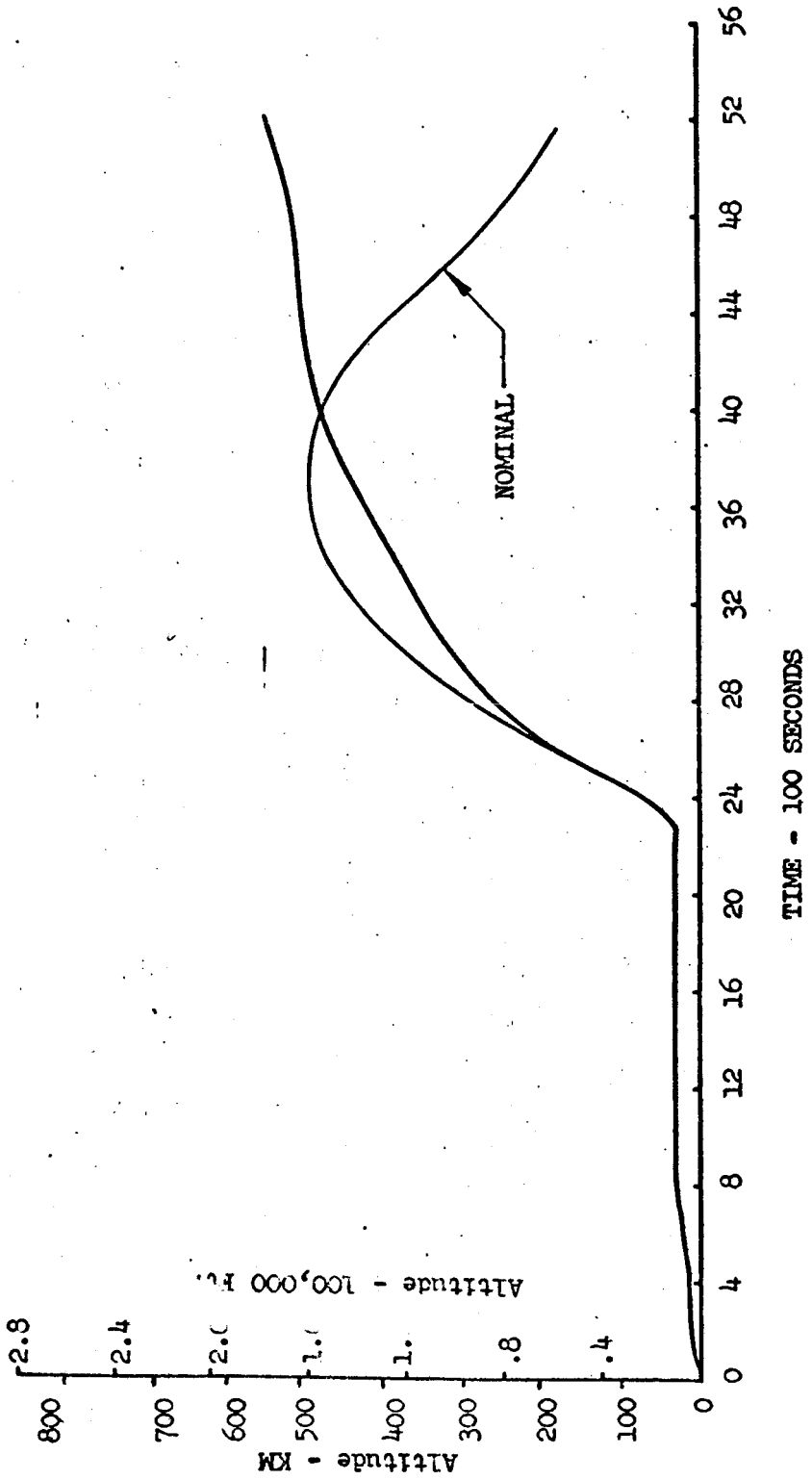

FINAL DYNAMIC PRESSURE HISTORY
FIXED STAGE PROGRAM

Figure 5-4

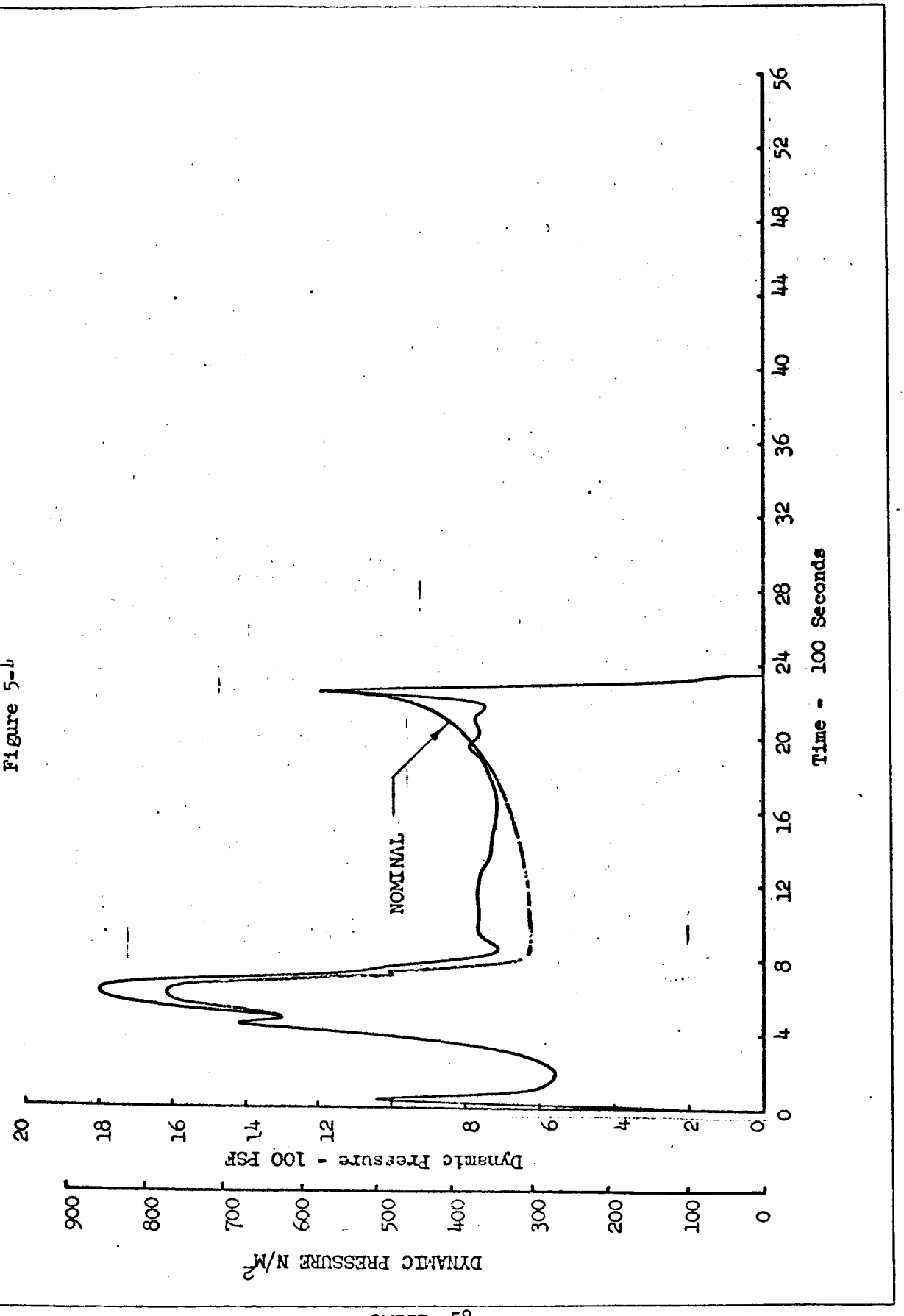

FINAL SCALAR PITCH CONTROL HISTORY

FIXED STAGE PROGRAM

Figure 5-5

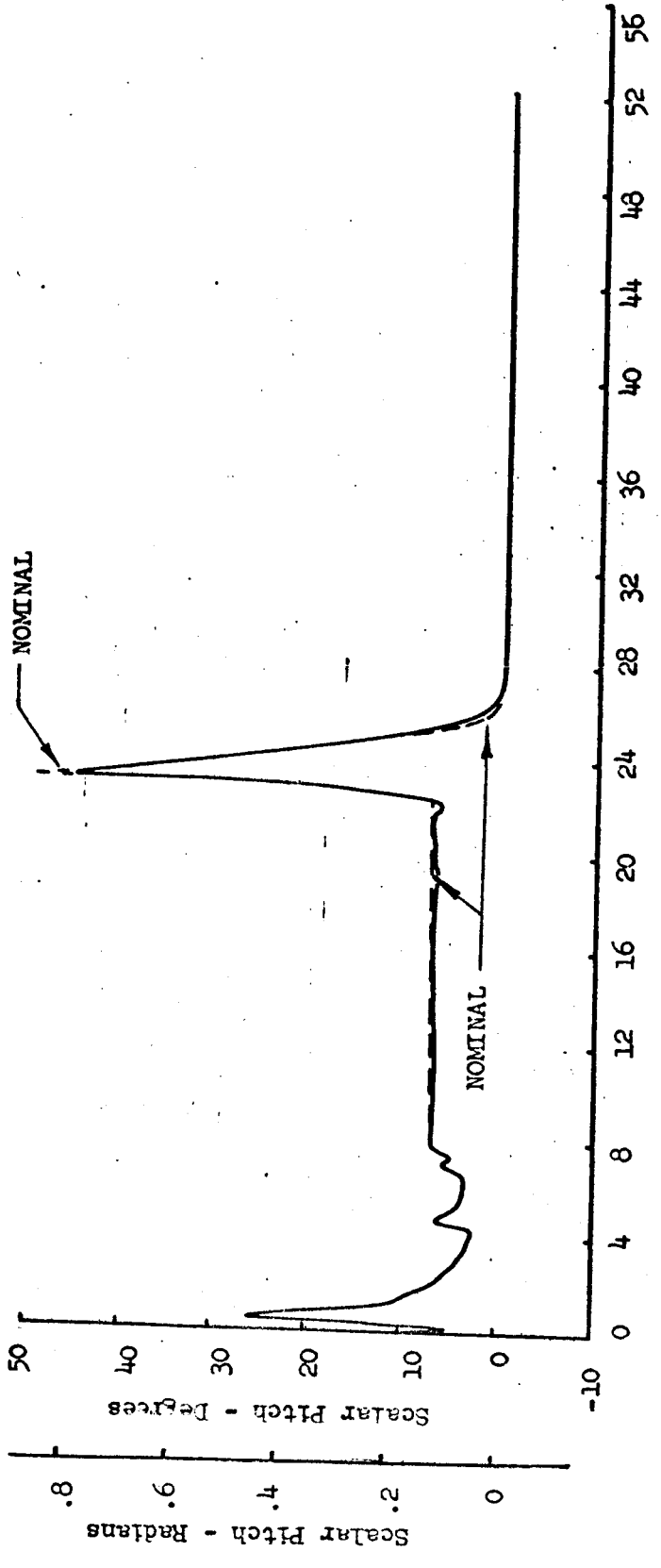

FINAL BANK ANGLE HISTORY

FIXED STAGE PROGRAM

FIGURE 5-6

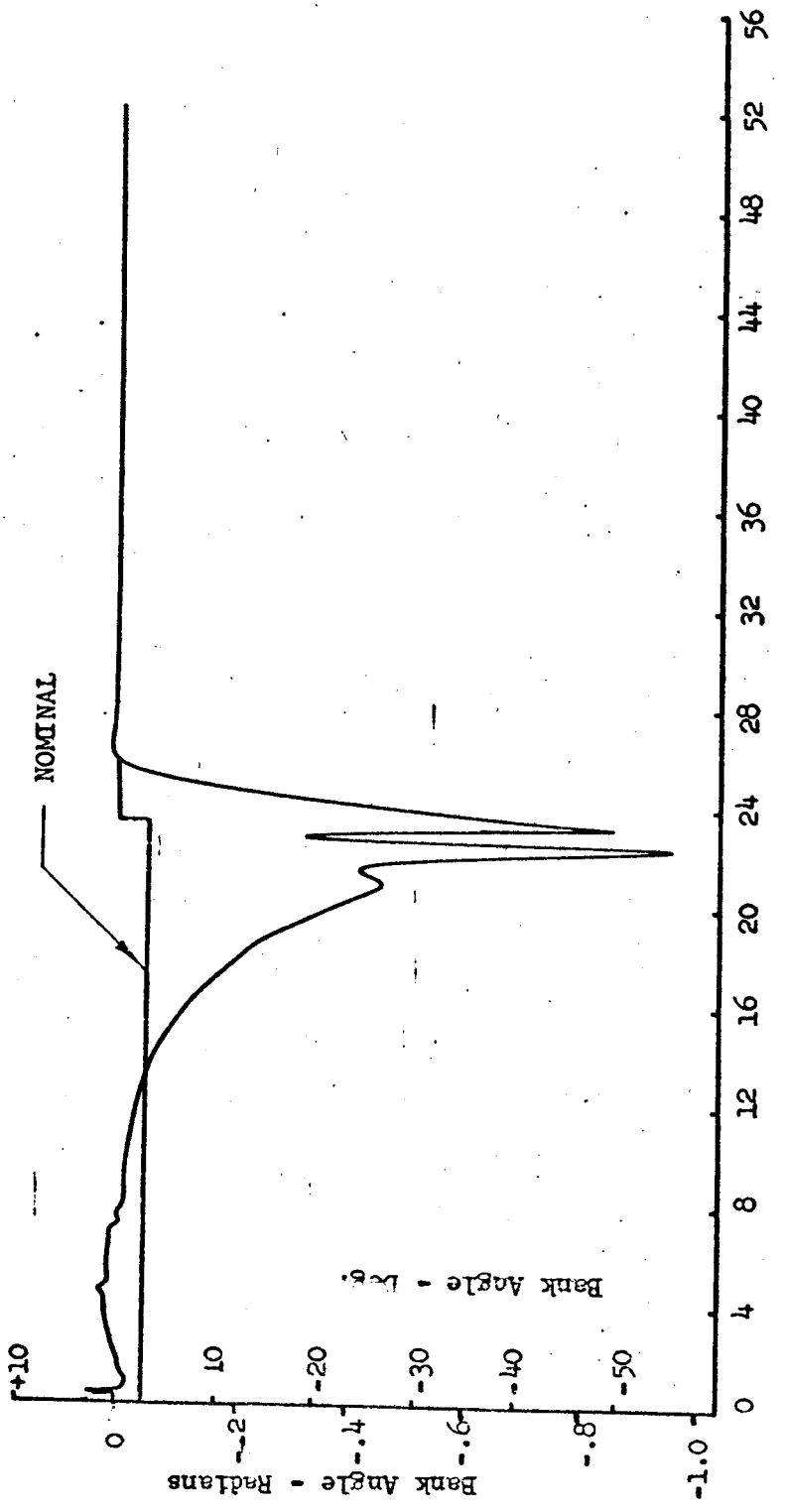

FINAL THROTTLE HISTORY
FIXED STAGE PROGRAM

Figure 5-7

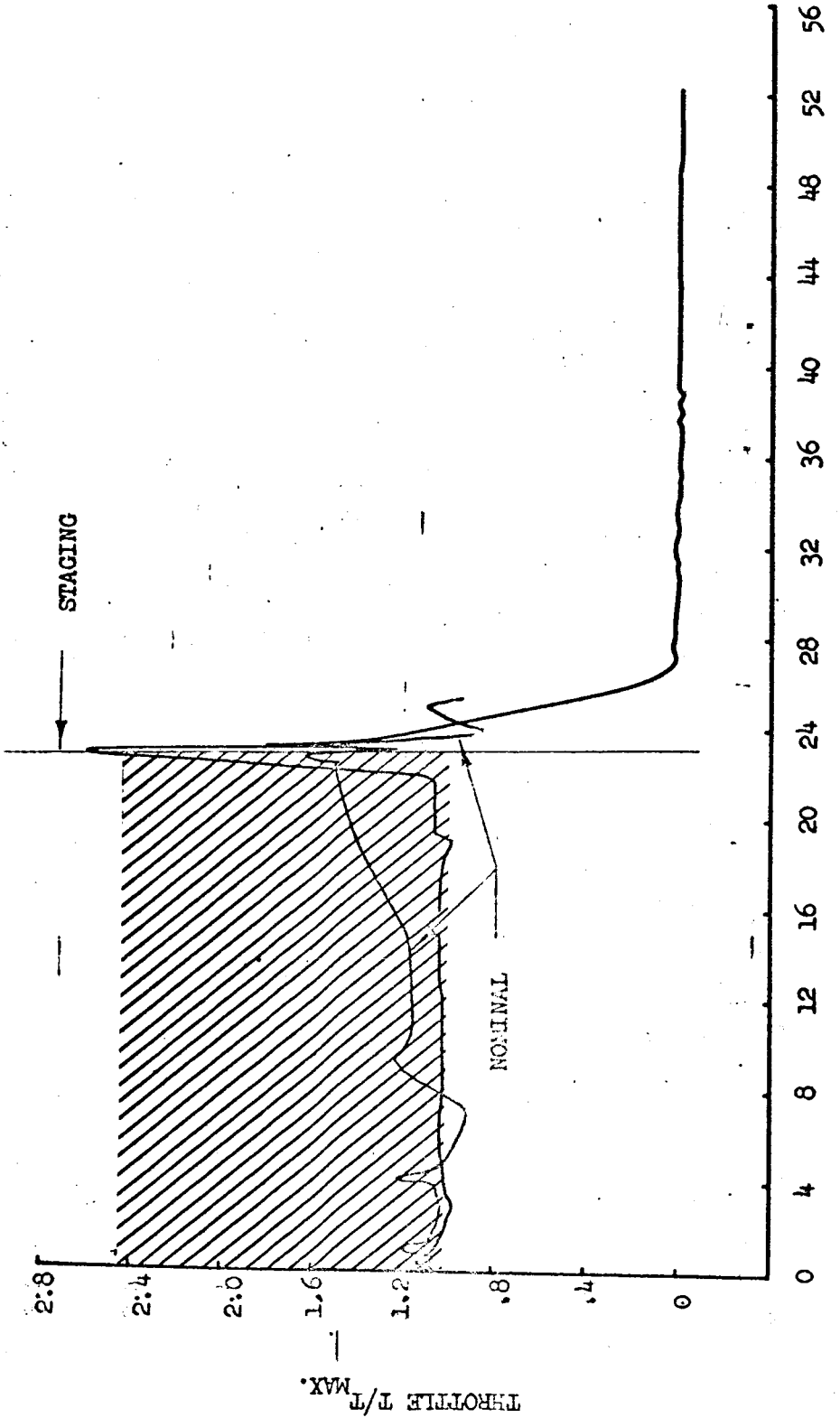

CONVERGENCE BEHAVIOR
STAGE 1/STAGE 2 OPTIMIZATION
Fixed Stage Time Program

Figure 5-8

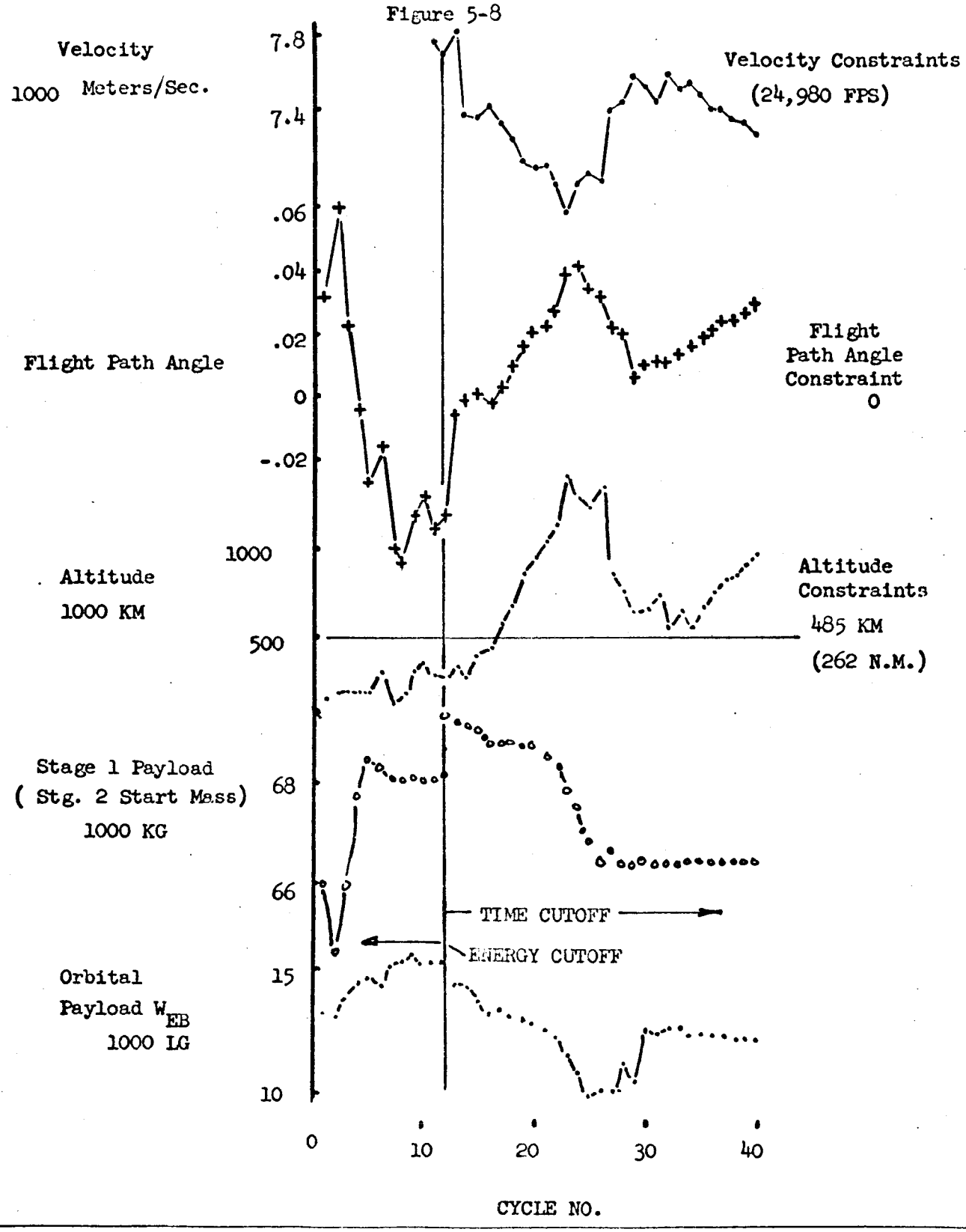

and a third at the end of Stage II coast. These modifications resulted in considerably different end conditions from the values obtained on cycle 32, particularly in the terminal altitude attained.

Since substantial alterations had to be made to the program of Reference 5 in order to solve the present problem, the program was first checked against a previously reported result. An orbital transfer problem involving a boost-coast-boost trajectory contained in Reference 4 was used for this purpose. The optimal-situation obtained showed agreement to four significant figures with the result presented on page 489 of Reference 4.

On completion of this test problem the optimal staging program was applied to the entire Stage I/Stage II trajectory. Convergence plots for these calculations are shown in Figures 5-9. It can be seen from the performance function convergence plot, Figure 5-9, that the terminal orbital mass is 14,200 kg (978 slugs). The launch vehicle configuration under investigation therefore provides an orbital mass to initial mass ratio of .063. That is, approximately 16 slugs of initial weight are required for each slug in orbit. This compares with a figure of 18.5 to 1 obtained in the Phase 1 study by more orthodox performance techniques. It can be seen from Figure 5-10 that all the terminal constraints imposed were essentially met. The convergence plots show a break at cycle 23. At this point the calculations were interrupted and for a period Stage I and Stage II were separately optimized. First, the terminal mass of Stage I was optimized to the staging conditions established by the Stage I/Stage II calculation at cycle 22. The behavior of the Stage I mass during these calculations is shown in Figure 5-10. Following the separate Stage I optimization calculation, Stage II of the vehicle was separately optimized from the new initial conditions established by the Stage I alone calculation. The behavior of the performance function mass in orbit during these calculations is shown in Figure 5-11. Following optimization of the separate stages they were brought together again and the complete Stage I/Stage II optimization was continued. The behavior of these calculations can be seen from Figure 5-9 following cycle 22. During this last period of calculation various combinations of weighting matrix and weighting parameters were employed. In the terminal phase of the calculation choice of weighting matrix or weighting parameters had little effect on the results, as might be anticipated.

The final control histories for the complete Stage 1/Stage 2 trajectory are shown in Figures 5-12 to 5-14. The final velocity-altitude profile for the complete mission is shown in Figure 5-15. Staging occurs at 2322.6 seconds. The Stage 1 cruise is a somewhat higher altitude than previously anticipated. A violation of the inequality constraints occurs just prior to staging because the calculation was not continued to a complete solution. The Stage 2 profile is considerably different than that

CONVERGENCE BEHAVIOR
STAGE 1/STAGE 2 OPTIMIZATION
OPTIMAL STAGING PROGRAM

Figure 5-9

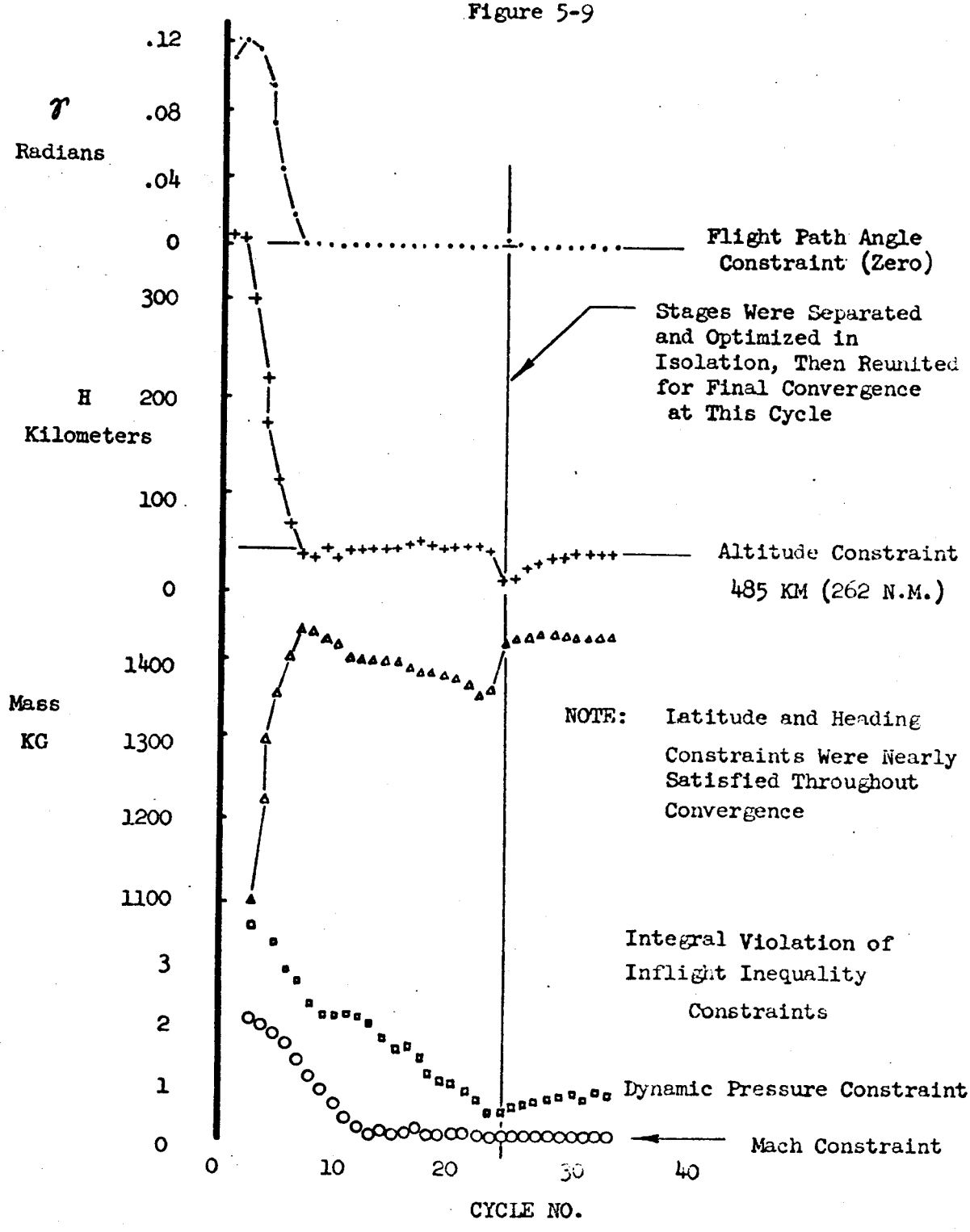

CONVERGENCE BEHAVIOR
STAGE 1 OPTIMIZATION
OPTIMAL STAGING PROGRAM

Figure 5-10

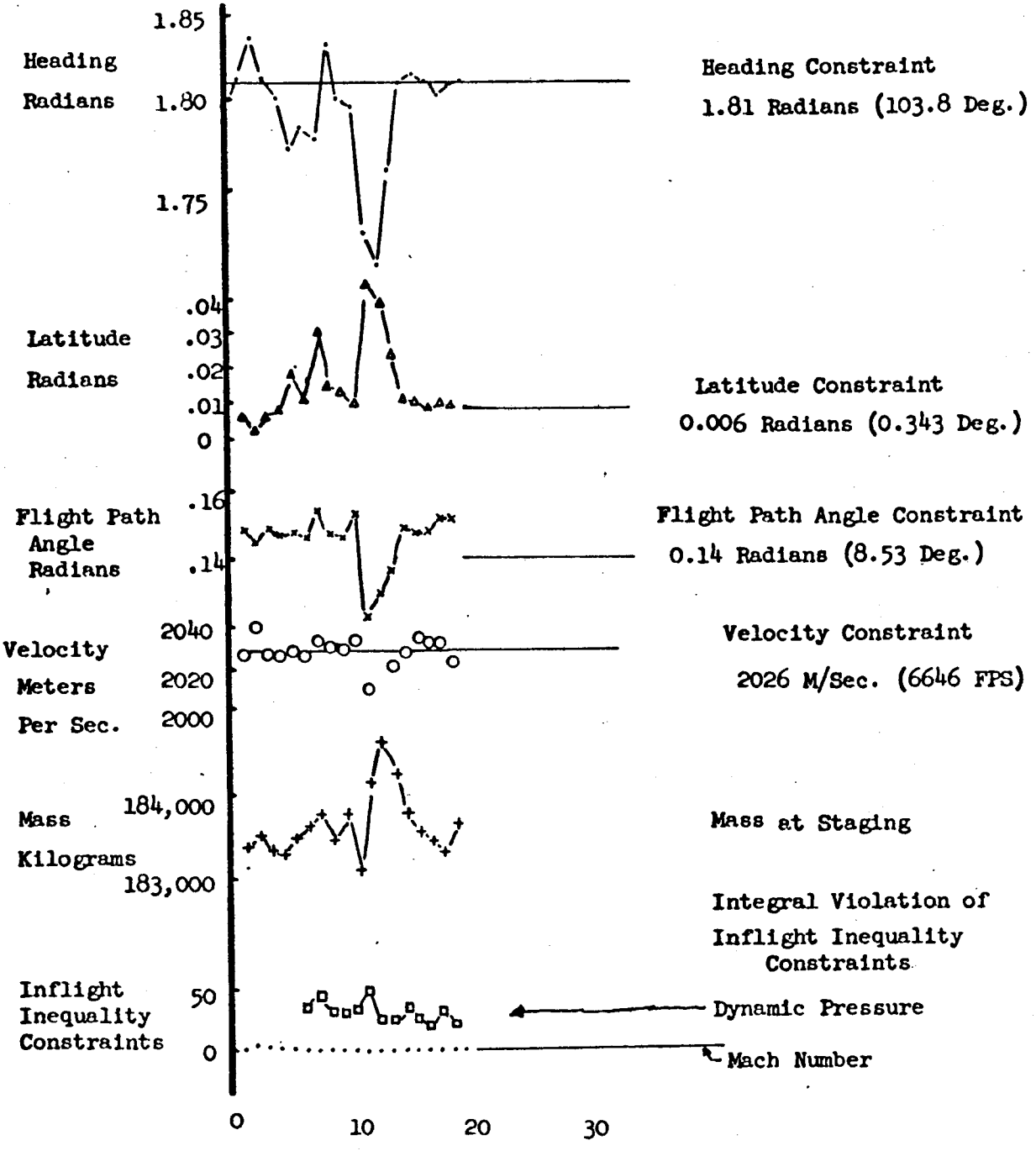

CONVERGENCE BEHAVIOR
STAGE 2 OPTIMIZATION
OPTIMAL STAGING PROGRAM

Figure 5-11

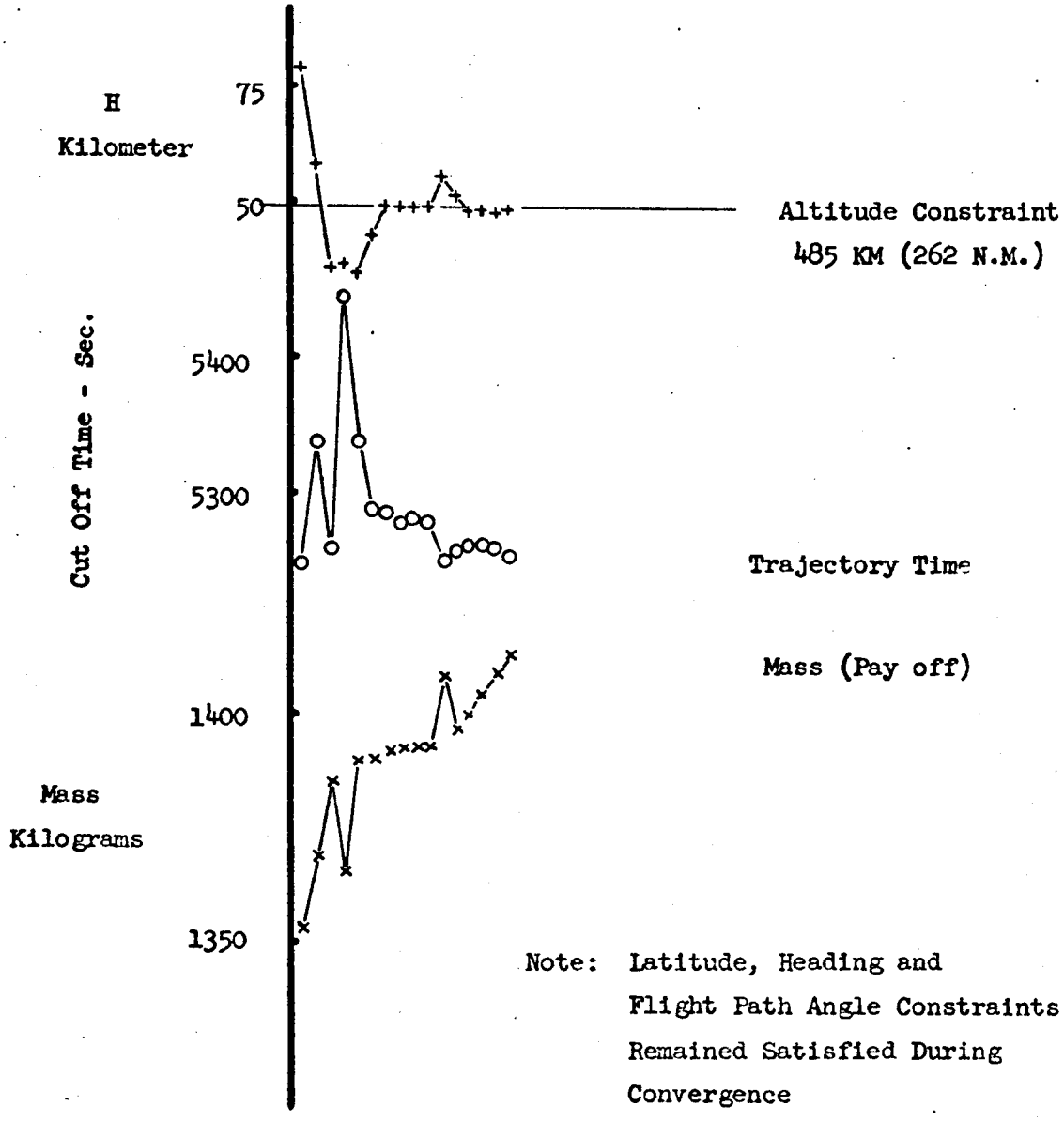

Note: Latitude, Heading and Flight Path Angle Constraints Remained Satisfied During Convergence

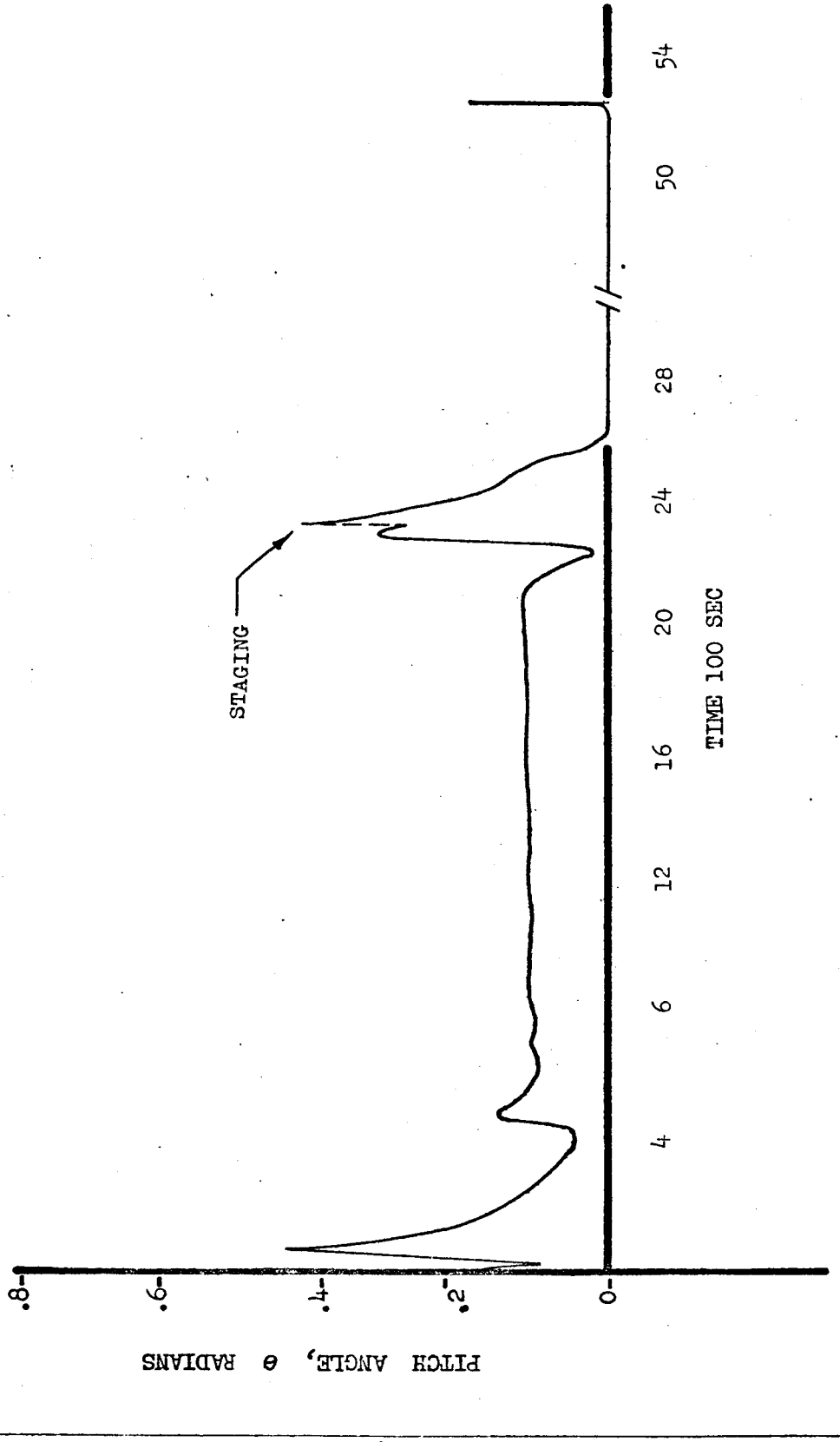

PITCH ANGLE CONTROL HISTORY
STAGE 1/STAGE 2 TRAJECTORY

FIGURE 5-12

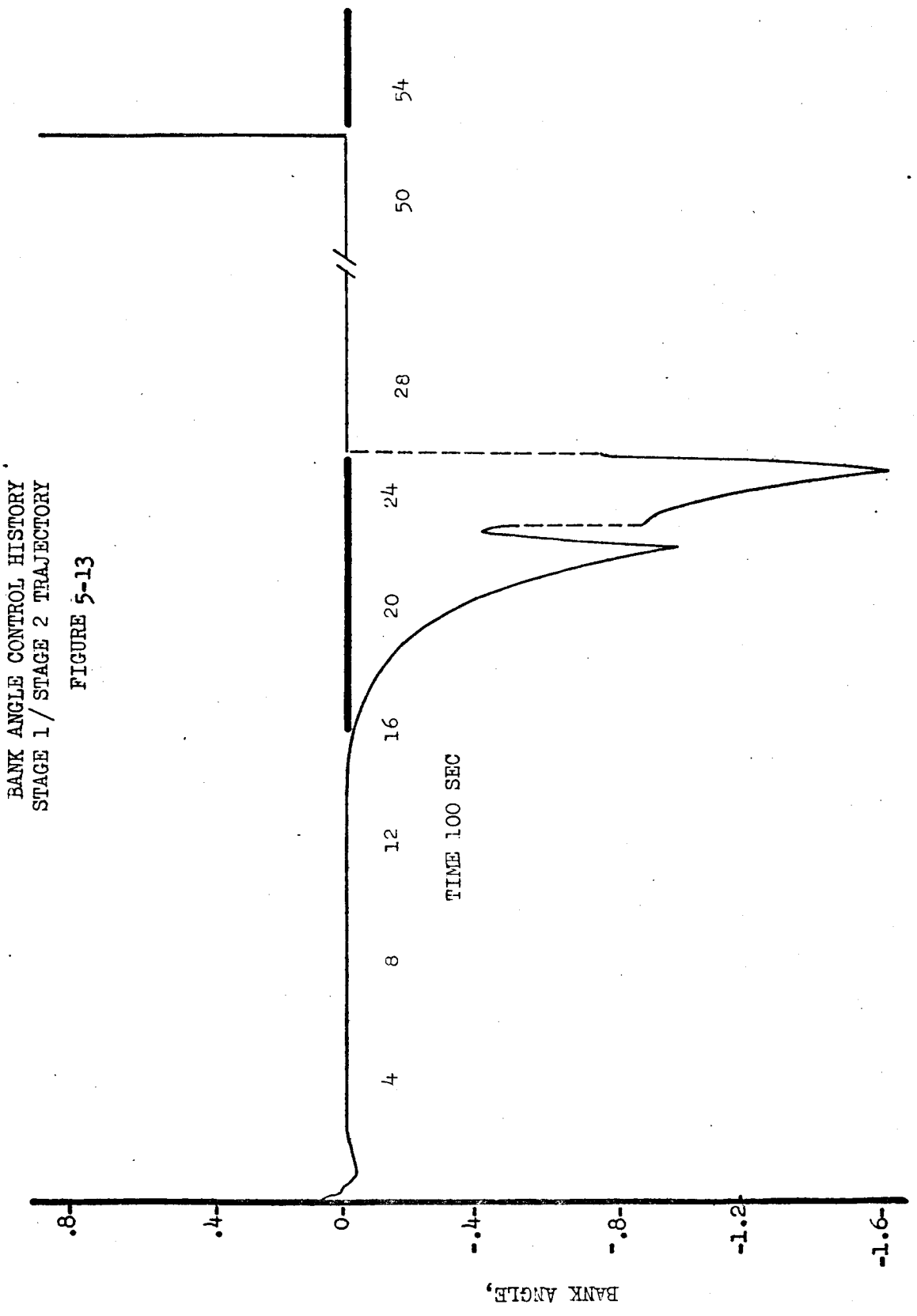

BANK ANGLE CONTROL HISTORY
STAGE 1 / STAGE 2 TRAJECTORY

FIGURE 5-13

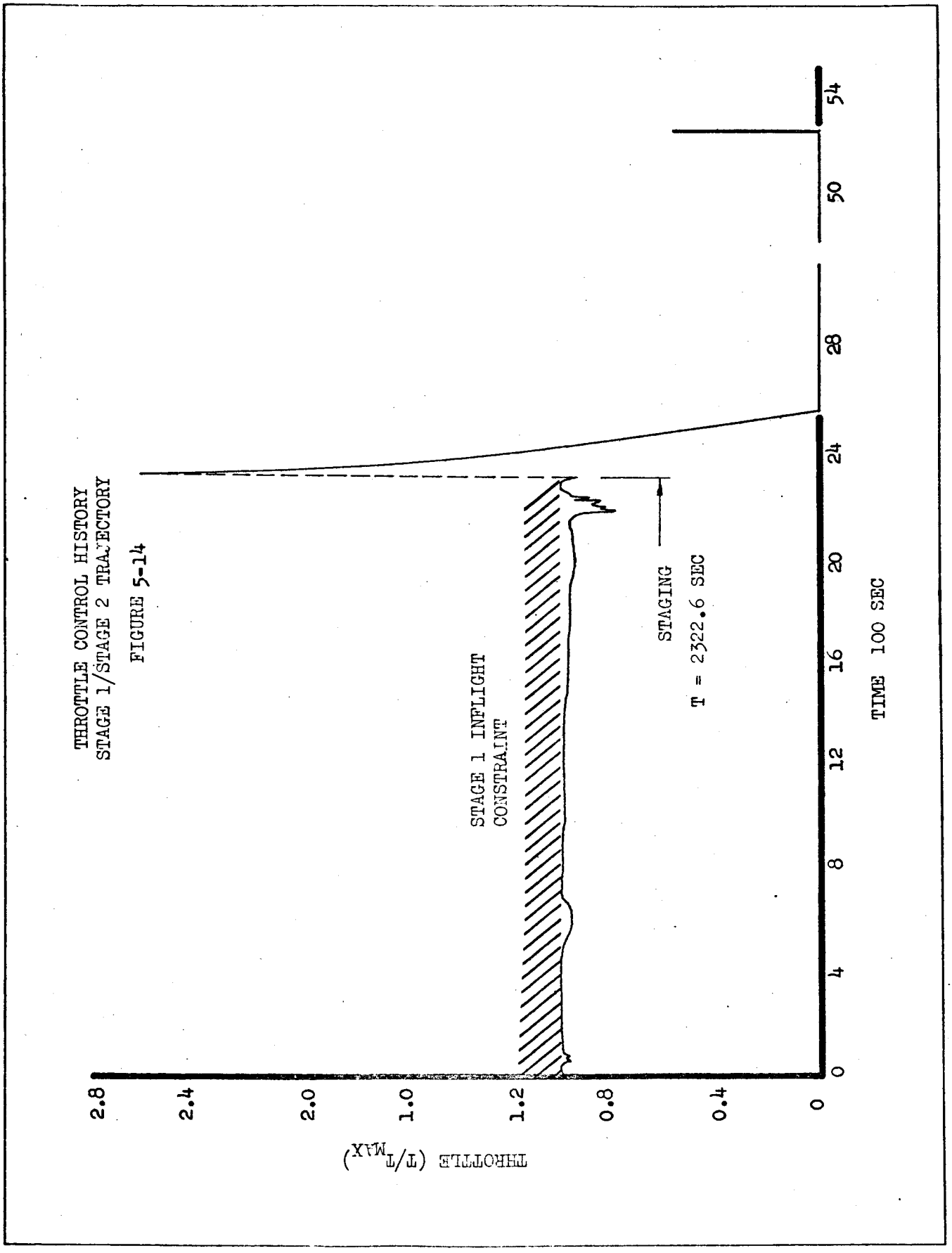

V-H PROFILE
STAGE 1/STAGE 2 TRAJECTORY

FIGURE 5-15

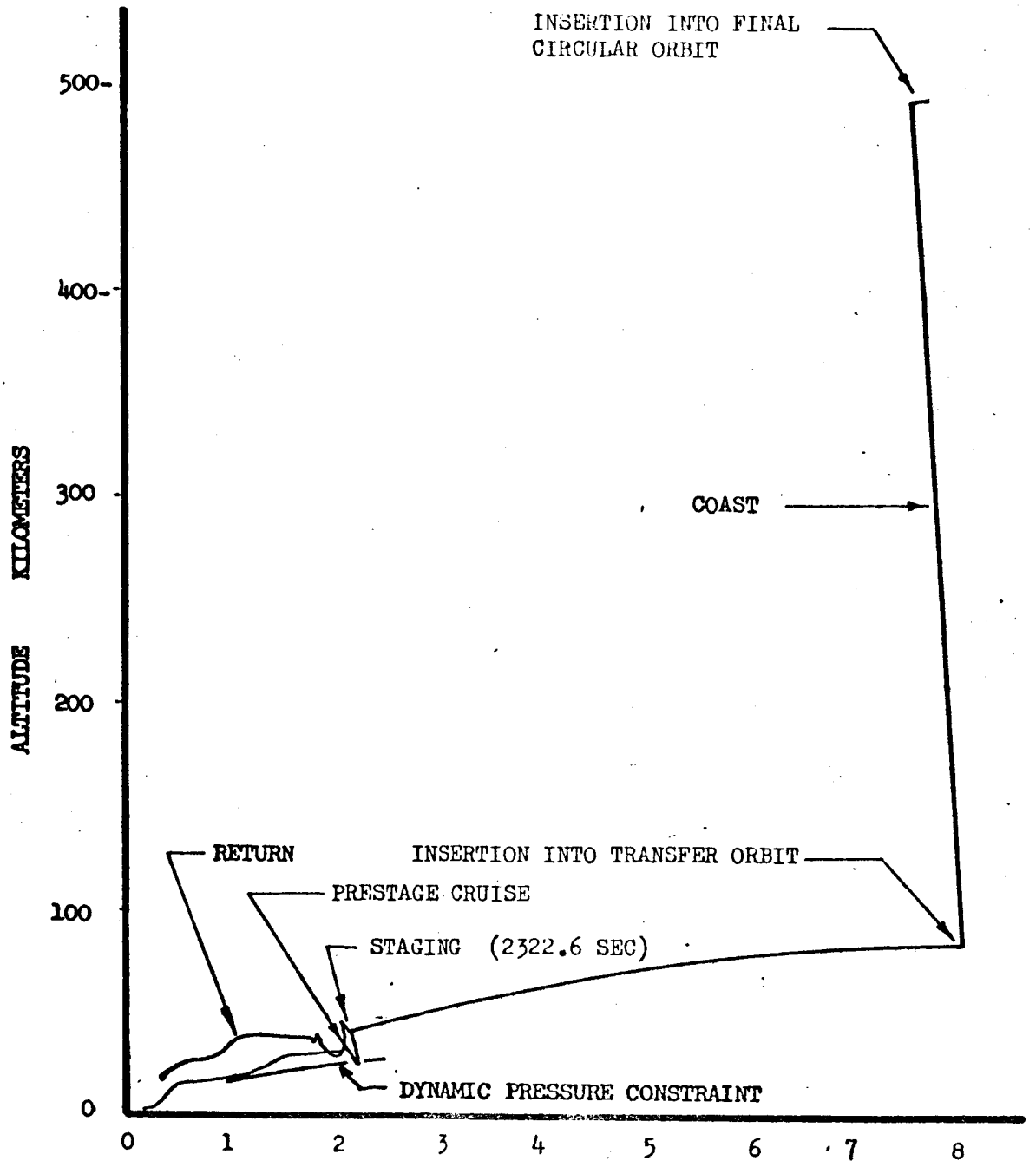

of Figure 5-2 using the fixed stage program. The trajectory is discussed in more detail in Section 6.

5.3 Stage 1 Return

Using the staging conditions established by this calculation the return trajectory was optimized as an independent problem. The initial conditions for this calculation at staging with a mass decrease of 118,500 kg (261,603 lbs.), are:

Velocity	=	2,115 m/sec (6,942 ft/sec).
Altitude	=	39.5 km (129/594 ft)
Gamma	=	9.10°
Latitude	=	0.523°
Longitude	=	6.711°
Heading	=	102.433°
Mass	=	118,500 kg (8,131 slugs)

The objective in this mission segment was to return to base with a minimum fuel expenditure. Accordingly the terminal constraints were chosen as:

Latitude	=	33.333°
Longitude	=	0°
Altitude	=	15.2 km (50,000 ft)

The first constraint, latitude was used as cutoff function since this appeared to be the most likely to increase in a monotonic fashion. Once again a smooth nominal was employed for the optimization calculation. The control histories used were:

Pitch Angle = 6° Constant
Bank Angle = 10° decreasing to 0
Throttle Constant = .7

The final optimal trajectory obtained after 25 iterations is shown in Figure 5-16. Convergence behavior during these calculations are shown in Figure 5-17. The final mass on the optimum trajectory is 107,000 kg (7,343 slugs) indicating a fuel expenditure of 11,470 kg (25,344 lbs.) This represents a reduction in return fuel requirements of 3,170 kg (7,000 lbs.) with amounts to a 28% reduction in the amount of fuel required, compared to the Phase I parametric study results.

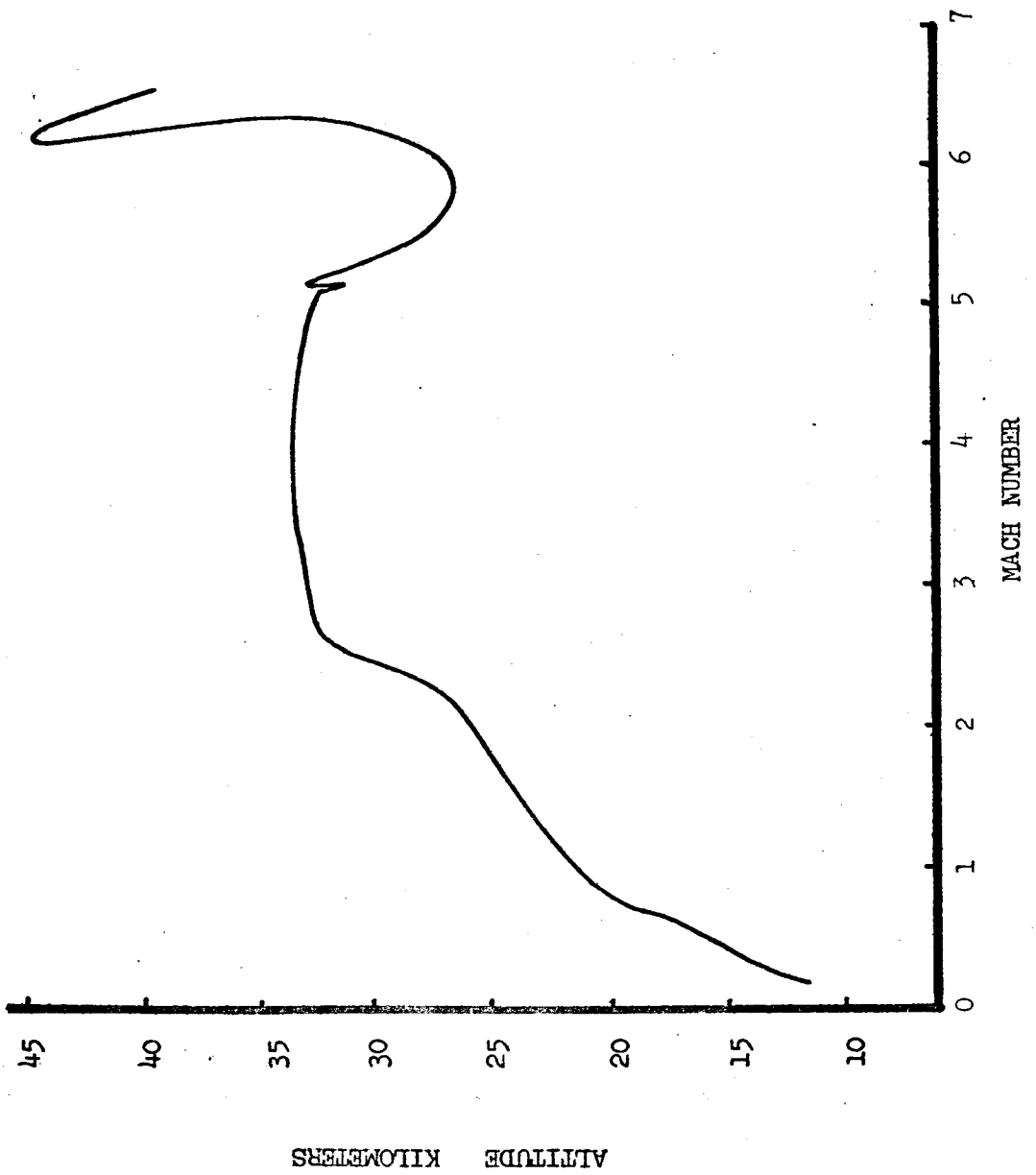

MACH ALTITUDE PROFILE
STAGE 1 RETURN

FIGURE 5-16

STAGE 1 RETURN

CONVERGENCE HISTORY

FIGURE 5-17

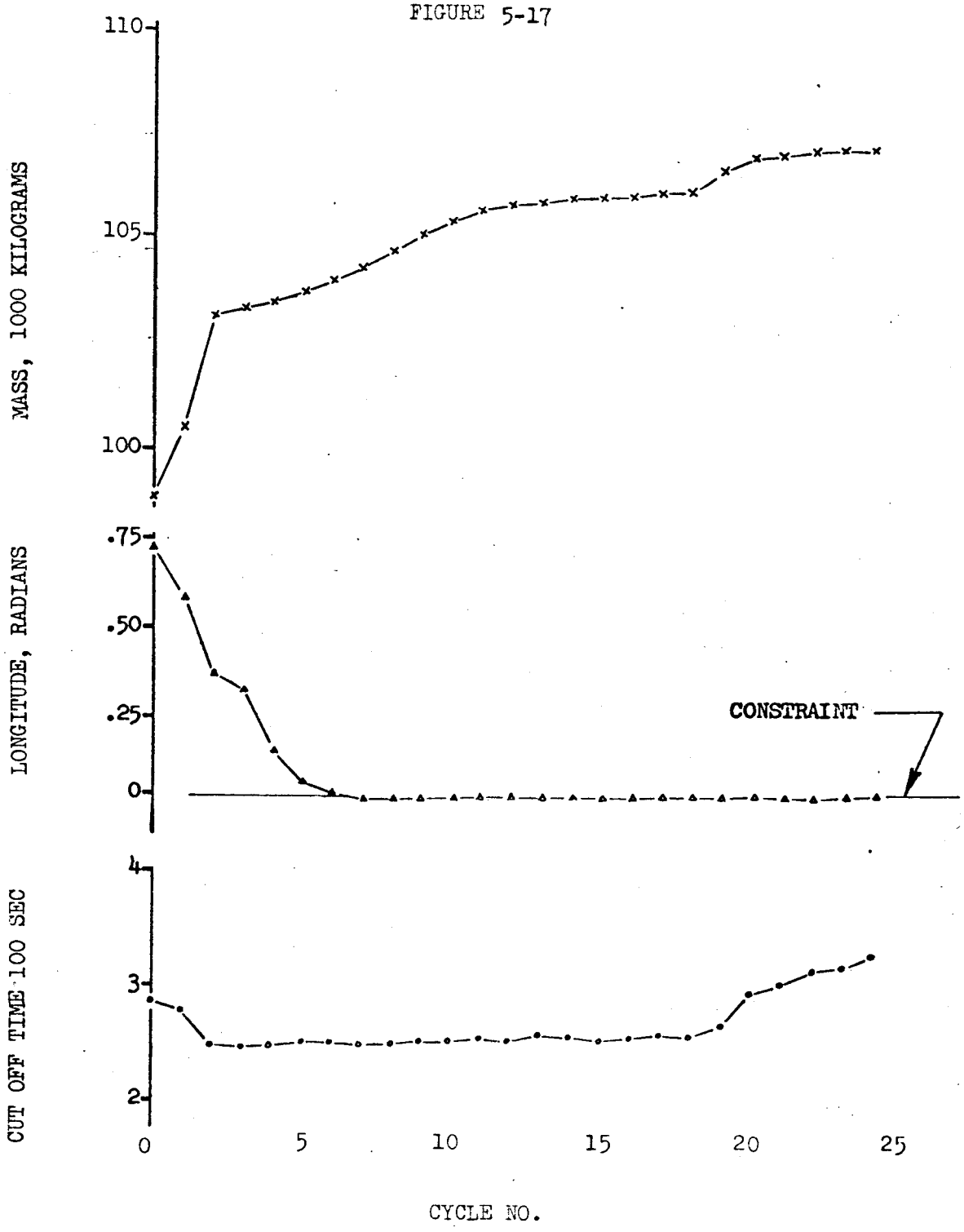

6.0 ANALYSIS OF THE TRAJECTORIES

Detailed discussion of each phase of the trajectory are contained below. For this discussion the mission has been divided into Stage I outbound mission, Stage II ascent to rendezvous, Stage I return, and the staging maneuver.

6.1 Stage I Outbound Flight Path

Details of the Stage I outbound and return segments are shown in Figures 6-1 to 6-3. Figure 6-1 shows the ground track with time ticks and pertinent state components identified. The staging point occurs at a longitude of 6.7° East and at a latitude of about 0.5° North. The fact that the Stage 2 launch does not occur in the equatorial plane was anticipated. The outbound cruise fuel used varies almost linearly with latitude change as shown in Figure 6-3 (the rate of fuel consumption is constant). However, the Stage II fuel required for small out-of-plane perturbations at this point varies parabolically, having zero slope for zero offset. A conventional analysis of this trade using a full 90° turn indicated suboptimal release point about a quarter of a degree North of the Equator. The optimal flight path which is obtained with the full trajectory dynamics, establishes the stage point at about half a degree North of the Equator, with release occurring at a heading angle 12° South of East. It should be remembered that this release point is obtained without considering the effect of the Stage I return path. Analysis of the effect of the return on a seven component state would be essentially speculation without the use of the full system dynamics.

It can be seen from the Mach - altitude profile of Figure 6-2 that a highly dynamic staging maneuver has been developed. It is called a synergetic zoom-turn because of its unique character. This is discussed in further detail below in Section 6.4. It is also apparent from Figure 6-2 that the acceleration from Mach 3 to Mach 7 does not follow the dynamic pressure inequality constraint boundary. Below Mach 3 the sonic boom overpressure limit is followed. On staging to the higher thrust ramjet engine, however the vehicle climbs until reaching Mach 5. Above this Mach number the vehicle tends to follow a dynamic pressure profile of about 11,800 N/M^2 (800 psf). The acceleration above Mach 5 is quite gradual taking about 890 seconds to reach cruise altitude. Figure 6-3 shows fuel consumption slope in this region to be closer to cruise than acceleration conditions.

Cruise occurs in the region of Mach 6.8, a somewhat lower velocity than had been anticipated from the steady state range equation. It can be seen from Figure 6-1 that cruise, in the classical sense, occurs for only about 1/3 of the outbound flight path. A pronounced knee occurs in the Mach-altitude profile at Mach 5. Analysis of the engine data indicates that this is the point at which the thrust coefficient of the ramjet engine first starts to fall off. It may also be noted that this is also the Mach Number at which the cruise dynamic pressure is first acquired. Either or both of these reasons influence the trajectory in this region.

GROUND TRACK
STAGE 1 & RETURN
FIGURE 6-1

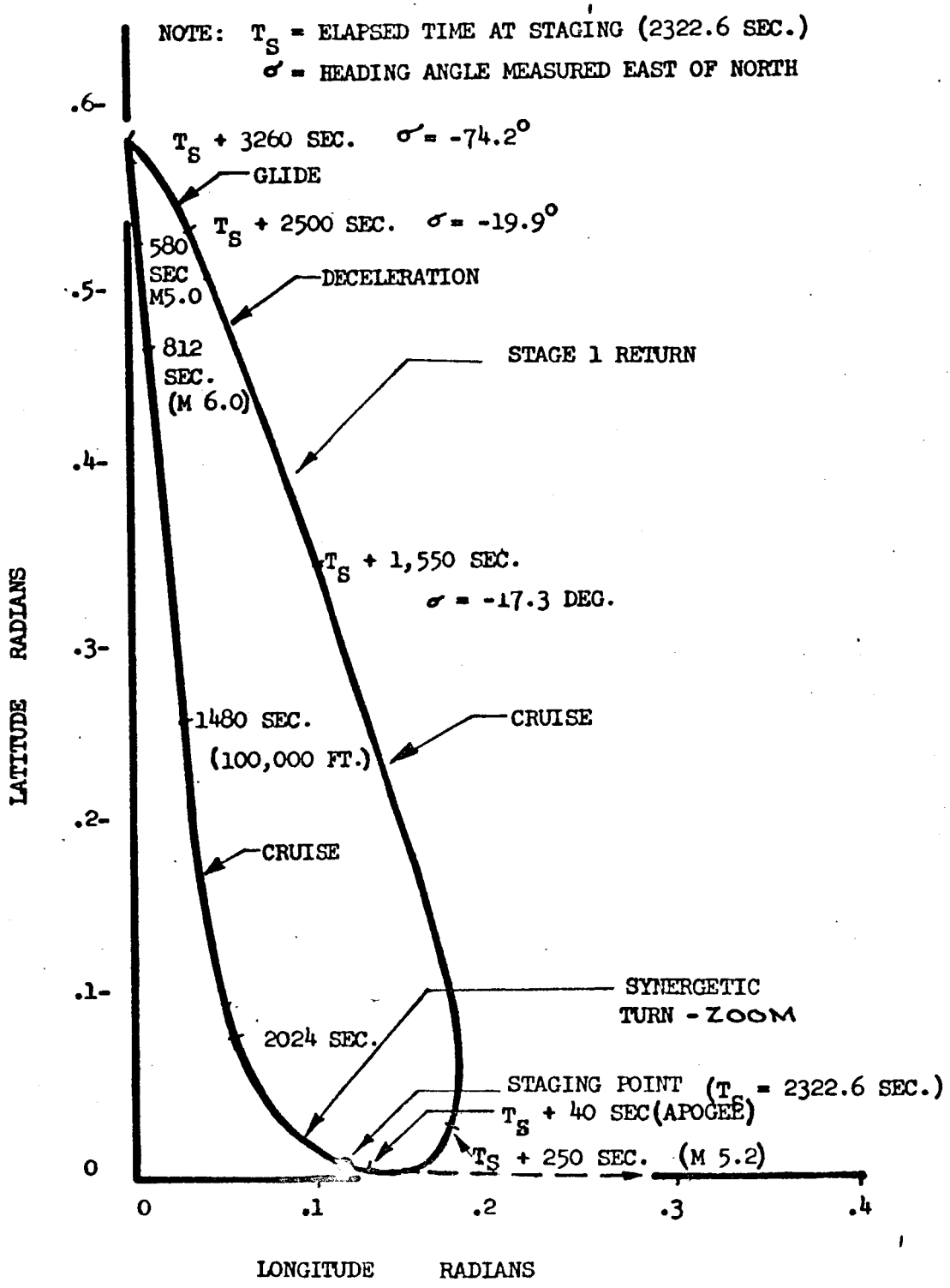

MACH ALTITUDE PROFILE
STAGE 1 AND RETURN

FIGURE 6-2

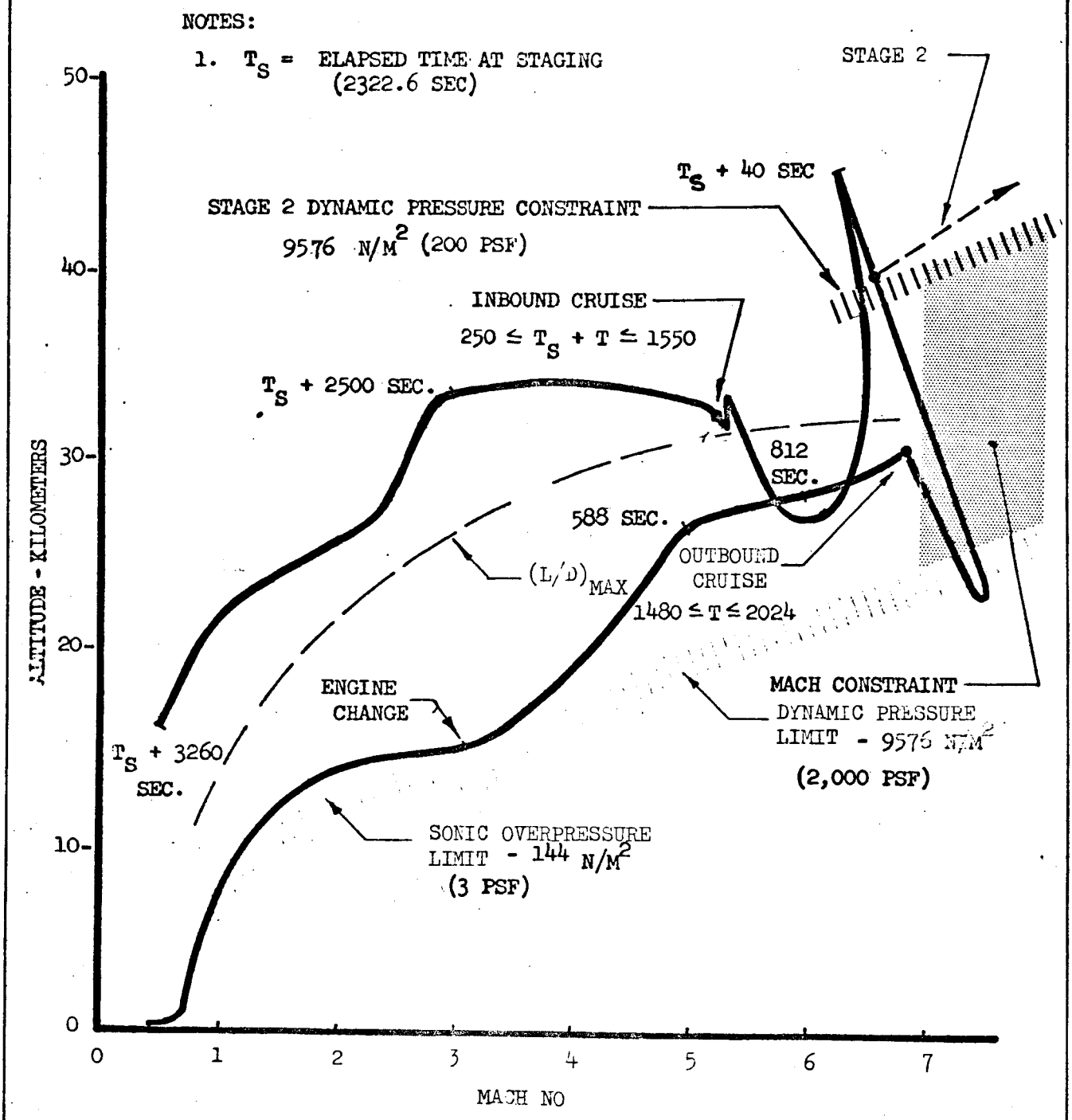

WEIGHT SCHEDULE
STAGE 1 AND STAGE 2
FIGURE 6-3

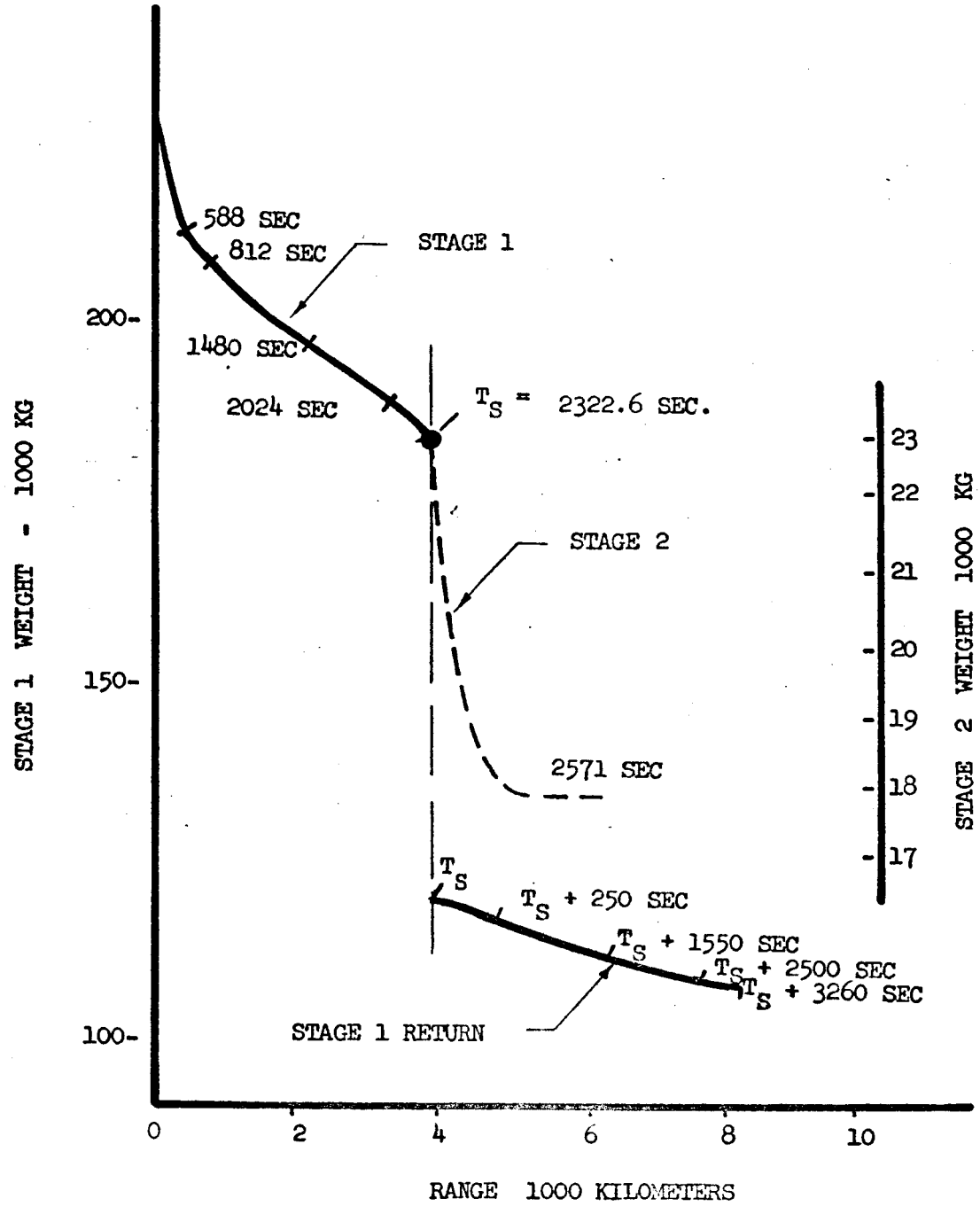

Analysis of the energy derivatives with respect to the mass flow rate for the acceleration profile would give further insight. This analysis is presently unavailable.

Figure 6-1 reveals that the major portion of the acceleration and cruise takes place at a heading approximately 15° East of South. The heading change from due South occurs quite rapidly at low speed. Turning losses at this speed are small. Apparently the optimization process is trading an increase in cruise duration against the losses during the high speed turn. Again it should be cautioned that this result is based solely on the Stage 1/Stage 2 optimal flight path with no regard to return. The Phase I parametric analysis on the other hand indicated a slight Westerly cruise component based on the relative efficiency of the inbound and outbound cruise. This is illustrated in Figure 6-3 by the relative slopes in the two mission segments. This same tendency may be present on the optimal flight path where a complete optimal staging multi-vehicle solution is obtained. The tool for this calculation does not exist at this time. In the absence of such a calculation the trades involved in staging position determination elude conventional analysis in view of the dynamic nature of the final flight path.

6.2 Stage 1 Return Trajectory

The stage 1 return trajectory is shown in Figure 6-1 to 6-3. The control histories are shown on Figures 6-4 to 6-6. The return mission can be divided into four segments for analysis: (1) a dynamic return to the cruise condition, (2) a cruising segment, (3) a deceleration at constant altitude to Mach 3, followed by (4), a deceleration glide to the terminal condition. The first segment of this mission is discussed in Section 6.4 as part of the staging maneuver. The steepest-descent generated cruise condition occurs at Mach 5.2 and 32.3 km (106,000 ft.). The cruise condition is acquired before completion of the initial turn. However, during the cruise portion of the turn, the heading change rate is quite moderate and diminishes to practically zero about a third of the way through the cruise segment. This is apparent from the bank angle history of Figure 6-5. The cruise condition is initially acquired at 250 seconds after staging and continues for 1300 seconds. The return cruise therefore occurs at a Mach number considerably below the design cruise Mach number of 7. Presumably it is more efficient to cruise at the recovery Mach number than to attempt a reacceleration to Mach 7 for the time periods involved. It may be noted that the cruise condition is somewhat above the max $\frac{L}{D}$ Mach-altitude line. Following cruise the constant altitude decelerating segment to Mach 3 is of almost 1,000 seconds duration, the Mach 3 condition occurring at time = 2500 seconds from staging. At this point a switch-over from ramjet engines to turbojet engines occurs. Simultaneously the final segment of the return commences. The decelerating glide is terminated at 3260 seconds from staging at approximately 15.2 km (50,000 ft.) altitude in a subsonic condition.

The remaining portion of the cruise segment and the

deceleration occur at almost constant heading angle. During the final glide an increase in bank angle occurs and the final turn is generated, ending in a near Westerly heading. Apparently the optimization process has detected a favorable trade between high speed turning losses and path length. The control histories of Figures 6-4 to 6-6 during this return mission are relatively smooth. The return does exhibit some of the characteristics of near orbital velocity re-entries, notably in the development of a skip like acquisition of the cruise condition, although the characteristic oscillatory motion of very high speed re-entries is practically absent.

Finally it is emphasized that though the return has been discussed in terms of a sequence of subarcs, the complete path from staging to mission termination was optimized as a single trajectory with only the end position as terminal constraints. It is anticipated that this segmentation will provide insight into the type of behavior which can be expected on other missions. For example, the cruise mission has been estimated by this technique and the results presented in Volume 4.

6.3 Stage 2 Ascent to Orbit

The Stage 2 velocity altitude path is contained in Figure 5-15. The optimal staging calculations have resulted in a well defined velocity-altitude profile. The first burn builds up energy practically normal to the energy contours. Constant energy coast follows. Insertion occurs with a small impulse at the coast termination. The trajectory history for the first burn period is shown in Figure 6-7 where velocity, altitude, pitch angle and heading are presented as a function of time. A somewhat unusual velocity history is discussed in detail in Section 6.4. Figure 6-8 presents the Stage 2 velocity losses compared with the vacuum solution. The vacuum solution was obtained using fixed thrust by the comparatively rapid computer program of Reference 8. The difference between the vacuum solution and the optimal staging solution can be attributed to the presence of the atmosphere in the optimal staging solution. The steepest descent process seeks a transfer orbit with lower perigee in a vacuum than in the presence of an atmosphere which reduces the thrust vectoring losses for the near horizontal launch of the second stage. However the benefit is nearly offset by an increase in gravity losses during the coast. The final orbital mass in both calculations was essentially equal. This may be attributable to the fact that the vacuum calculation uses constant thrust whereas the optimal Stage 1/Stage 2 calculation was performed using the assumption of throttleable engines throughout the entire flight path including Stage 2. This point has not been analysed in detail.

6.4 The Staging Maneuver

Staging maneuver details are contained in Figure 6-9 to 6-14 . For the purpose of this section the staging maneuver is defined as that part of the mission lying between Stage 1 outbound cruise termination through the stage point to the start of Stage 1 return cruise, and includes the first burn of the second stage module.

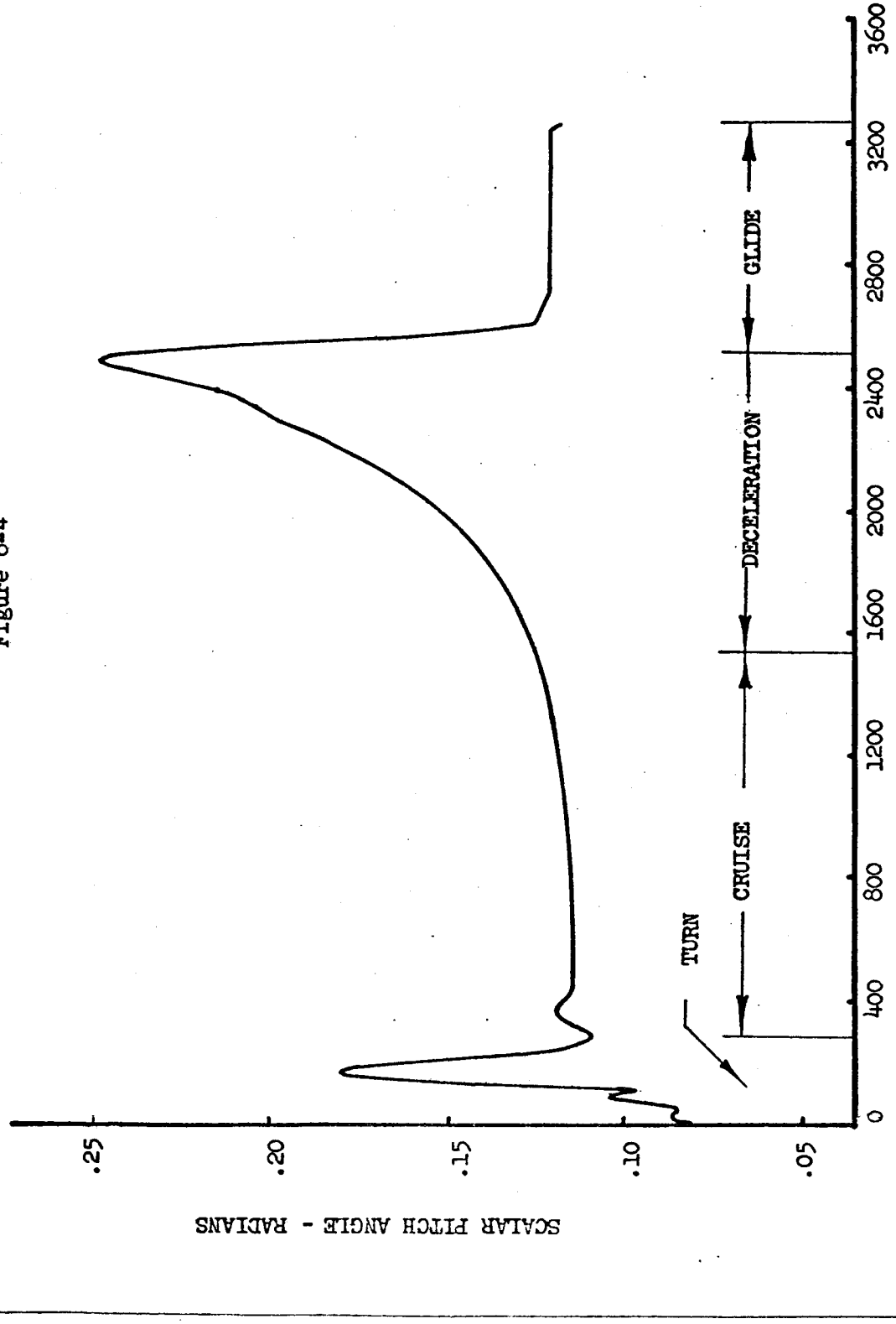

SCALAR PITCH HISTORY
STAGE 1 RETURN

Figure 6-4

BANK ANGLE HISTORY
STAGE 1 RETURN

Figure 6-5

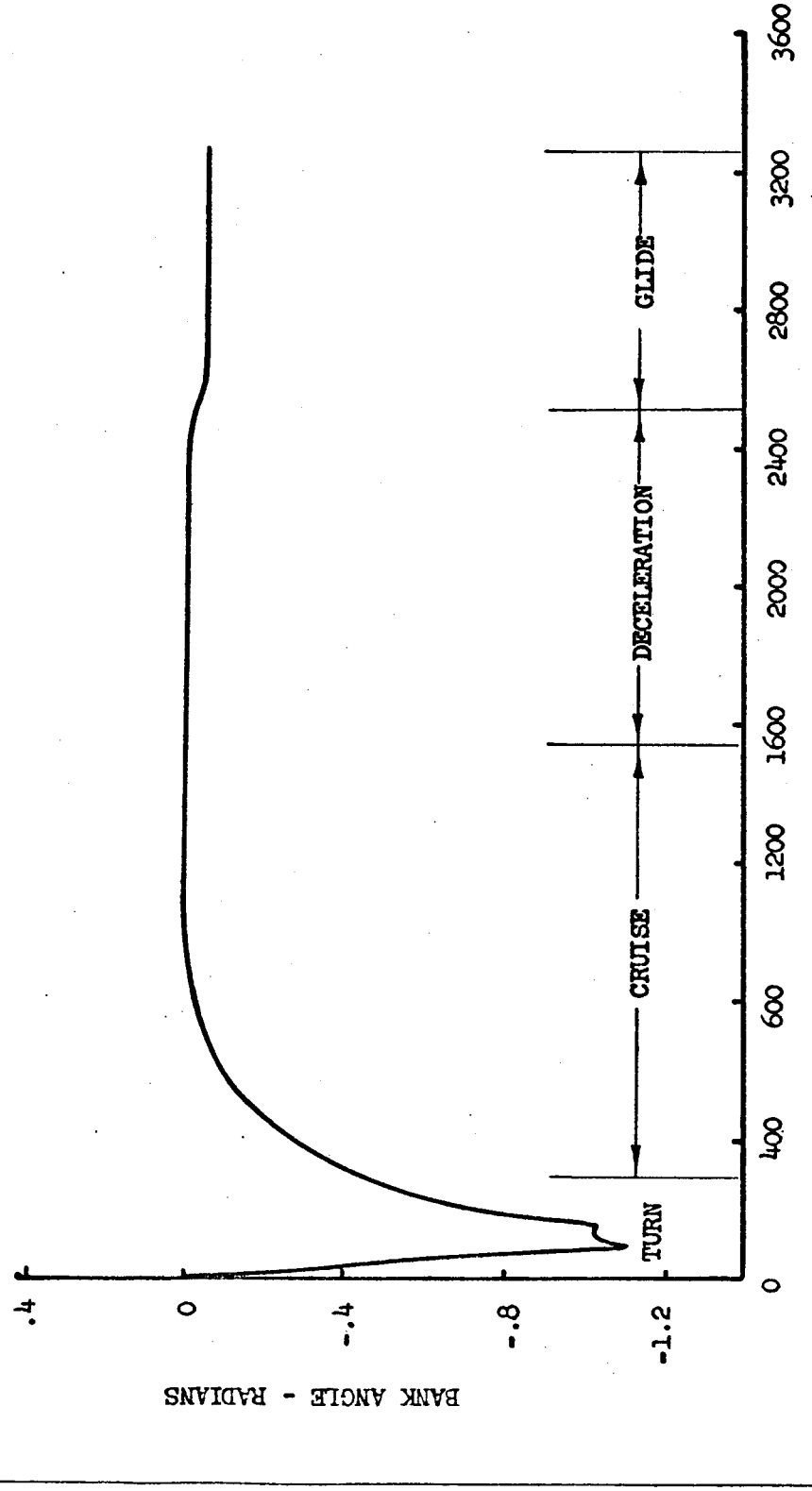

THROTTLE HISTORY

STAGE 1 RETURN

Figure 6-6

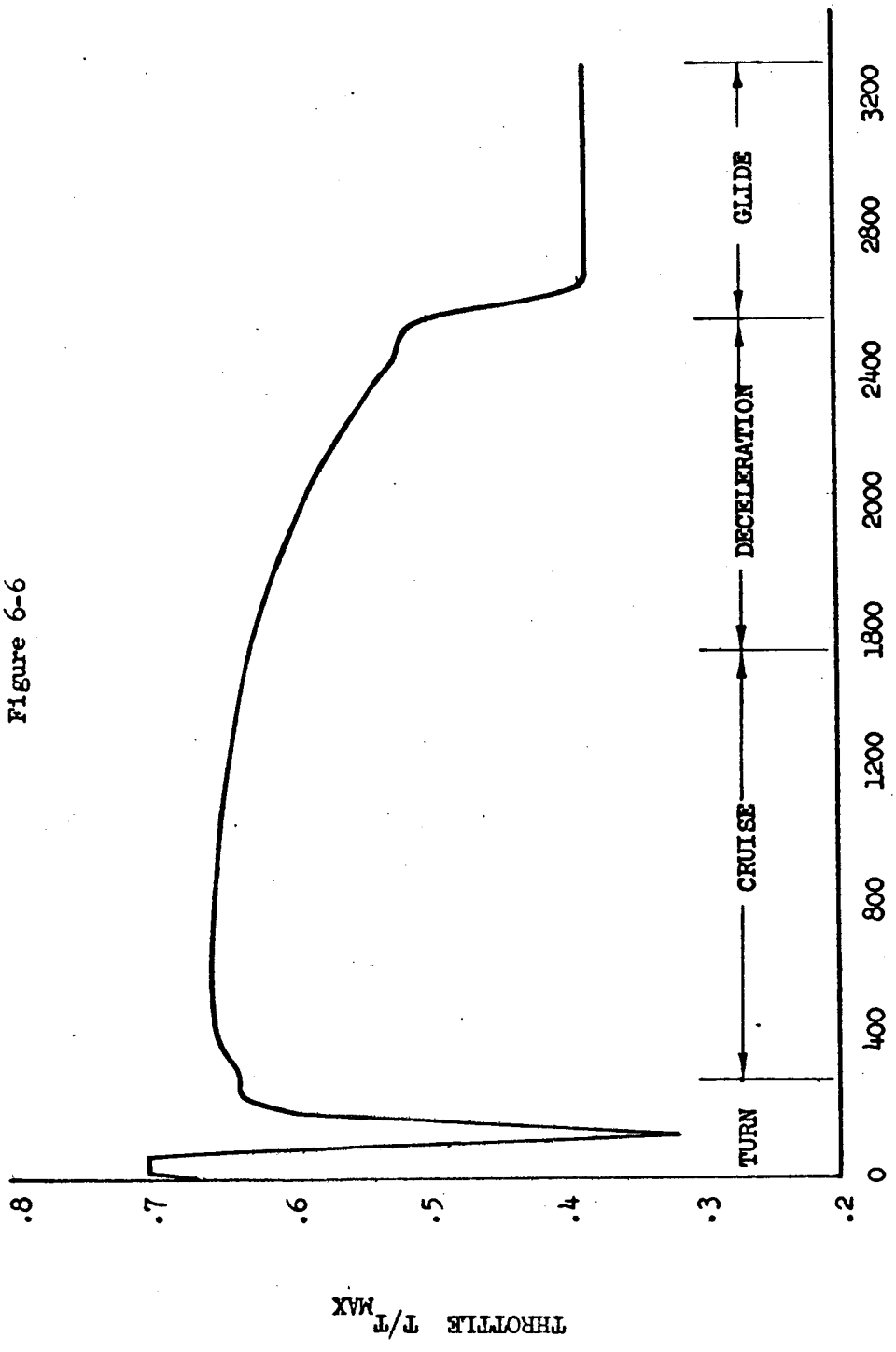

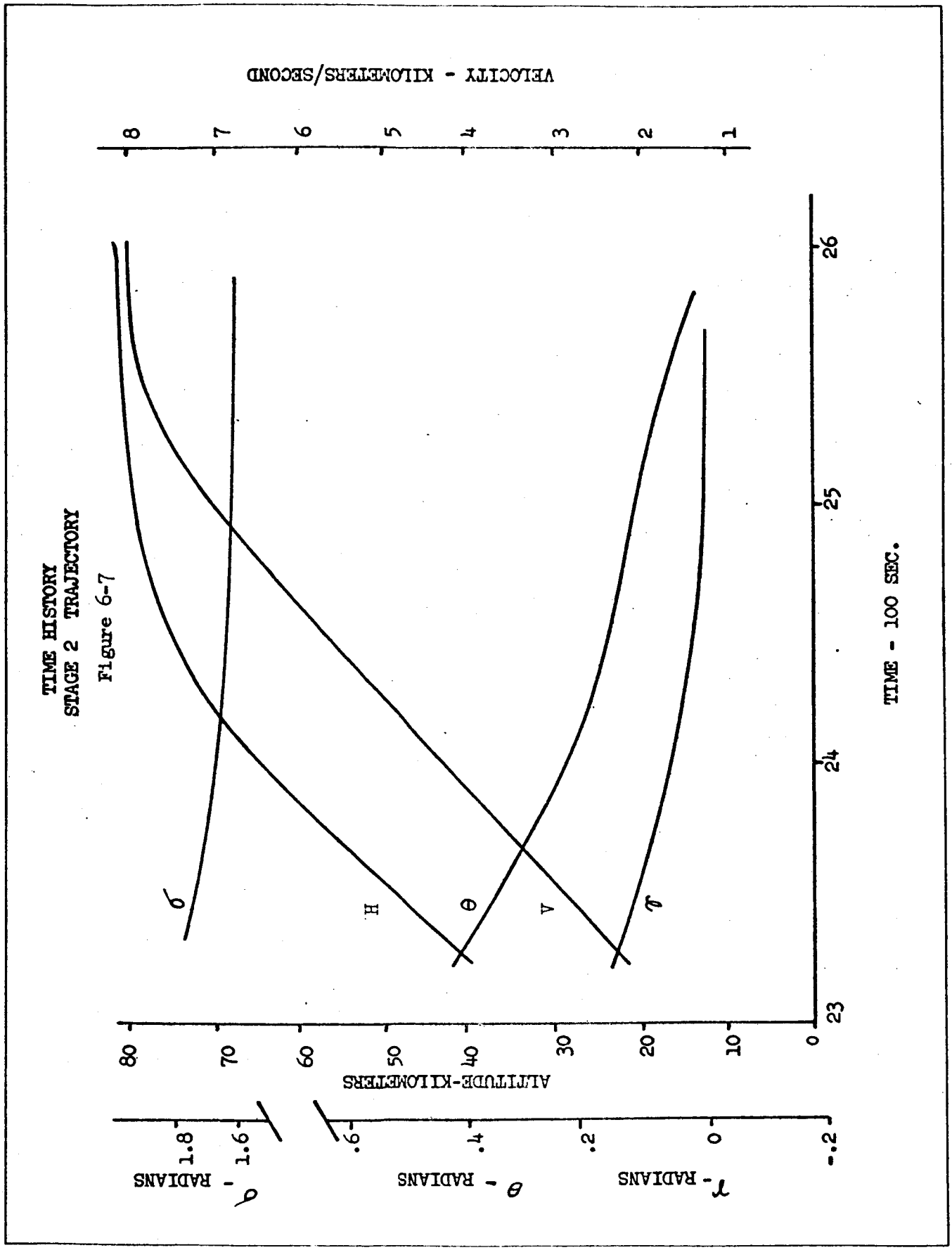

TIME HISTORY
STAGE 2 TRAJECTORY

Figure 6-7

TOTAL VELOCITY LOSSES

STAGE 2

Figure 6-8

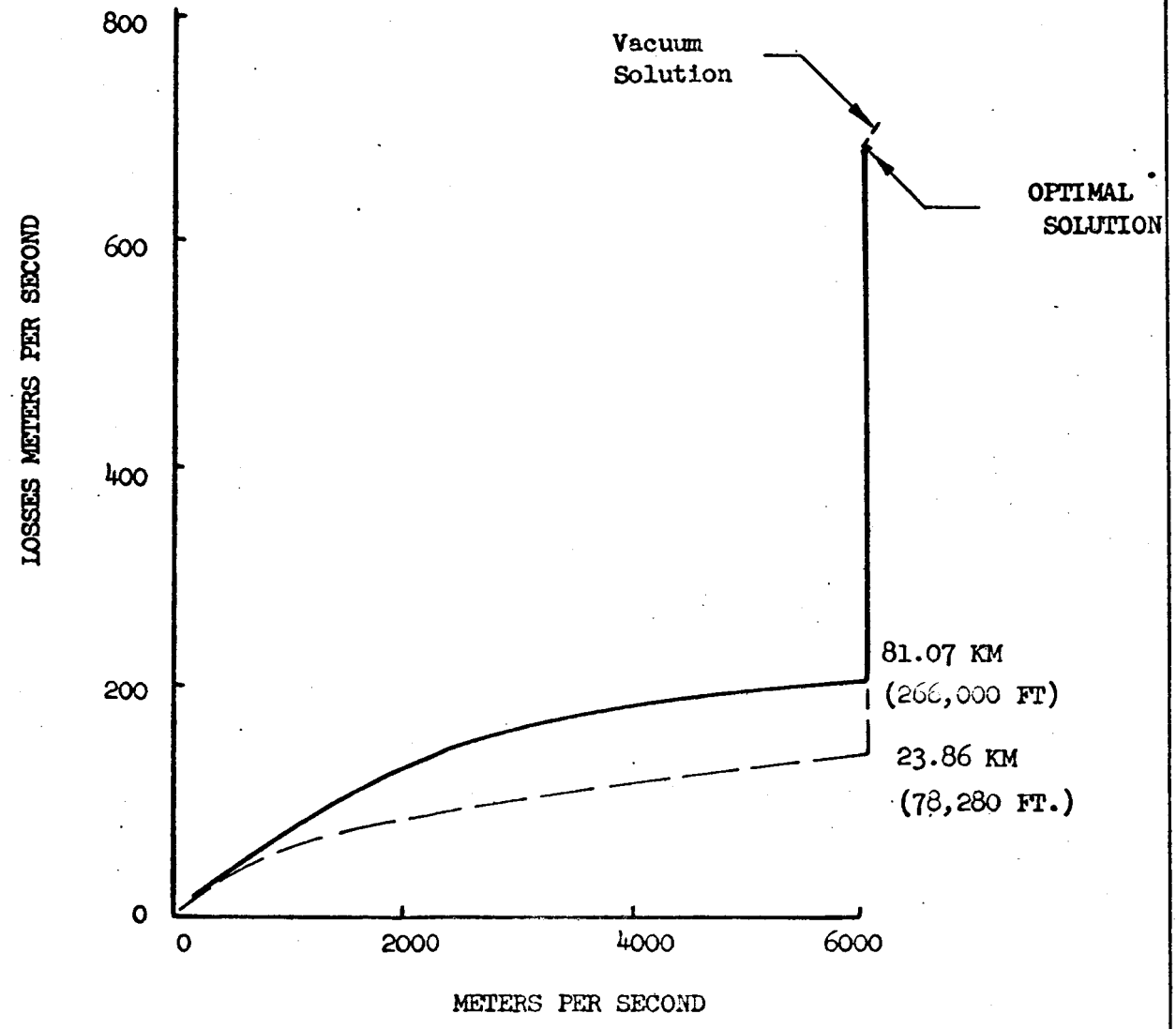

VELOCITY ALTITUDE PROFILE
STAGING MANEUVER
FIGURE 6-9

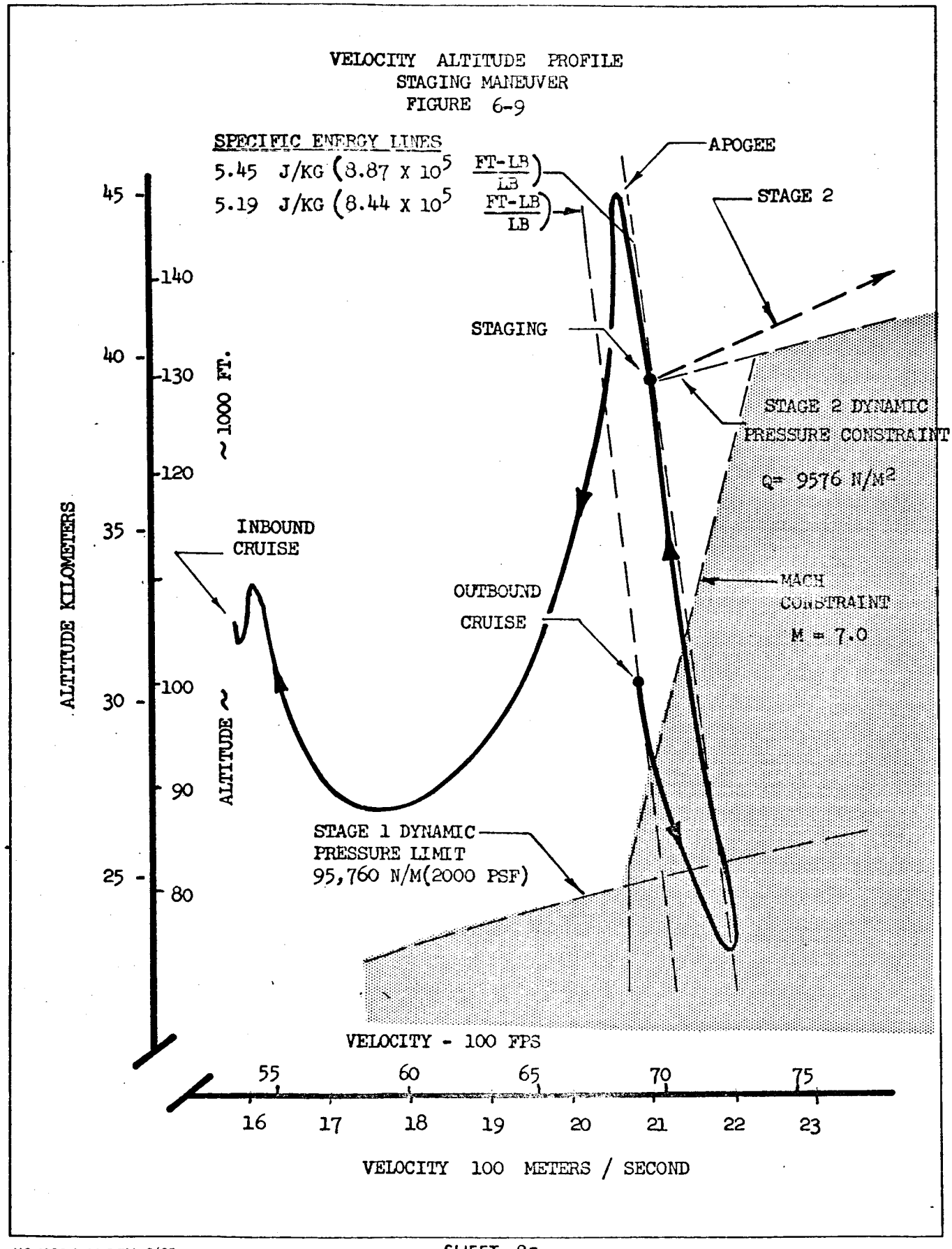

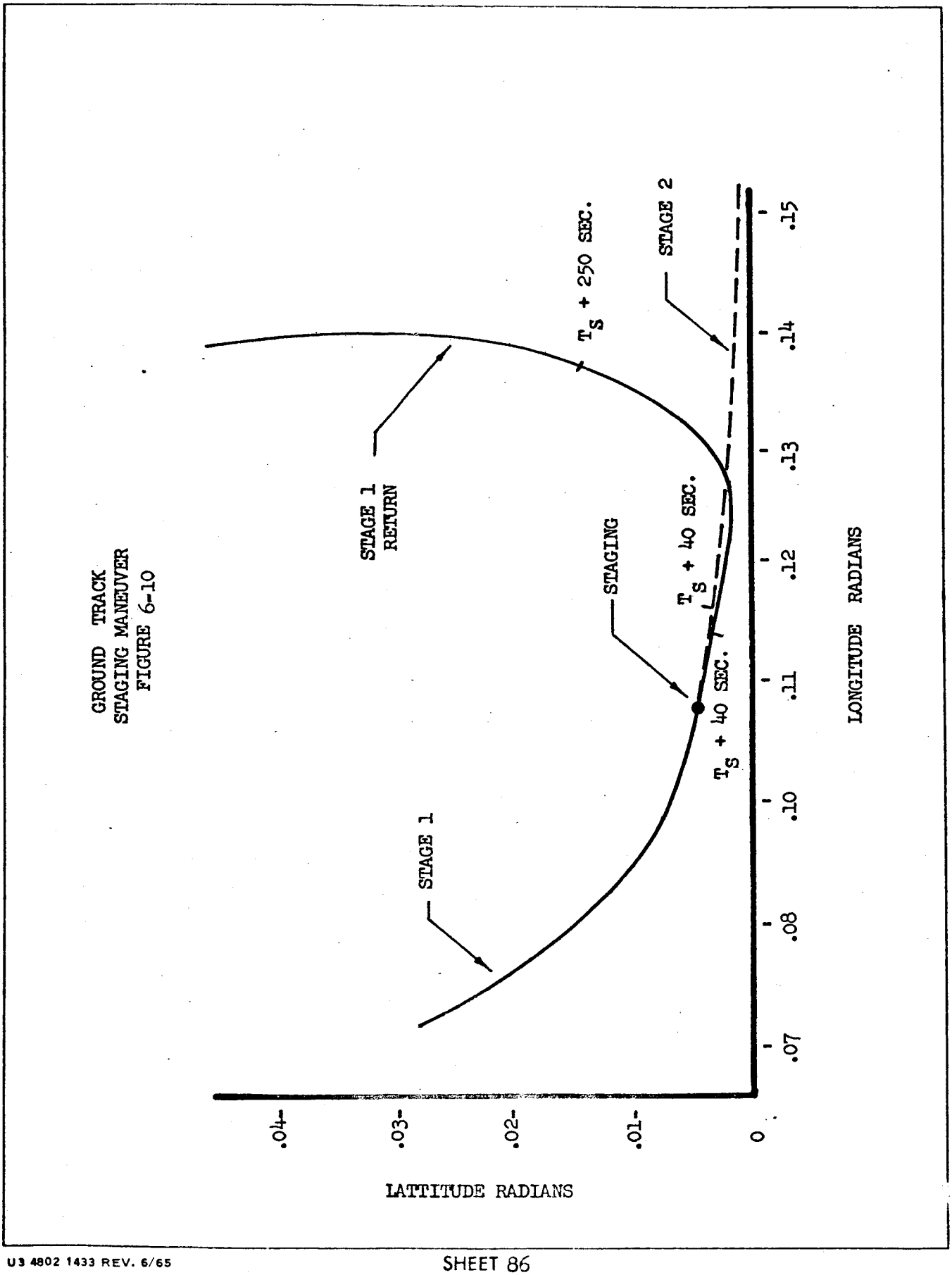

CONTROL HISTORIES
STAGING MANEUVER
FIGURE 6-11

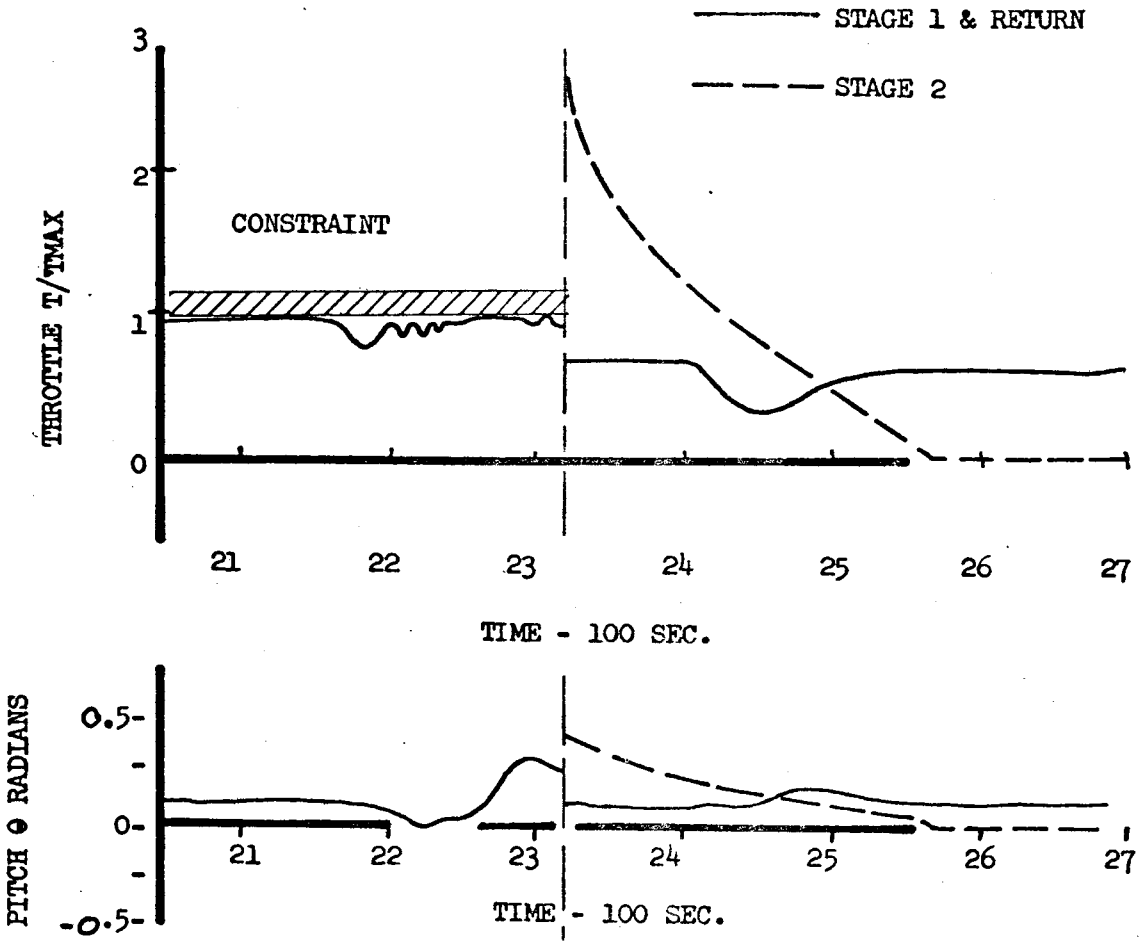

VELOCITY VECTOR ANGLES
STAGING MANEUVER
FIGURE 6-12

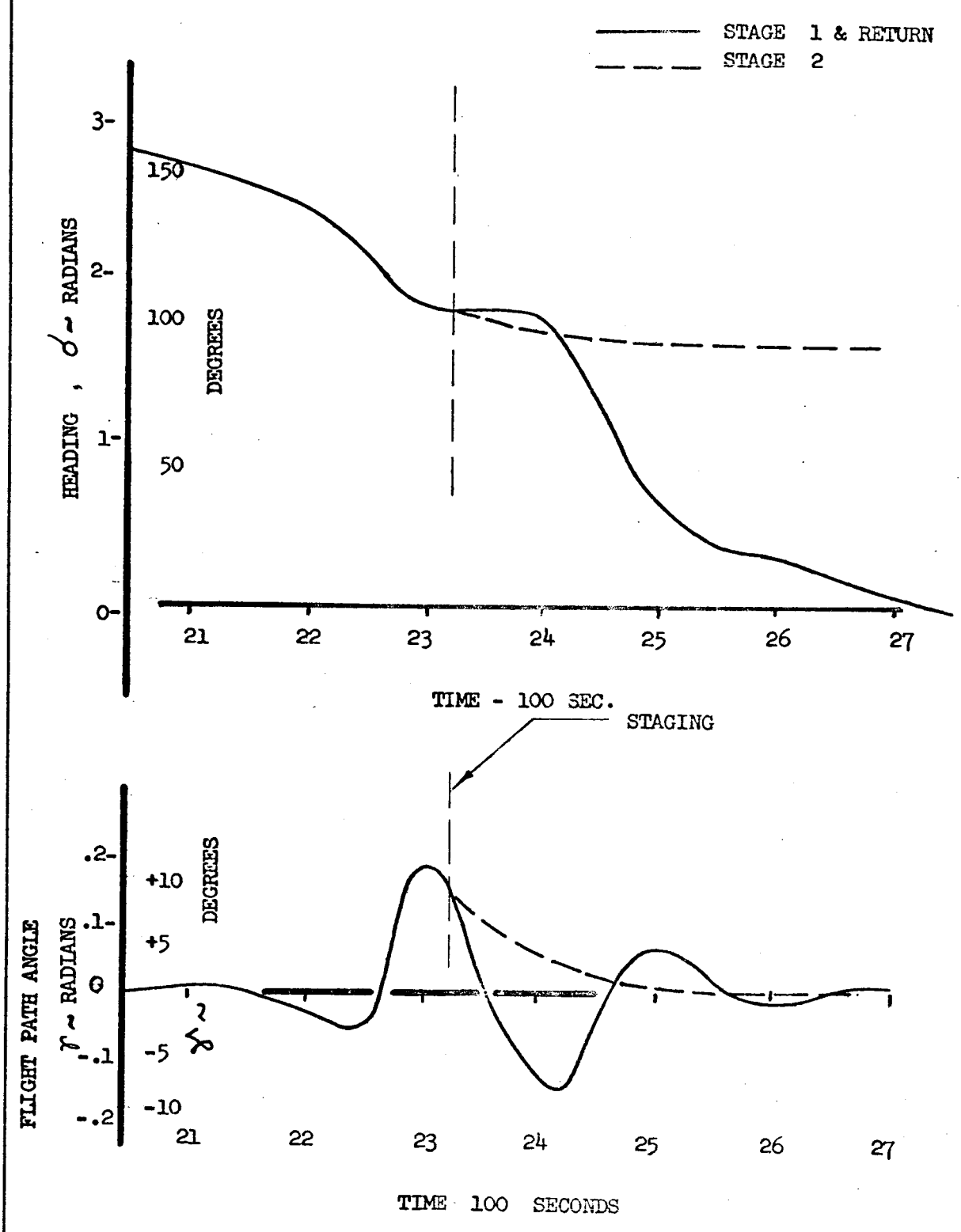

ALTITUDE PROFILE
STAGING MANEUVER
Figure 6-13

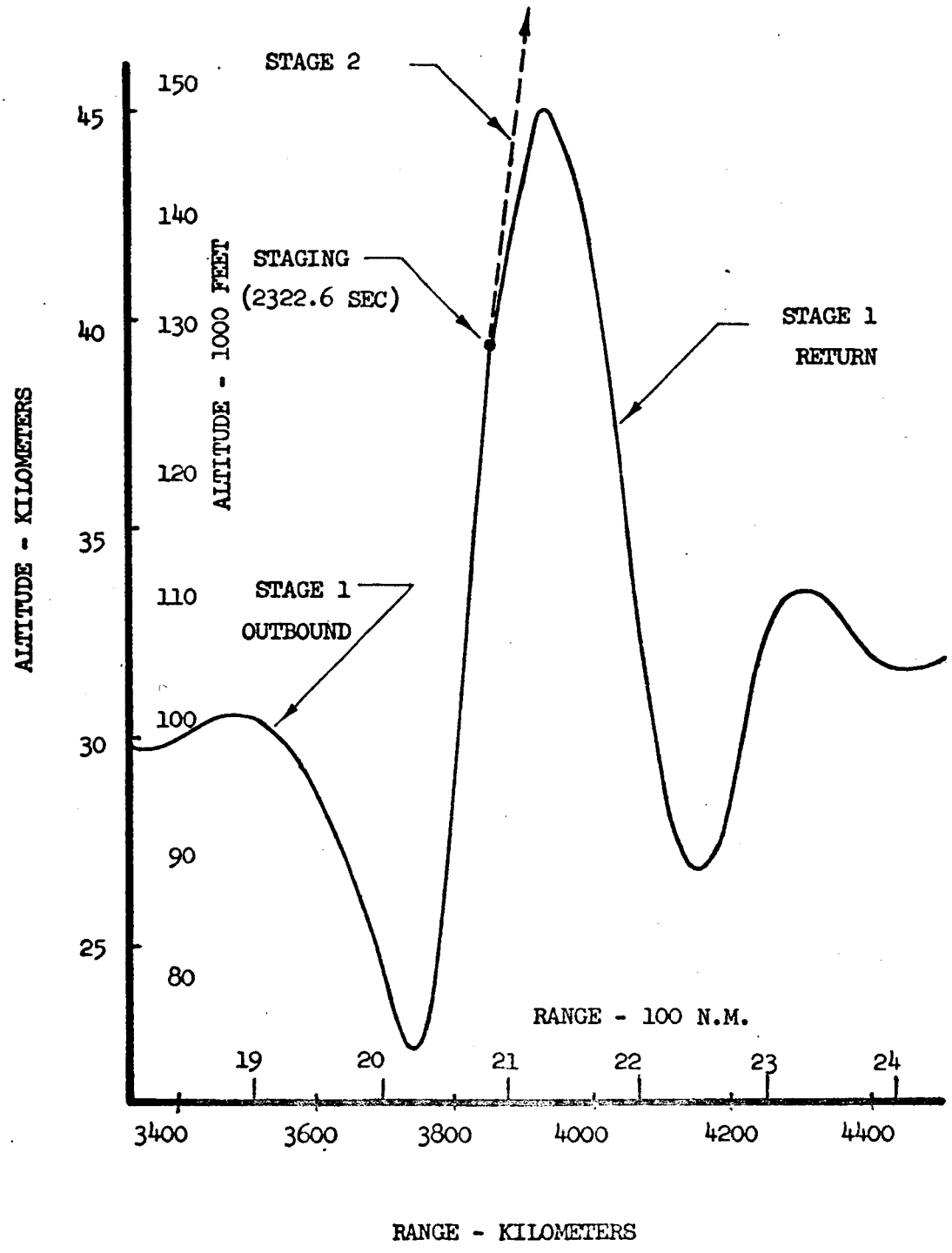

TOTAL LOAD FACTOR
STAGING MANEUVER
FIGURE 6-14

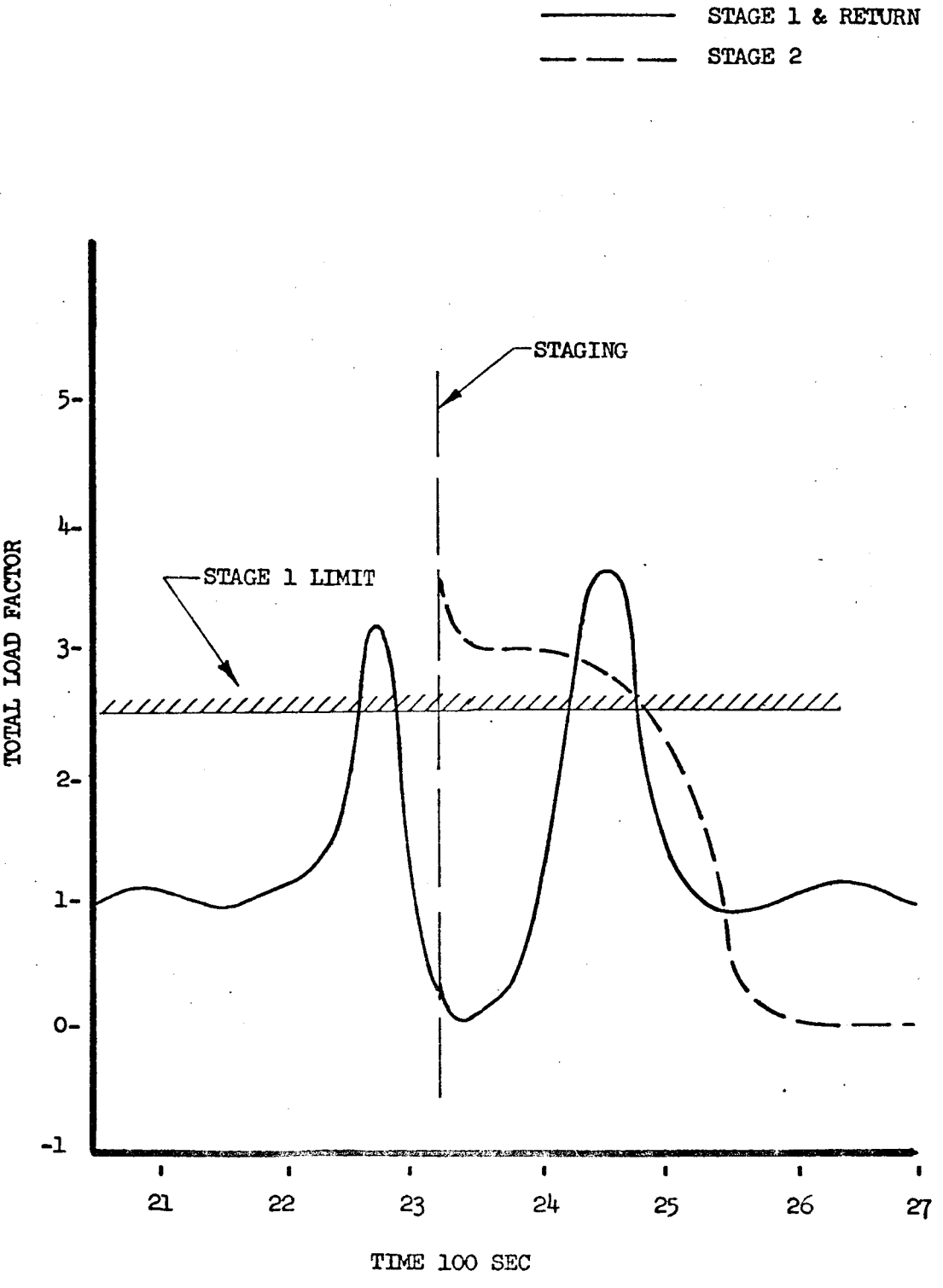

The Mach-Altitude plot of Figure 6-9 reveals that this portion of the mission is extremely dynamic involving an integrated combination of turn into orbit plane, pull-up, and recovery on the part of the first stage. It is obvious from Figure 6-9 that from a flight path performance viewpoint the staging maneuver ideally consists of a synergetic zoom-turn. The ground track of Figure 6-10 reveals considerable heading change during this maneuver. The Stage 1 dynamic pressure inequality constraint of 2000 psf is briefly violated during this maneuver as are the Mach number and load factor constraints. Limitations in available computer time prevented elimination of the violations. The maneuver satisfies the Stage 2 dynamic pressure inequality constraints of 9,560 N/M^2 (200 psf). A significant energy gain of approximately 5% of the total first stage specific energy occurs during this maneuver. This maneuver is retained as the nominal for lambda guidance studies since at this point the vehicle design and materials technology remains in a flexible state. The control histories during the synergetic zoom-turn are contained in Figure 6-11. The throttle history exhibits some oscillation during the dive. Total energy is gained during the dive. The pull-up portion of the zoom occurs at almost constant specific energy. The flight path angle history is presented in Figure 6-12. It can be seen that the stage point does not occur at maximum flight path. It is thought that this release below maximum flight path angle is related to the reflex in the velocity-altitude profile of Figure 6-9 which occurs immediately below staging. This reflex recovers most of the specific energy of the initial pull-up.

The relative position of the vehicle stages following Stage 2 release is apparent from Figures 6-10 and 6-13. The Stage 1 ground track during return crosses that of the Stage 2 module. For at this point Stage 1 has little turning ability while Stage 2 is developing a considerable portion of the orbital plane change required. This is apparent from the bank angle history of Figure 6-11. A detailed study of the separation flight mechanics was beyond the scope of the present study. Following apogee of the pullup maneuver Stage 1 descends below 27 km (90,000 ft.) turning rapidly during this pull out maneuver. Cruise condition is then acquired following climb to cruise altitude and the small oscillation. This maneuver is shown in Figure 6-13.

The most significant features of the Stage 2 first burn are the large bank angles and the monotonically decreasing throttle history exhibited in Figure 6-11. The large bank angle is associated with the plane change required during Stage 2. The transverse force remains small due to the small pitch angle. The decreasing throttle history may be associated with the presence of an atmosphere. An interesting bi-product of this throttle history is the resulting load factor history presented in Figure 6-14. Stage 2 load factors remain moderate during this part of the mission. The two load factor violations of Stage 1 are also apparent from this diagram. Further iteration of the steepest-descent program is required to design a nominal path that does not have these violations.

7.0 SUMMARY

7.1 Comparison of Phase I and Phase II Results

Figure 7-1 is a weight summary which compares Phase I and Phase II results for the 3704 km (2000 N.M.) mission. The difference between Phase I and Phase II resulted in a 29% increase in orbital payload. The Phase II trajectory can be characterized by an improvement in the climb profile, the cruise efficiency, shorter Stage I ground track and a more efficient staging maneuver. The climb fuel was improved by climbing to cruise conditions at Mach 5.0 then performing a slow acceleration along the cruise dynamic pressure line as shown in Figure 7-2. The cruise efficiency was improved by flying higher and using all the available thrust. In Phase I studies the cruise altitude was reduced to allow turn capability at constant altitude. The Phase II optimization studies showed this to be unnecessary in view of the development of a synergetic turn-zoom for total Stage 1 specific energy gain. The improvement in climb and cruise efficiency are shown in Figure 7-3. Similar results can be shown for the Stage 1 return. Finally the staging maneuver influences the improvement in performance because of a 5% gain in total Stage 1 specific energy mentioned above, and more importantly a sizeable reduction in the Stage 1 path length as shown in Figure 7-4. It should be noted that the comparison is for a Phase I path which is uncorrected for inbound/outbound cruise fuel trade but is indicative of the path lengths involved. The savings can be summarized as follows:

Stage 1 Outbound Fuel	7080 kg (15,600 lb.)
Stage 1 Return Fuel	3340 kg (7370 lb.)

The Stage 2 mass ratio for Phase II is 4.49 compared with 4.65 for Phase I. These performance improvements of Stage 1 and Stage 2 result in a net payload in orbit increase of 1800 kg (3970 lb).

7.2 Optimization Development

The Phase II performance results were obtained with the optimal staging technique proposed in Reference 2. Results obtained by the application of this technique have previously been reported in Reference 4.

The present results provide confirmation of the feasibility of simultaneously perturbing the combination of continuous control histories and the parameters determining the stage durations. Convergence problems were negligible apart from some experimentation with the stage point weighting parameters. The separation of the Stage I/Stage II trajectory into two separate problems after several cycles of convergence of the combined Stage I/Stage II problem was primarily intended as a device for reducing total elapsed computer time. A secondary objective was to verify the trajectory shaping capability of the optimal staging algorithm. The time saving would now appear to be negligible and the validity of the algorithm seems to be supported by the fact that no significant changes in the trajectory were introduced when the stages were separated in the above

manner. It is therefore recommended that in future studies the complete problem be treated by the optimal staging algorithm.

The need for further development of flight path optimization computer programs is apparent from the present study. The device of treating the Stage I Outbound-Stage II Ascent to orbit problem as an entity followed by an independent optimization of the Stage I return undoubtedly involves some performance loss. The complete solution of the problem would require a multi-vehicle optimization computer program in order to satisfy the split end conditions imposed by the conditions of Stage I return to base and Stage II ascent to orbit. Further the design rules for transferring the mass between Stage I and Stage II at staging would have to be incorporated into the computation, the mechanism for this is provided by the state stage transfer matrices, $[P_s]$, and the independent state stage perturbations, $[dX_s]$, introduced in Section 3.

In conclusion it would appear that the optimal staging technique of Reference 2 affords a practical means for solving complex atmosphere multi-stage flight path optimization problems. Further development of flight path optimization programs should be undertaken to combine optimal staging with multi-vehicle capability in order to solve the forthcoming generation of trajectory shaping problems. This is essential if future vehicles are to be operated efficiently, for it would appear from this study that approximate methods of determining the flight path of vehicles of the type considered here may result in significant but unnecessary performance losses of the system.

3704 KM (2000 N.M.) MISSION WEIGHT COMPARISON

Figure 7-1

WEIGHT BREAKDOWN	MASS - KG (LBS) PHASE 2	MASS - KG (LBS) PHASE 1
Gross Weight KG (LB)	226,750* (500,000 lb)	226,750 (500,000 lb)
Stage 1 (Stage Wt.)	159,429 (351,552 lb)	169,836 (374,500 lb)
Structures	104,396 (230,200 lb)	104,396 (230,200 lb)
Fuel	55,033 (121,352 lb)	65,440 (144,300 lb)
Stage 2 (Stage 1 Payload)	67,321 (148,448 lb)	56,914 (125,500 lb)
Structure	6,981 (15,393 lb)	6,009 (13,250 lb)
Propellant	52,318 (115,365 lb)	44,683 (98,530 lb)
Payload	8,022 (17,690 lb)	6,222 (13,720 lb)

*907 kg (2000 lb) allowance for take-off and heading change.

CLIMB/ACCELERATION PROFILE
PHASE I/PHASE II COMPARISON
Figure 7-2

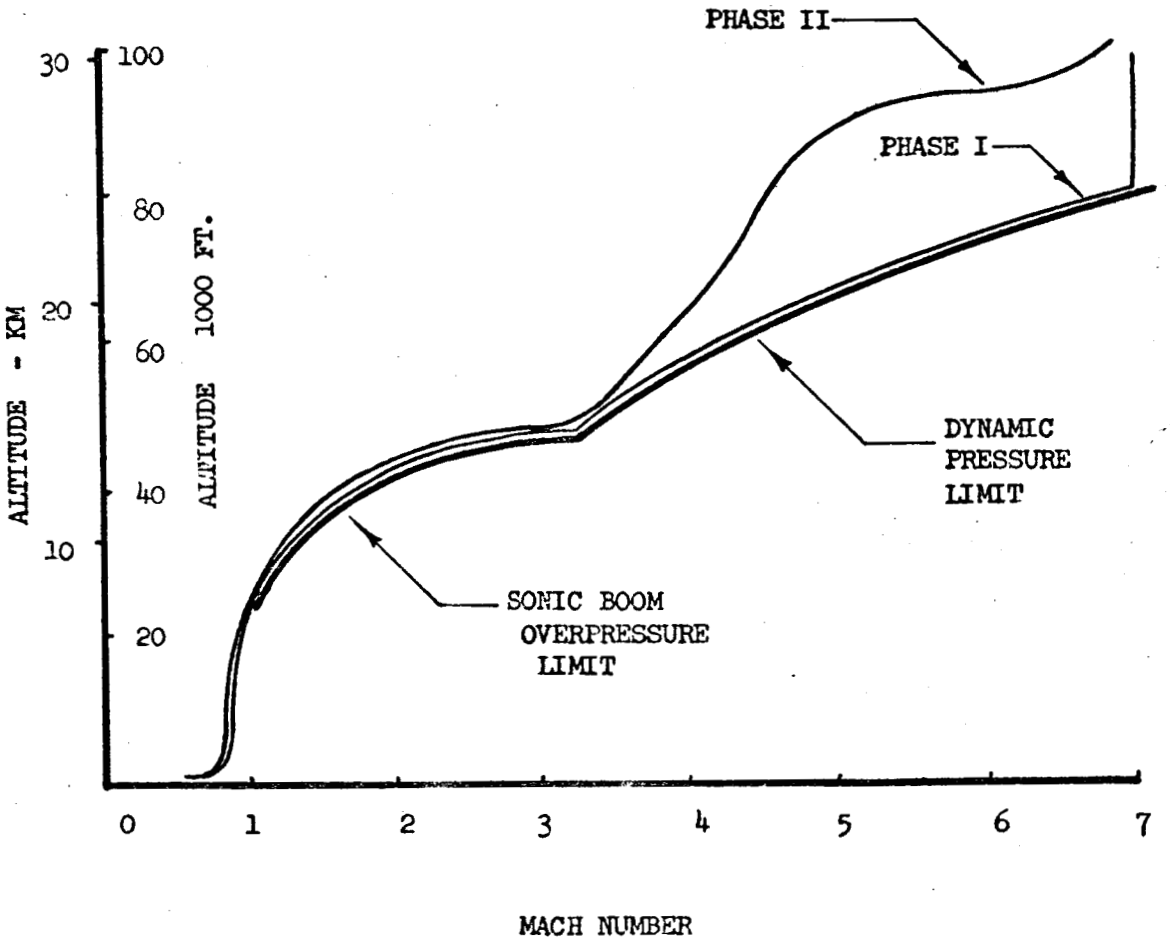

CLIMB AND CRUISE MASS FLOW
PHASE I/PHASE II COMPARISON

Figure 7-3

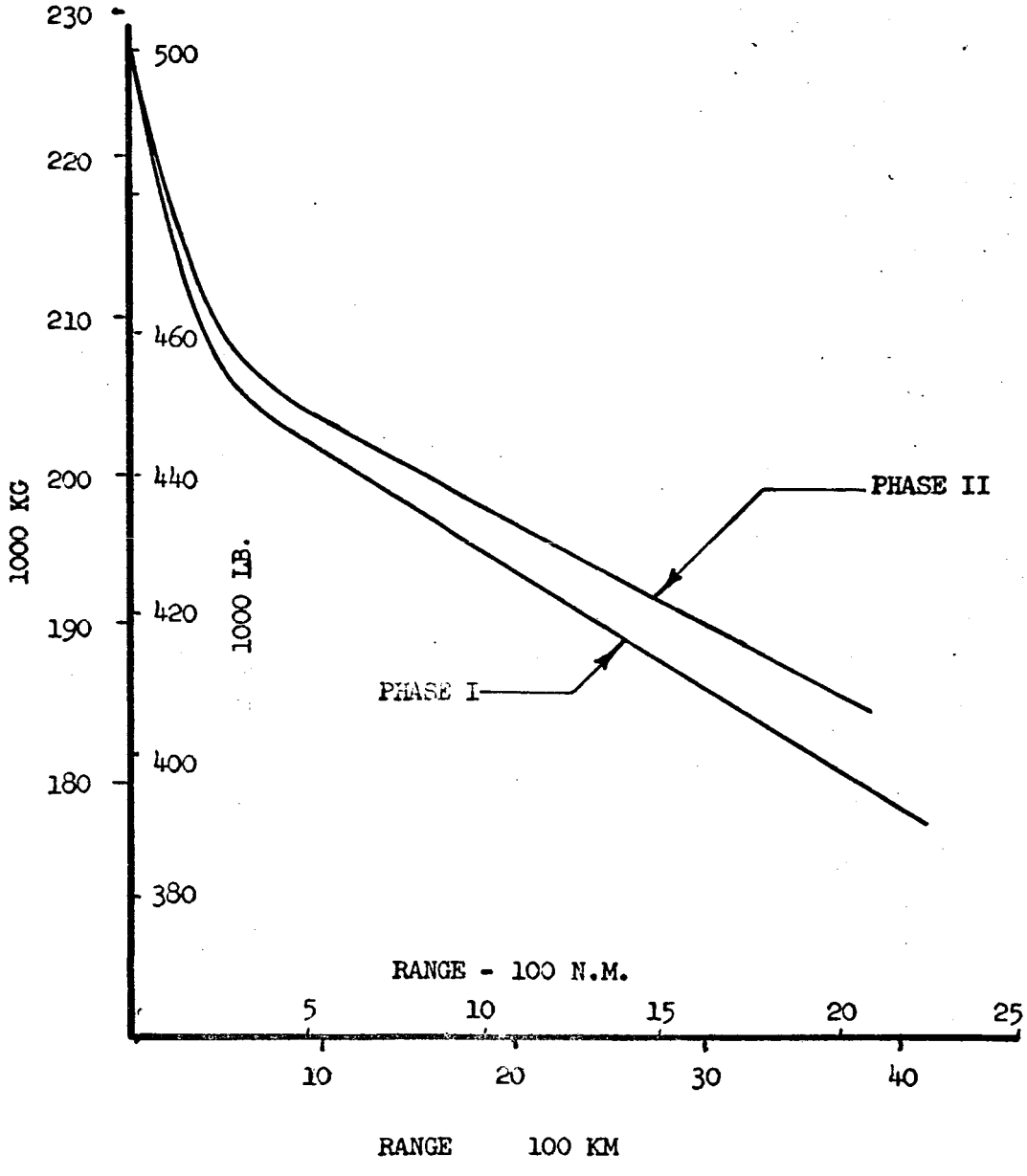

STAGE I GROUND TRACK
PHASE I/PHASE II COMPARISON

Figure 7-4

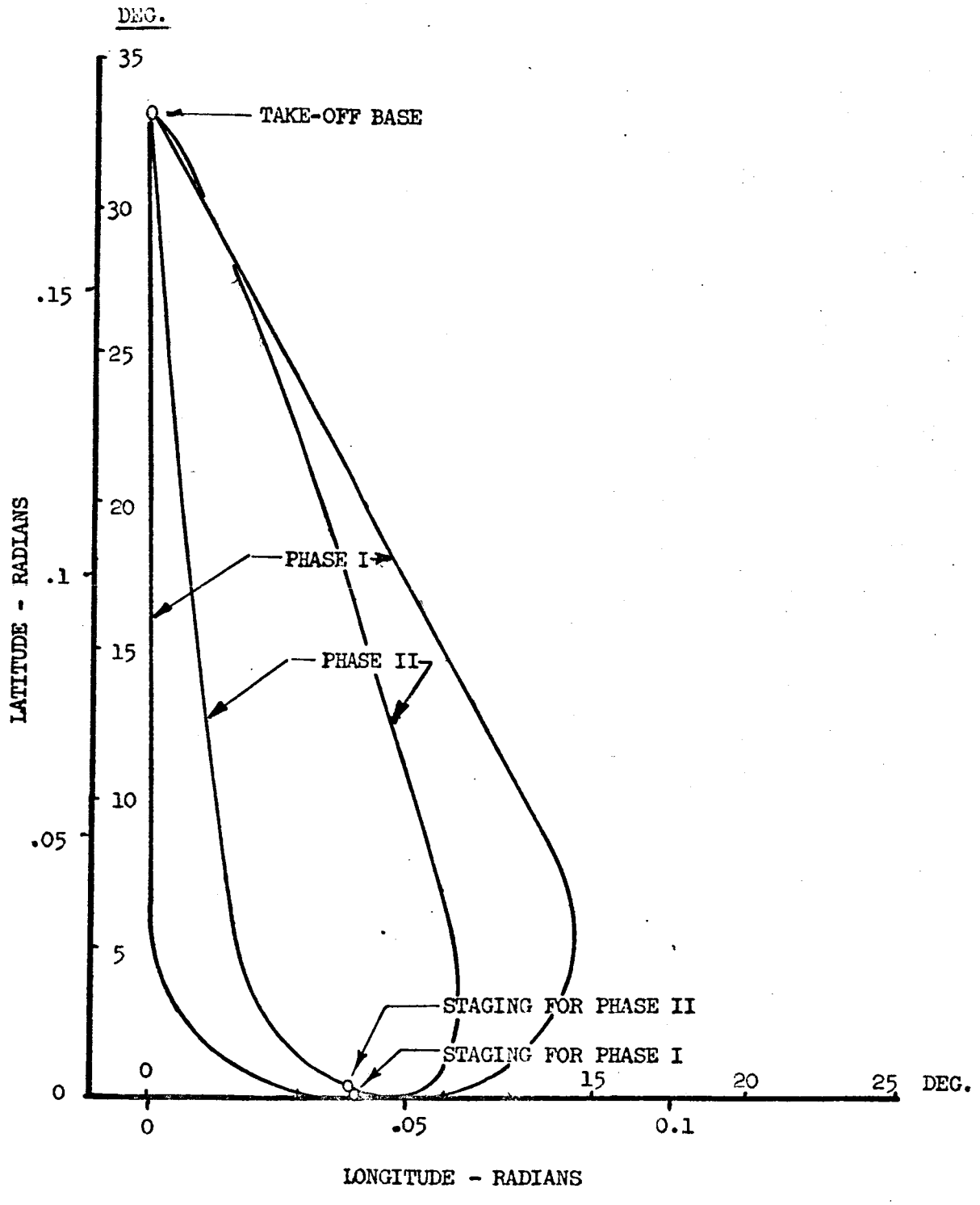

SYMBOLS

(Reproduced from Reference 2)

A	Non-dimensional acceleration dose
$\bar{A}$	Non-dimensional acceleration dose with damping included
A_1, A_2, A_i	Integral measure of an inequality constraint violation
A_{ii}	Weighting matrix constant
A_m^s	Defined by Eqn. (7.2.4)
A_s^N	Defined by Eqn. (6.2.26)
$A(t)$	Control variable perturbation mode shape
$\mathring{A}(t)$	Desired control variable history for a vehicle flight path
$\dot{A}(t)$	Time derivative of non-dimensional acceleration dose
a, $a(t)$	Instantaneous acceleration
a_n	Acceleration in direction n
B_A	Bank angle
B_{ii}	Weighting matrix constant
B_m^s	Defined by Eqn. (7.2.5)
B_s^N	Defined as a column matrix by Eqn. (6.2.27), as a rectangular matrix in Eqn. (6.5.1)
C	The C^{th} iteration in a descent
$C_{D_\alpha}, C_{D_\alpha 2}, C_{D_\beta}, C_{D_\beta 2}, C_{D_{\alpha\beta}}$	Drag force slopes
C_{ii}	Weighting matrix constant
C_L, C_D, C_Y	Lift, drag and side force coefficients
$C_{L_o}, C_{D_o}, C_{Y_o}$	Lift, drag and side force coefficients when $\alpha = \beta = 0$
$C_{L_\alpha}, C_{L_\alpha 2}, C_{L_\beta}, C_{L_\beta 2}, C_{L_{\alpha\beta}}$	Lift force slopes
C_m^s	Defined by Eqn. (7.2.6)
C_N, C_A, C_Y	Force coefficients in body axis system
C_s^N	Defined by Eqn. (6.2.28)

C_{Y_α}, $C_{Y_{\alpha^2}}$, C_{Y_β}, $C_{Y_{\beta^2}}$, $C_{Y_{\alpha\beta}}$	Side force slopes
C_ψ	Non-dimensional amount of constraint error to be eliminated in a given cycle
c_q	Stagnation point heating coefficient
D	Any function to which an inequality constraint is to be added
D	Drag force
D	Summation defined by Eqn. (6.3.10)
DA^2	Algebraic control variable perturbation magnitude
D_{ii}	Weighting matrix constant
DP^2, DC^2	Control variable perturbation magnitudes
DP^2_{N-1}, DP^2_{N-2}	Value of DP^2 on final trajectory on last and last but one iterations
$DP_0{}^2$	Trial value of DP^2
$DP_1{}^2$	Minimum control variable perturbation magnitude which will eliminate a given constraint error
$DP_2{}^2$	Control variable perturbation magnitude when constraints are unaltered
DT^2	Stage point perturbation magnitude
$\bar{D}_U$, $\bar{D}_L$, $\bar{D}$	Upper and lower inequality constraints
D_1	Time history of D when inequality constraint is not satisfied
D_2	Time history of D when inequality constraint is satisfied
$df(\epsilon)$, df	Predicted change in a function for a very small perturbation
$d\beta$	Combined change in terminal constraints and initial state variable values
$d\beta^*$	Combination of $d\beta$ and cut-off function error
$d\phi$, $d\psi$, $d\Omega$	Change in payoff, constraint and cut-off functions

$d\phi_k$	Predicted change in ϕ for a step-size of magnitude k
$d\phi_o$, $d\psi_o$	Trial value of $d\phi$ or $d\psi$
E	Magnitude of maximum control variable error
E	A function to which a point constraint is to be applied
E	Distance between an interceptor and the first of two targets
$\bar{E}$, $\bar{E}(t)$	A point constraint
E_1	A function which fails to satisfy a point constraint
E_2	A function which satisfies a point constraint
F	Total vehicle force vector
F, F(t)	Matrix of partial derivatives $\frac{\partial f_i}{\partial x_j}$
F_n	Force in direction n
F_{x_e}, F_{y_e}, F_{z_e}	Components of force in X_e, Y_e, Z_e system
f, $f(x_n(t), \alpha_n(t), t)$	Function which gives the time derivative of a state variable
$\bar{f}$, $f(\bar{x}(t), \bar{\alpha}(t), t)$	Function which gives the time derivative of a state variable on the nominal trajectory
$f(X_i)$	Algebraic function of the variables X_i
f_1, f_2, f_v	Functions defining the state variables in the algebraic steepest descent analysis
G, G(t)	Matrix of partial derivatives, $\frac{\partial f_i}{\partial \alpha_j}$
grad ϕ	Gradient of ϕ when constraints are satisfied
g, g(x(T),T)	Any additional optimization function
g(x,y,z)	An algebraic constraint function

$H(D-\bar{D})$	Heaviside step function used to handle inequality constraints
h	Altitude
h_{min}	Minimum value of altitude permitted
h_s	Height of satellite's orbit
h_1, h_2	Height of target vehicles in interception problem
$I^{(-)}$, $I^{(+)}$	Number of regions in which $\lambda_{\phi\Omega}G$ is negative or positive
$I_{\phi\phi}$, $I_{\psi\phi}$, $I_{\psi\psi}$	Integrals of payoff and constraint sensitivities over whole trajectory
$I_{\phi\phi}(t')$, $I_{\psi\phi}(t')$, $I_{\psi\psi}(t')$	Integrals of payoff and constraint function sensitivities in the interval $t' \leq t \leq T$
i	Subscript indicating an element in the i^{th} row of a matrix
i,j,k	Unit vectors in direction of X_e, Y_e, Z_e
$J_{\phi\phi}$, $J_{\psi\phi}$, $J_{\psi\psi}$	Integrals defined by Eqns. (6.3.15) to (6.3.17)
j	Subscript indicating an element in the j^{th} column of a matrix
K_{N_ϕ}, K_{N_ψ}	Integrals defined by Eqns. (6.2.33) and (6.2.34)
K_s	Integrals defined by Eqn. (6.2.14)
$K_{\phi\phi}$, $K_{\psi\phi}$, $K_{\psi\psi}$	Functions defined by Eqns. (6.4.25) to (6.4.27)
k	Magnitude of control variable perturbation
k	Step-size parameter
$k(a,t-t')$	Acceleration dose damping function
k_{high}, k_{low}	Working limits on step-size parameter k
$k_{\phi TVL}$, $k_{\psi TVL}$	Value of step-size parameter based on dimensional change of payoff or constraint functions
L	Lift force
$L(t)$, $\dot{L}(t)$	Solution to the adjoint equations which at some time $t = T$, becomes the unit matrix
$L(t')$, $L(\bar{t})$	Particular values of $L(t)$ at $t = t'$ or $\bar{t}$
$L_{\phi\phi}$, $L_{\psi\phi}$, $L_{\psi\psi}$	Integrals defined by Eqns. (6.3.7) to (6.3.9)

M	The number of control variables
M_N	Mach number
M_μ, M_ω	Constants used to improve convergence in numerical solution of variational equations
$M_{\phi\phi}$, $M_{\psi\phi}$	Functions defined by Eqns. (7.4.7) and (7.4.9)
m	Subscript or superscript indicating a typical control variable
m	Vehicle mass
m	Exponent of density in stagnation point heating
$\dot{m}$	Time derivative of vehicle mass
N	Exponent in approximate step function
N	The number of state variables
N	The number of completed iterations
N	Throttle setting
n	A direction
n	Exponent on velocity in stagnation point heating
n	Subscript or superscript indicating a typical state variable
$n_{f,a,y}$	Body axis forces
O(P), O(Q)	Orders of magnitude
P	Argument of an order of magnitude
P	The number of constraints
P_1, P_2, etc.	Trajectories followed if the errors at the first, second, etc., predetermined sampling points are uncorrected.
p	Suffix indicating a typical constraint
P_s	Matrix which transforms state variable perturbations to the left of the s^{th} stage point into those on the right

Q	Rate at which heat is created at the stagnation point
Q_s	Product of P_s and $\bar{\lambda}_{x\Omega s}$'
Q_1, Q_2, etc.	Expected trajectory after errors at first, second, etc., predetermined sampling points are corrected for
q	Dynamic pressure
R	Radius vector from center of the earth to vehicle
R	Range inhibiting force
R_e	Planet equatorial radius
R_p	Planet polar radius
r,s	Suffix indicating r^{th} and s^{th} control variables
S	A switching function
S	Vehicle reference area
S', $\bar{S}$	Number of stages being specified directly and optimized, respectively.
S^{ϕ}	A typical control variable sensitivity
S_r, S_s, S_t	Typical control variable sensitivities of order R,S,T, respectively
S^{ϕ}_{α}	Integrated payoff function sensitivities
$S^{\phi}_{\alpha\psi}$	Integrated mixed payoff function sensitivities
s', $\bar{s}$	Suffix indicating typical stage points being specified directly and optimized, respectively.
s^{ϕ}_{α}	Instantaneous payoff function sensitivities
$s^{\phi}_{\alpha\psi}$	Mixed control variable sensitivities
T	Trajectory termination time
$T_i(-)$, $T_i(0)$, $T_i(+)$	Upper time boundary on the i^{th} region in which $\lambda_{\phi\Omega}G$ is negative, zero, or positive, respectively
T_s	Cut-off point for s^{th} stage in stage time
T_1, T_2	Actual conditions at predetermined sampling points along a trajectory
T_1', T_2', etc.	Anticipated conditions at predetermined sampling points along a trajectory
t	The independent variable, in this report time
t	A time point between the time an error is noted, t', and the trajectory termination

t'	Time at which an acceleration dose is received
t'	Time at which an error in a desired flight path is detected
t'	Time at which a function which fails to satisfy a point constraint is nearest to doing so
t'	A point in time separating regions of differing control variable power
t'	Time at which a stage point occurs
t'	A point at which it is desired to impose boundary conditions on the adjoint equation solution
$t_i(-)$, $t_i(0)$, $t_i(+)$	Lower time boundary on the i^{th} region in which $\lambda_{\phi\Omega}G$ is negative, zero, or positive, respectively
t'_s	Time at which the s^{th} stage point occurs
t_{max}	Maximum value of time permitted.
t_o	Trajectory commencement time
U	Weighting function used in penalty function technique, Eqn. (6.4.42)
U, $\bar{U}$	Augmented payoff function
u,v,w	Velocity components of body axis system
u_e, v_e, w_e	State variables of velocity in X_e, Y_e, Z_e system
V, V_e	Vehicle velocity vector
V_{c_s}	Satellite velocity
V_I	Inertial velocity
$V_{\bar{s}}$	Stage point weighting functions
V_1, V_2	Velocity of targets in interception problem
W, $W(t)$	Control variable weighting function
W_α	Algebraic control variable weighting function
X_e, Y_e, Z_e	Rotating rectangular coordinate system at center of the earth
$\dot{X}_e$, $\dot{Y}_e$, $\dot{Z}_e$	Velocity components in X_e, Y_e, Z_e system
$\ddot{X}_e$, $\ddot{Y}_e$, $\ddot{Z}_e$	Acceleration components in X_e, Y_e, Z_e system
$\dot{X}_g$, $\dot{Y}_g$, $\dot{Z}_g$	Velocity components in local geocentric coordinates
X_i	Algebraic variables
$X(t)$	Desired flight path of a vehicle

$x_e(t)$, $\dot{x}_e$	A state variable and its derivative used in point constraint analysis
$x_n(t)$	The n^{th} state variable history
$\dot{x}_n(t)$	The nth state variable time derivative
x_o, x_{1_o}, x_{2_o}	Position of interceptor, and two target vehicles at $t = t_o$
$\dot{x}_s(T_s)$, $\dot{\bar{x}}_s$	Value of state variable derivative at $\tau = T_s$
$x(t)$	A state variable history
$\bar{x}(t)$	A nominal state variable history
$x(t_o)$, x_o	Initial state variable value
$x(T_s)$	Values of state variables at $\tau = T_s$
x_u, $x_u(t)$, x_L, $x_L(t)$	State variables which measure the integrated violation of an inequality constraint
$\dot{x}_u$, $\dot{x}_L$	Time derivatives of x_u, x_L
x,y,z	Body axis coordinates
x_1, x_2, x_v	State variables in algebraic steepest descent analysis
x , $\dot{x}$ (t)	A state variable and its derivative, used in the penalty function analysis
Y	Side force
$z(x,y)$	An algebraic function which is to be maximized
α , $\alpha(t)$	Control variable, control variable history
α	Angle of attack
$\alpha_m(t)$	The m^{th} control variable history
$\bar{\alpha}_m(t)$, $\bar{\alpha}(t)$	Nominal control variable history
α_1, α_2	A powerful and a weak control variable
α_1, α_2	Control variables in algebraic steepest descent solution

β	Sideslip angle
γ_I	Inertial flight path climb angle
ΔC_ψ	Attempted incremental change in C_ψ on each cycle
$\overline{\Delta P}_i^*$, $\overline{\Delta P}_s^*$, $\overline{\Delta P}_r^*$	Integral measure of total change in the i^{th}, s^{th} or r^{th} control variable between nominal and optimal trajectories
$\overline{\Delta P}_i(C)$, $\overline{\Delta P}_s(C)$, $\overline{\Delta P}_r(C)$	Integral measure of change in the i^{th}, s^{th} or r^{th} control variable, between the nominal and C^{th} iteration
$\overline{\Delta P}_s(\infty)$, $\overline{P}_r(\infty)$	Integral measure of change in the s^{th} or r^{th} control variable history as the number of ierations increases without limit
ΔP^2	Magnitude of control variable correction
ΔT	Change in cut-off time
ΔT_s	Stage time perturbation at the termination of the s^{th} stage
$\Delta T_s'$	Directly specified stage point perturbations
$\Delta T_{\overline{s}}$	Optimal stage point perturbations
ΔU	Change in augmented function produced by control variable perturbation
$\Delta f(\epsilon)$, Δf	Actual change in a function during a very small perturbation
$\Delta \alpha i$	Difference between nominal and optimal values of i^{th} control variable at any point
$\overline{\Delta \alpha_s}$	Mean control variable change as the number of interations increases without limit
$\overline{\Delta \alpha^*_s}$	Mean control variable change between nominal and optimal trajectories
$\Delta \alpha(t)$	A control variable history correction or error
$\Delta \alpha(t')$	Size of a pulse correction to the control variable history at $t = t'$
$\Delta \beta$	Defined by Eqn. (III.23)
$\Delta \phi$, $\Delta \psi$	Terminal errors introduced by uncorrected state variable error at $t = t'$
$\Delta \phi(k), \Delta \psi(k)$	Actual change in payoff or constraint functions for a perturbation step-size of magnitude k
$\Delta \Omega$	Cut-off function error introduced by terminating trajectory at the predicted time at which $\Omega = 0$
$\Delta \Omega_s$	Perturbation in the s^{th} stage point cut-off function
$\Delta \psi(-), \Delta \psi(+)$	Upper and lower bounds on constraint function changes caused trajectory errors
Δx_s, Δx_s^P	Additional state variable perturbations specified directly by at the commencement of the s^{th} stage

$\Delta x(t')$	Error in desired flight path at $t = t'$
$\Delta\varphi(-)$, $\Delta\varphi(+)$	Upper and lower bounds on constraint function changes caused by trajectory errors
Δx_1^{ϕ}, Δx_1^{θ}	Perturbations in latitude and longitude at commencement of first stage
δU, $\delta\bar{U}$	Change in augmented payoff function
$\delta(d\phi)$	Change in ϕ caused by a pulse in the control variables at $t = t'$
δk	Change in control variable perturbation magnitude
$\delta(t-t')$	Dirac Delta Function applied at $t = t'$
$\delta x(t)$	State variable perturbation
$\delta x(\bar{t})$	State variable error induced at $t = \bar{t}$ by uncorrected error at $t = t'$
$\delta x_s(T_s + \Delta T_s)$	State variable perturbations at the termination of the s^{th} stage
$\delta x_s(0)$, δx_s	State variable perturbations at the commencement of the s^{th} stage
$\delta x_{s+1}(-)$, $\delta x_{s+1}(+)$	State variable perturbations induced by perturbations in preceding portion of the trajectory to the left and right of the s^{th} stage point
$\delta\alpha(t)$, $\delta\alpha$	Control variable variation (perturbation)
$\delta^2\alpha$, $\delta(\delta\alpha)$	Control variable second variation
$\delta\alpha_{ij}$, $\delta\alpha_{sj}$, $\delta\alpha_{rj}$	Change in the i^{th}, s^{th} or r^{th} control variable on the j^{th} descent
$\delta\alpha_o$	Trial value of $\delta\alpha$
$\delta\alpha_k$	Values of $\delta\alpha$ corresponding to a value k of the step-size parameter
$\delta\alpha(t)_{min}$, $\delta\alpha(t)_{max}$	The maximum and minimum control variable perturbation magnitudes at any point along the trajectory
$\delta\alpha_1$	Control variable perturbation corresponding to DP_1^2
$\delta\alpha_2$	Control variable perturbation which leaves the constraints unaltered
$\delta\Gamma$	Defined by Eqn. (6.2.50)
$\delta\bar{\Gamma}$	Defined by Eqn. (7.4.1)

$\delta\Psi(T_s)$	Change in Ψ_s at $\tau_s = T_s$
$\delta\phi$, $\delta\psi$, $\delta\Omega$	Change in payoff, constraint and cut-off functions
θ_I	Inertial longitude
θ_L	Longitude
Λ	Sum of a set of vector solutions, or multiple of a solution, to the adjoint equations
$\Lambda_{\phi\Omega}$, $\Lambda_{\psi\Omega}$	Adjoint variables defined by Eqns. (6.2.35) and (6.2.36)
λ , $\lambda(t)$	The adjoint variables
$\dot{\lambda}$, $\dot{\lambda}(t)$	The adjoint variable derivatives
λ_T	Thrust angle rotation
λ_e, $\dot{\lambda}_e$	Adjoint variable corresponding to a point constraint state variable
λ_i, $\dot{\lambda}_i$	Adjoint variables which do not correspond to a point constraint state variable
λ_j, $\dot{\lambda}_j$	Vector solution to the adjoint equation and its time derivative
$\lambda_s^{(-)}$, $\lambda_s^{(+)}$	Values of the adjoint variables to the left and right of a stage point
λ_{x_s}, $\lambda_{x\Omega_s}$	Adjoint variables corresponding to the choice $\Psi = x$
$\overline{\lambda}_{x\Omega_s}$, $\lambda_{x\Omega_s}(0)$	Value of $\lambda_{x\Omega_s}$ at $\tau_s = 0$
λ_ϕ, $\lambda_\phi(t)$	Payoff function adjoint variable, measures sensitivity of ϕ at unperturbed cut-off time to state variable changes at t
λ_ψ, $\lambda_\psi(t)$	Constraint function adjoint variable, measures sensitivity of constraint at unperturbed cut-off time to state variable changes at t
λ_Ω, $\lambda_\Omega(t)$	Cut-off function adjoint variable, measures sensitivity of Ω at unperturbed cut-off time to state variable changes at t
λ_{Ψ_s}, λ_{Ω_s}, $\lambda_{\Psi\Omega_s}$	Adjoint variables defined in the s^{th} stage
$\lambda_{\phi\Omega}$, $\lambda_{\phi\Omega}(t)$	Payoff function sensitivity to state variable changes at t
$\lambda_{\psi\Omega}$, $\lambda_{\psi\Omega}(t)$	Constraint function changes to state variable changes at t

Ψ, $\Psi(x)$	Algebraic constraint function
Ψ_s, $\Psi_s(T_s + \Delta T_s)$	The value of any function of the state variables and stage time at the s^{th} stage termination
$\dot{\Psi}_s$, $\dot{\Psi}_s(T_s + \Delta T_s)$	Time derivative of Ψ_s
Ψ_1, Ψ_2	Constraints in algebraic steepest descent analysis
ψ, $\psi(x_n(T),T)$	A constraint function
$\dot{\psi}$, $\dot{\psi}(T)$	Constraint function time derivative at trajectory
ψ_{ERR}	Control system constants, Section I.4.5
ψ_{FWD}, ψ_{BWD}	Permissable favorable or unfavorable non-dimensional change in constraints
ψ_{NL}	Non-linearity of constraints
ψ_{NL_o}	Desired non-linearity of constraints
ψ_{TOL}	Desired accuracy of constraints
$\psi_\alpha(t')$	Constraint function sensitivity to control variable pulse at $t = t'$, in optimal staging problem
$\psi_{\Delta x_s}$	Constraint function sensitivity to perturbations in the state variable which are directly specified at the commencement of the s^{th} stage
$\psi_{\Delta T_s}$	Constraint function sensitivity to stage point perturbations
Ω, $\Omega(x_n(T),T)$	The trajectory final cut-off function
$\dot{\Omega}$, $\dot{\Omega}(T)$	Cut-off function time derivative at trajectory termination
Ω_s, $\Omega_s(x(T_s), T_s)$	Cut-off function for s^{th} stage
$\dot{\Omega}_s(T_s)$	Time derivative of s^{th} stage cut-off function at T_s
Ω	Longitude of ascending node
ω	Lagrangean multiplier on stage point perturbations
ω_p	Magnitude of earth's angular velocity
ω_p	Earth's angular velocity vector
ω_s	Angular velocity of satellite

ω_0, ω_1	Particular values of ω used in numerical solution of variational equations
$\Phi, \Phi(x)$	Algebraic payoff function
$\phi, \phi(x_n(T),T)$	The payoff function
$\dot{\phi}, \dot{\phi}(T)$	Payoff function time derivative at trajectory termination
ϕ_{ADV}	Maximum permissable adverse change in payoff function
ϕ_{max}	The greatest absolute value of the payoff function over the preceding iterations
L	Latitude
ϕ_{NL}	Payoff function non-linearity
ϕ_{NL_o}	Desired payoff function non-linearity
ϕ_T	Thrust cone angle
$\phi_\alpha(t)$	Payoff function sensitivity to control variable pulses at $t = t'$, in optimal staging problem
$\phi_{\Delta T_s}$	Payoff function sensitivity to stage point perturbations
$\phi_{\Delta x_s}$	Payoff function sensitivity to state variable perturbations which are directly specified at the commencement of the s^{th} stage
φ	Central angle measured from ascending node
φ_s	Satellite central angle
$\mu\varphi s_o$	Initial satellite central angle
	Lagrangean Multiplier for control variable magnitude constraint
μ_g	Gravitational constant
μ_0, μ_1	Particular values of μ used in numerical solution of variational equations
ν	Lagrangean Multiplier for terminal constraints
ϑ	Lagrangean Multiplier used in optimal staging analysis
ϑ_0, ϑ_1	Particular values of used in numerical solution of variational equations
σ_I	Inertial heading angle

τ	Stage time
$\tau(a)$	The length of time that a vehicle or crew can withstand an acceleration a
τ_s	Stage time in the s^{th} stage
υ	Longitude difference between vehicle and ascending node

Matrix Notation

$[\ ]$	Rectangular matrix
$\{\ \}$	Column matrix
$[\ ]$	Row matrix
$[\ ]$	Diagonal matrix
$'$	Transposed matrix
$[\ ]^{-1}$	Inverse matrix

REFERENCES

1. A. E. Bryson and W. F. Denham, A Steepest-Ascent Method for Solving Optimum Programming Problems, Raytheon Report B31303.

2. D. S. Hague, Three-Degree-of-Freedom Problem Optimization Formulation, Volume 3 Analytical Development, FDL-TDR-64-1, Part I, Volume 3, AF Flight Dynamics Laboratory, Air Force Systems Command, Wright-Patterson AFB, October 1964.

3. A. A. Morgan and G. W. Braudaway, An Explicit Multi-Stage Boost Guidance for Minimum Fuel Consumption, Boeing Document D2-90200, November 1962.

4. D. S. Hague, "The Optimization of Multiple-Arc Trajectories by the Steepest-Descent Method", pp 489-517; Recent Advances in Optimization Techniques, edited by Lavi and Vogl, John Wiley, 1966.

5. FDL-TDR-64-1, Part II, Volume 3, Users Manual for Part I, Volume 3 (reference 2 above).

6. Part I of D2-113016-5.

7. L. H. Stein, M. L. Matthews, and J. W. Frenk, "STOP-A Computer Program for Supersonic Transport Trajectory Optimization", Contract NAS 1-5293, Final Report, January 1967.

8. D. W. Hahn and B. F. Itzen, "The Space Trajectory Optimization/Steepest Ascent Digital Computer Program (AS2080)", Boeing Document D2-23374, June 1964.

9. W. F. Denham and A. E. Bryson, Jr., "Optimal Programming Problems With Inequality Constraints II: Solution by Steepest-Ascent", AIAA Journal, January 1964, pp. 25-34.

10. A. E. Bryson, Jr., W. F. Denham, S. E. Dreyfus, "Optimal Programming Problems With Inequality Constraints I: Necessary Conditions for Extremal Solutions", AIAA Journal, November 1963, pp 2544-2550.

11. Optimization Techniques with Applications to Aerospace Systems, edited by George Leitmann, Academic Press, 1962.